SRESA's International Journal of

LIFE CYCLE RELIABILITY AND SAFETY ENGINEERING

Vol.4 **Issue No.4** **Oct –Dec 2015** **ISSN – 2250 0820**

"Special Issue on REACTOR PHYSICS AND SAFETY"

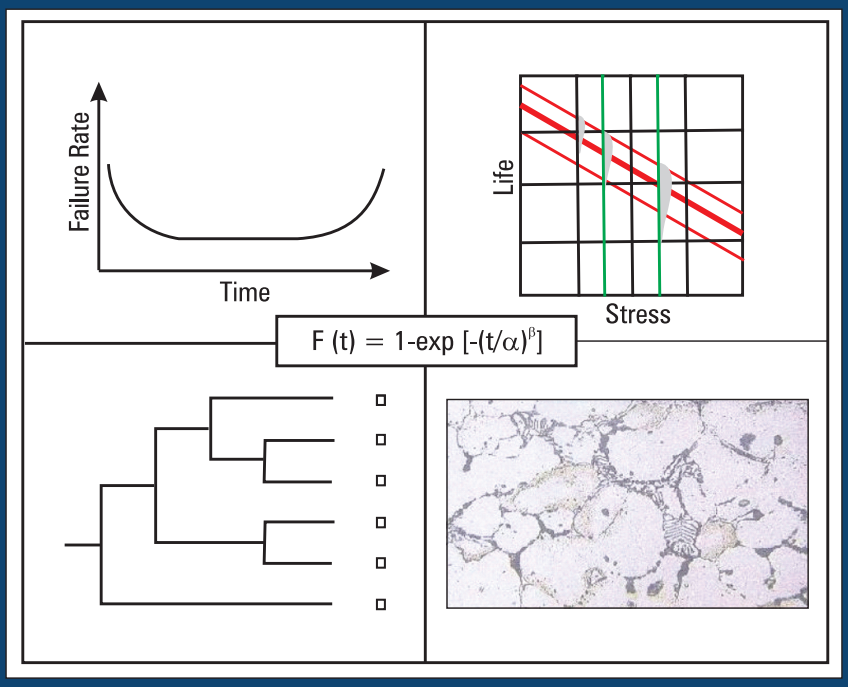

Guest Editor:
Tej Singh

Society for Reliability and Safety
website: http://www.sresa.org.in

SRESA Journal of Life Cycle Reliability and Safety Engineering

Extensive work is being performed world over on assessment of Reliability and Safety for engineering systems in support of decisions. The increasing number of risk-based / risk-informed applications being developed world over is a testimony to the growth of this field. Here, along with probabilistic methods, deterministic methods including Physics-of-Failure based approach is playing an important role. The International Journal of Life Cycle Reliability and Safety Engineering provides a unique medium for researchers and academicians to contribute articles based on their R&D work, applied work and review work, in the area of Reliability, Safety and related fields. Articles based on technology development will also be published as Technical Notes. Review articles on Books published in the subject area of the journal will also form part of the publication.

Society for Reliability and Safety has been actively working for developing means and methods for improving system reliability. Publications of quarterly News Letters and this journal are some of the areas the society is vigorously pursuing for societal benefits. Manuscript in the subject areas can be communicated to the Chief Editors. Manuscript will be reviewed by the experts in the respective area of the work and comments will be communicated to the corresponding author. The reviewed final manuscript will be published and the author will be communicated the publication details. Instruction for preparing the manuscript has been given on inside page of the end cover page of each issue. The rights of publication rest with the Chief-Editors.

SCOPE OF JOURNAL

System Reliability analysis	**Structural Reliability**	**Risk-based applications**
Statistical tools and methods	Remaining life prediction	Technical specification optimization
Probabilistic Safety Assessment	Reliability based design	Risk-informed approach
Quantitative methods	Physics-of-Failure methods	Risk-based ISI
Human factor modeling	Probabilistic Fracture Mechanics	Risk-based maintenance
Common Cause Failure analysis	Passive system reliability	Risk-monitor
Life testing methods	Precursor event analysis	Prognostics & health management
Software reliability	Bayesian modeling	Severe accident management
Uncertainty modeling	Artificial intelligence in risk and reliability modeling	Risk-based Operator support systems
Dynamic reliability models	Design of Experiments	Role of risk-based approach in Regulatory reviews
Sensitivity analysis	Fuzzy approach in risk analysis	Advanced electronic systems reliability modeling
Decision support systems	Cognitive framework	Risk-informed asset management

SRESA AND ITS OBJECTIVES

a) To promote and develop the science of reliability and safety.

b) To encourage research in the area of reliability and safety engineering technology & allied fields.

c) To hold meetings for presentation and discussion of scientific and technical issues related to safety and reliability.

d) To evolve a unified standard code of practice in safety and reliability engineering for assurance of quality based professional engineering services.

e) To publish journals, books, reports and other information, alone or in collaboration with other organizations, and to disseminate information, knowledge and practice of ensuring quality services in the field of Reliability and Safety.

f) To organize reliability and safety engineering courses and / or services for any kind of energy systems like nuclear and thermal power plants, research reactors, other nuclear and radiation facilities, conventional process and chemical industries.

g) To co-operate with government agencies, educational institutions and research oganisations

SRESA's International Journal of

LIFE CYCLE RELIABILITY AND SAFETY ENGINEERING

Vol.4 Issue No.4 Oct–Dec 2015 ISSN – 2250 0820

"Special Issue on REACTOR PHYSICS AND SAFETY"

Guest Editor

Tej Singh

SOCIETY FOR RELIABILITY AND SAFETY

Typeset & Printed

EBENEZER PRINTING HOUSE
Unit No. 5 & 11, 2nd Floor, Hind Services Industries,
Veer Savarkar Marg,
Dadar (west), Mumbai -28
Tel.: 2446 2632/ 3872
E-mail: outwork@gmail.com

Guest Editorial

In three stage nuclear power programme of India, fast reactors come in second stage. Plutonium produced in Indian PHWRs are planned to be used in fast reactors. Use of Plutonium compensates smaller neutron cross section in fast energy range as compared to thermal. Fast reactors are capable to provide higher breeding and burnup of fuel. Moreover, they are capable to incinerate minor actinides and transmute long-lived fission products, which is not possible in thermal reactor due to poor neutron economy and soft neutron spectrum. The inherent safety features of fast reactors coupled with engineered safety features allow their safe and reliable operation under normal and accidental conditions (protected and un-protected). Efforts are being put to achieve a design which gives improved safety, sustainability, non-proliferation resistance, low nuclear waste and reduced economy. In India, metal FBRs with higher breeding ratio and low doubling time is considered for the future because of its higher breeding potential and inherent safety characteristics. The advances in the FBR design with improved safety features are briefly mentioned in the first paper.

The second paper gives an overview of two methods viz. Nodal Expansion Method and Finite Difference Method (FDM) used for reactor core calculation. In general, core calculation is done in two steps. In first step known as lattice level calculation, neutron transport equation is solved for a lattice to generate few group homogenized cross section from multigroup cross section library. In second step known as core level calculation, neutron diffusion equation is solved using few group homogenized cross section, calculated in lattice level, to calculate the reactor core parameters. Nodal Expansion Method (NEM) and Finite Difference Method (FDM) are two techniques which are frequently used to carry out the core level calculation. In NEM, neutron flux in a mesh is expanded in terms of polynomials which help in taking bigger mesh size in calculation whereas in FDM, constant flux is assumed within a mesh which is valid for mesh size not more than neutron diffusion length.

For transient analysis of Compact High Temperature Reactor (CHTR), integrated 3D space-time neutron kinetics with thermal-hydraulic feedback code system is being developed which is discussed in third paper. ARCH (code for Analysis of Reactor transients in Cartesian and Hexagon geometries) has been developed with IQS module for efficient 3D space time analysis with adiabatic Doppler feedback capability. In the adiabatic model of fuel temperature feedback, the transfer of the excess heat from the fuel to the coolant during transient is neglected. The Doppler feedback in ARCH-IQS with adiabatic heating has been validated with AER benchmark. The anticipated transients without scram (ATWS) case in CHTR as well as in AHWR have been analyzed with adiabatic fuel temperature feedback model in ARCH-IQS.

By measuring stable reactor period, reactivity can be determined from the in-hour formula. But this technique is appropriate for positive reactor period only. Fourth paper of the journal describes inverse kinetics method which can be used to determine reactivity under any operating condition of the reactor. In this method, the variation of neutron density with time is used to determine the variation of precursor concentration and reactivity with time. The process begins with the assumption of a functional form of the neutron density variation between two successive time intervals. This leads to an approximate estimate of the precursor concentration and thus the reactivity at the current time. This method can be used to obtain worth of any reactivity device either in critical or subcritical state of the reactor. Care must be taken while using the method for low reactor power or subcritical reactor where the contribution from source term becomes important. In this paper, different cases have been discussed wherein standard methods have been applied to measure reactivity of shut off rods under different conditions, bringing out the importance of the source term, wherever it arises.

Reactor noise methods have long been used for measurement of kinetics parameters and diagnosis of faults in research and power reactors. The methodologies for theoretical treatment of reactor noise and analysis of experimental results are well established for traditional reactors. With recent worldwide interest in accelerator driven sub-critical systems (ADS) for waste management and thorium utilization, various methods for sub-criticality monitoring of such systems are being studied. Due to their passive nature, noise techniques are expected to be useful for the purpose. The statistical properties of the external neutron source in an ADS are

different from that in traditional reactors. For such sources, a new theoretical approach has been developed. The fifth paper in the journal titled "Reactor noise and its role in safety of critical and accelerator driven sub-critical systems", gives a short review of the theoretical and experimental methods used for studying reactor noise in critical systems. This is followed by salient features and some results of the reactor noise theory for ADS and summary and conclusions.

Development and benchmarking of two computer codes namely SAC-RIT (Safety Analysis Code for Reactivity Initiated Transient) and RITAC (Reactivity Initiated Transients Analysis Code) based on coupling of point kinetics and thermal-hydraulics have been described in sixth paper. These codes have been developed to analyze reactivity initiated transients related with upcoming projects like 2 MW Upgraded Apsara and 30 MW HFRR being designed at BARC. The aim is to carry out reactivity initiated transient analysis for nuclear research reactors with plate/pin type fuel assemblies. In SAC-RIT, point kinetics equations are solved using fourth order Runge-Kutta method while thermal hydraulics equations are solved using explicit finite difference method. In RITAC, point kinetics equations are solved using piece-wise constant approximation (PCA) method while thermal hydraulics equations are solved using finite difference method along with Crank-Nicholson technique. Thermal hydraulic modeling is done using two phase homogeneous flow model of the coolant for two representative channels: one average and one hottest channel. In the thermal hydraulics model, the wall to fluid heat transfer mode consists of liquid phase natural convection, liquid phase forced convection, nucleate boiling, sub-cooled nucleate boiling, saturated boiling, transition boiling, film boiling and vapor phase convection. Both the codes have been benchmarked against the transient analysis of 10 MW MTR.

Seventh paper describes the modified point kinetics equations and its solution for Molten Salt Reactor (MSR). The modification is adopted in order to take into account the delayed neutron precursors drift and the subsequent decay in the primary loop along with zero-dimensional thermo-hydraulic equations. Two methods (say delay differential equation solver and Tayler series expansion) are used to solve the coupled set of differential equations. This resulting program is used to analyses the Molten Salt Reactor Experiment (MSRE) for both U235 based fuel mixture and the U233/U235/Pu239 based fuel mixtures. The loss of reactivity due to recirculation of fuel salt in steady state Molten Salt Reactor Experiment (MSRE) operation has been estimated. The step reactivity initiated power and temperature transients in MSRE fueled with Th232-U233 and U235 based fuel salts have been analyzed.

Tej Singh
Guest Editor
Bhabha Atomic Research Centre, Mumbai, India

Tej Singh, *a post graduate in Physics from Agra University, Uttar Pradesh, joined Research Reactor Services Division of BARC in the year 1990 after completion of one year orientation course in Nuclear Engineering from 33rd batch (Physics Discipline), BARC training school. His fields of interest are operation, design and safety of Nuclear Research Reactors. He started his career as operational reactor physicist in Cirus reactor. At present, he is heading the Reactor Physics and Nuclear Engineering Section of Research Reactor Services Division. He is responsible to provide Reactor Physics support for safe and smooth operation of the research reactors at Trombay, Mumbai. He is also responsible for Reactor Physics and shielding design of upcoming Research Reactors, like upgraded Apsara, High Flux Research Reactor (HFRR) and 125 MW Thermal Research Reactor. Shri Singh has developed computer codes NEMSQR and HEXNEM, based on nodal expansion method, for reactor core calculations and safety analysis codes RITAC and SACRIT based on point kinetics model coupled with thermal hydraulics.*

Life Cycle Reliability and Safety Engineering
Vol.4 Issue 4(2015) 01-10

Fast Reactor Physics and Safety

T. Sathiyasheela*, Anuraj, V. L, G. S. Srinivasan, K. Devan
Reactor Neutronics Division, Reactor Design Group, Indira Gandhi Centre for Atomic Research, Kalpakkam-603 102, Tamil Nadu, e-mail: sheela@igcar.gov.in

Abstract:

Fast reactors have attractive neutronics properties which provide higher breeding and burnup of fuel. With closed fuel cycle, it is possible to achieve higher fuel utilization of about 70%. The other advantage of fast reactors is their capability to incinerate minor actinides and transmute long-lived fission products. The inherent safety features of fast reactors coupled with engineered safety features allow their safe and reliable operation under normal and accidental conditions (protected and un-protected). The sodium-cooled systems have been selected as one of the systems under Generation-IV International Forum(GIF) to achieve a design which gives improved safety, sustainability,non-proliferation resistance, low nuclear waste and reduced economy. In India, metal FBRs with higher breeding ratio and low doubling time is considered for the future because of its higher breeding potential and inherent safety characteristics. The advances in the FBR design with improved safety features are briefly mentioned in this paper.

Keywords: Reactivity, Inherent reactivity feedback, Positive void, Fuel slumping, CDA, Shutdown system, Gen-IV, Design Extension Condition.

1. Introduction

The principle of controlled chain reaction makes the possibility of producing electricity from nuclear energy in a nuclear reactor. It had been demonstrated in the Experimental Breeder Reactor I (EBR-I) on 20th December, 1951. Thenuclear reactorsdesigned today are either of thermal or fast,depending upon the average energy of neutrons involved in nuclear fission reaction (0.025 eV in thermal reactors and hundreds of keV in fast reactors). Most of the reactors currently in operation are thermal reactors. The concept of fast reactor has been developed to meet the two main objectives of efficient fuel utilization and minor actinide incineration. So far many small experimental and commercial fast reactors have been constructed world-wide and demonstrated its safe and reliable operation, meeting all its design challenges. It included the world's first plutonium based reactor, Clementine (USA), the experimental breeder reactor I (EBR-I) for demonstrating electricity generation and breeding and EBR-II to demonstrate the reactor operation using closed fuel cycle. In addition, many zero power critical facilities, viz. ZPR and ZPPR (USA), BR, BFS (Russia) and RAPSODIE and MASURCA (France) and FCA (Japan), etc. was also built to study the various neutronics aspects of fast reactor cores. Based on the experience gained, several small, medium and large power reactors were also built in various countries (examples: CEFR in China, BN-350 in Kazakhstan, BN-600 and BN-800 in Russian Federation, MONJU in Japan, PHENIX and SUPERPHENIX etc.). In India, the fast reactor study was initiated in 1972 and subsequently the PURNIMA reactor was commissioned. Later on, a 40 MWt mixed carbide Fast Breeder Test Reactor (FBTR) was built and made critical in 1985. Since then it is being used for various irradiation studies towards the development of advanced fuels and structural materials for use in future fast reactors. Based on the operational experience gained from FBTR, India has constructed a 500 MWe Prototype Fast Breeder Reactor (PFBR) [Chetal,2009], which is expected to be commissioned by this year end. At present, countries like Russia, France, Japan, India, China and South Korea are actively pursuing fast reactor studies. In parallel, the Generation-IV International Forum (GIF) is also investigating six nuclear energy systems to meet the challenging goals of efficient fuel utilization with minimum nuclear waste, improved safety,enhanced proliferation resistance and low cost [Bouchard, 2008]. The reactor systemschosen are Very High-Temperature Reactor (VHTR), Sodium-cooled Fast Reactor (SFR), Gas-cooled Fast Reactor (GFR), Lead-cooled Fast Reactor (LFR), Molten Salt Reactor (MSR) and Super-Critical Water-cooled Reactor (SCWR).

In this paper, we discuss some important physics aspects of sodium cooled fast reactors and their safety characteristics.

2. A brief Overview of Fast Reactors and Their Characteristics

In fast reactors, no specific moderators are provided in the design. The fission neutrons undergo very little moderation mainly by in-elastic scattering reaction with fuel, structural materials and sodium. The fast reactor neutron flux spectrum is generally peaked in the energy range of ~ few tens of keV to MeV (Figure.1). Because of this, there will be a strong overlap between fission neutrons and the neutrons that undergoes fission. Neutron flux shows lot of dips due to resonances of neutron interaction cross section of core materials. The effect of these flux depression (called self-shielding effect) on neutron interaction with materials has to be accurately taken care of in the core neutronics studies. The resonance region, viz. both resolved and un-resolved, is thus very important in fast reactor analysis.

It is well known that neutron interaction cross section reduces in harder neutron spectrum. A closer look at the neutron cross section of core materials results the following important facts:

- For fissile nuclides, fission cross section is higher in thermal region compared to capture reaction. In fast region, fission cross section does not fall rapidly as the capture reaction.
- Fertile nuclides have fission cross section in the fast energy region.
- The combination of increased fission to capture ratio, and increase in the number of neutron yield due to fission (ν), yields more excess number of neutrons per neutron absorbed. It is represented by a parameter 'η', called as 'reproduction factor'. This is the parameter deciding the breeding potential of fuels. The minimum condition for breeding is η should be greater than 2. Pu-239 has the highest η-value in the fast energy region, compared to other fissile nuclides namely U-233 and U-235 (see Figure 2 and Table 1). Breeding potential of a typical 1200 MWt FBR with oxide, carbide and metallic fuel is 1.3, 1.4 and 1.6 respectively [Walter & Reynolds, 1981]. Metal fuel has higher breeding ratio due to harder neutron spectrum.

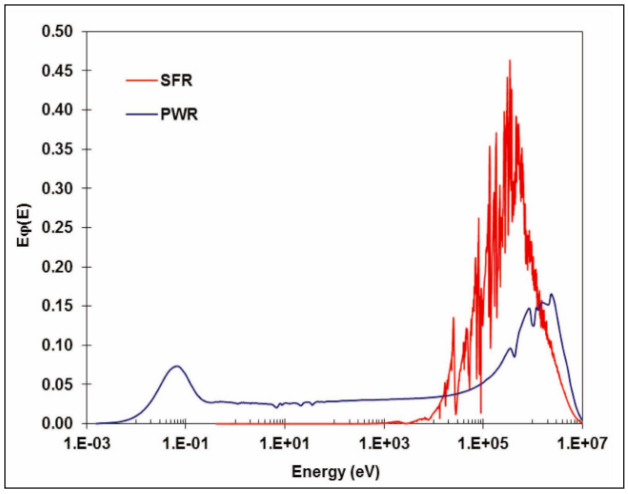

Figure 1: Comparison of a typical SFR and PWR flux spectra

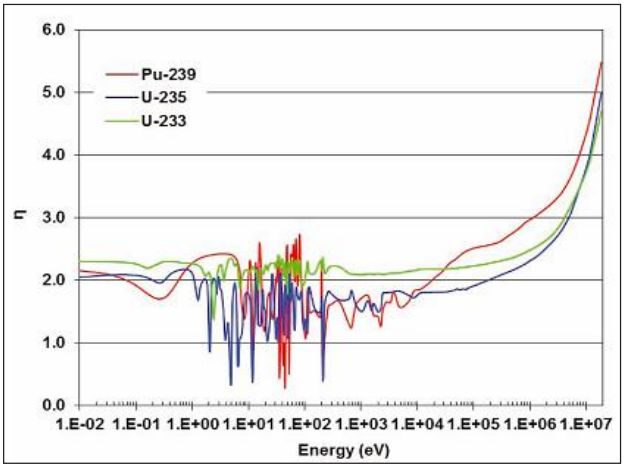

Figure 2: Comparison of η-value for U-233, U-235 and Pu-239

Table 1: Comparison of η-values for a Typical LWR and LMFBR

Reactor Type	Pu-239	U-235	U-233
LWR	2.04	2.06	2.33
LMFBR (oxide)	2.45	2.10	2.31

- In fast spectrum, U-238 has significant neutron capture, which enables more internal breeding and low burnup swing. Higher fertile capture and low fission cross section in fissile nuclides necessitates fuel enrichment (10-30%).
- In harder spectrum, parasitic neutron capture is less and it leads to better neutron economy. It is possible to use conventional stainless steel as the structural material. In addition, the effect of fission product poisoning is found to ne not very significant in fast reactors.
- The mean free path of about 10-20 cm in FBRs compared to ~2 cm in LWRs.The reactor core is tightly-coupled. The heterogeneity effect is relatively unimportant in fast reactors.
- Larger mean free path of fast neutrons lead to increased neutron leakage from the core. They are used for breeding fissile material by using external radial and axial blankets. It is very

important to provide good reflector savings in the design.

- The reactor core size is generally very small with high power density.
- The parameters affecting the reactor safety are low effective delayed neutron fraction (β-eff) and shorter prompt neutron life time. Significant negative feedback is possible because of Doppler Effect in U-238 capture resonances.

2.1 Salient Features of Fast Reactor Core

The design of a fast reactor is a multi-disciplinary activity involving physics, chemistry, electronics and all branches of engineering. Based on the primary coolant system design the reactor can be either pool-type (example: PFBR) or loop-type (example: FBTR). In the pool-type design, reactor core is immersed in a pool of primary sodium in the reactor vessel. The primary sodium is circulated through the core by using sodium pumps kept inside the vessel, whereas in the loop type design, heat from the core is removed by circulating primary sodium with the help of sodium pumps kept outside the reactor vessel. The primary sodium circuit removes the nuclear heat generated in the core and transfers to the secondary system through

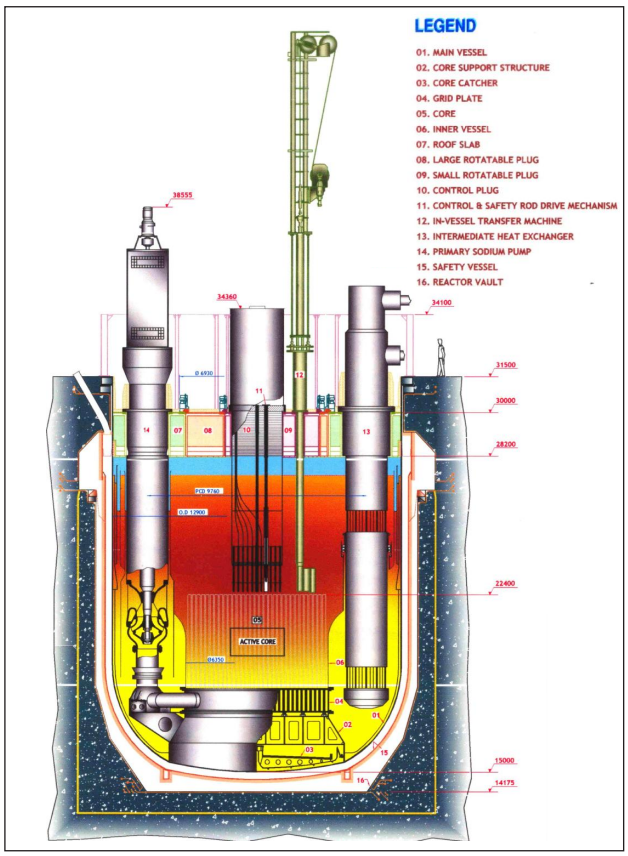

Figure 3: A sketch showing PFBR core and its internals in the reactor vessel

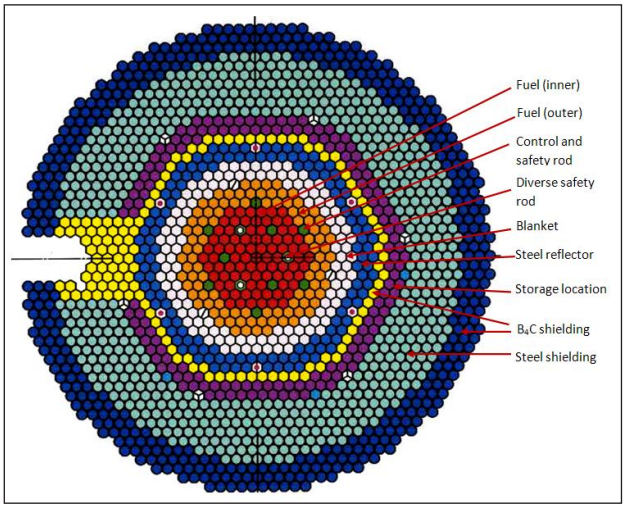

Figure 4: A sketch of PFBR core arrangement (homogeneous)

intermediate heat exchangers (IHXs). The secondary system transfers this heat to steam/water system through steam generators. Figure 3 gives a sketch of PFBR core (pool-type) and its core internals.

The first part of the core design requires the selection of materials for fuel, structural materials and coolant for the reactor system. The core size and neutron spectrum is optimized to meet the various design objectives. It requires the volume fraction of fuel, steel and coolant volume fraction inside the core. The design of sub-assemblies is very crucial for achieving the desired neutron spectrum. The fuel pin design ensures the specified linear heating for a fixed sodium flow. Neutronics computations are performed to optimize various design parameters like (a) fuel and absorber rod material enrichments, (b) core excess reactivity, (b) cycle length (c) shutdown margin, (d) temperature and power coefficients (e) burnup swing (f) fuel management, (g) breeding ratio and doubling time and (h) kinetics parameters like delayed neutron fraction, prompt neutron life time, (i) detector responses for core monitoring etc.

In a country like India, where there is a limited availability of nuclear fuel, it is desired to optimize reactors such a way that the energy extracted from the nuclear fuel is the highest (high burnup). For PFBR, maximum burnup targeted is 100 GWd/t. Higher burnup is possible with increased LHR (450 W/cm for PFBR) and longer residence time (180 effective full power days for PFBR). The limiting factor of burnup in fast reactor is the radiation damage in structural materials. To achieve higher fuel utilization, it is essential to breed more fissile fuel and re-cycle it as the fuel for the next cycle. A recent study has shown that it is possible to re-cycle plutonium up to 12 cycles

in PFBR without violating the safety parameters. A homogeneous core concept is generally used in fast reactors in which the fertile breeding material is arranged external to the core as radial and axial blankets (Figure. 4). There is also in-core breeding from the fertile material which is mixed along with the fuel. Minimum fuel inventory and maximum breeding is the design objectives of India. It is to be noted that Gen-IV objective does not account for the breeding. Since metal fuel has the higher breeding potential, India has the plan to build many metal FBRs for the future to achieve energy security. Metal FBRs have shown good inherent safety charactersagainst the possible unprotected transients [Sathiyasheela et al., 2013].

Spent fuel in any reactor has vast amount of radio-toxicity. Unless the disposal of this radio-toxicity is addressed, nuclear power program is incomplete. Nuclear waste is the combination of fission product, depleted uranium, plutonium and higher actinides etc. Radio-toxicity of fission product reduces below the specified limit by 300 years through natural radioactive decay process. But, plutonium and other minor actinides take more than 10,000 years to reduce below the natural background radioactivity. So, providing long surveillance for such radioactive waste is very difficult. On the other hand, fast reactor can be designed to run with minor actinides, depleted uranium and plutonium. In fast reactors, minor actinides are annihilated through fission (known as incineration) and long lived fission products absorb a neutron and undergo transmutation and become either more stable nuclei or short lived nuclei. Most of the minor actinides are fertile nuclei, which undergo fission in the higher energy range. So, incineration of minor actinides requires a high energy neutron, as the fission to capture ratio is more in this energy range. In addition, the transmutation requires excess of neutron. So, fast reactor is the ideal system to reduce the radio active management period through incineration and transmutation, below 300 years. However, fast reactor fuel with minor actinide reduces the safety coefficients, which should be considered during reactor optimization.

To summarize, fast reactors have the following important core characteristics:

- Smaller core size
- Larger critical mass
- Higher fuel enrichment (10-30%)
- Triangular lattice arrangement
- Thin fuel pins to provide large heat transfer area.
- High power density
- High specific power
- Liquid metal coolant
- High burnup
- High fuel and clad temperatures
- High thermodynamic efficiency (~40%)
- High breeding
- High neutron flux ($3 - 8 \times 10^{15}$ n/cm^2/s)
- High radiation damage (due to high flux and hard spectrum)
- Less reactivity control margin (low β-eff & shorter prompt neutron life time)
- Capable of multiple re-cycling of reprocessed fuel.
- Possible for minor actinide incineration.

3. Fast Reactor Safety

Since fast reactor core has higher power density, liquid metal coolant like sodium is used as the coolant. It removes large amount of heat from a small volume of core without much neutron moderation.In India, good amount of experience is gained by using liquid sodium as the coolant in FBTR. PFBR also uses liquid sodium coolant. Though there are advantages of using sodium as a coolant, there are safety concerns also with respect to core neutronics and operational point of view. Higher enrichment of fuel in fast reactor makes the situation difficult to control under accident condition due to coolant boiling and fuel melting because of the core not in most reactive configuration as in thermal reactors. In thermal reactors, if there is any change in geometrical configuration due to fuel melting or coolant boiling etc., it will change the moderator/fuel ratio and makes the reactor sub-critical. But, in fast reactors, heat transfer from the fuel without proper heat sink may lead to fuel melting. It is possible that gross melting of fuel will lead to slumping and change of reactor configuration. Slumping of fuel further accelerates the neutron production. So, higher fissile enrichment is a safety concern in fast reactors.Similarly, higher enrichment of plutonium fuel reduces effective delayed neutron fraction (β) to almost half of the thermal reactor value. This implies a lower safety margin to achieve super prompt criticality. But, it is always possible to optimize the core with more inherent safetycharacteristics with the added engineered safety features so that the reactor safety is ensured during the above mentioned

situations. In this discussion, safety of medium sized pool-type reactor similar to PFBR is addressed.

3.1 Reactor Transients

When the reactor is in the critical state, the effective multiplication factor (k_{eff}), ratio of number of neutrons produced in the present generation to the previous generation, is equal to unity. If there is any deviation from criticality, then the reactor is said to be in super critical state if $k_{eff}>1$ or in the sub- critical state if $k_{eff}< 1$. Reactivity (ρ) explains the fractional change in multiplication factor from criticality. If $\rho>0$, then the reactor is said to in super-critical and $\rho<0$, then the reactor is said to be in sub-critical. Positive/ negative reactivity may be added to the system as an operational requirement. After achieving criticalitythe reactor power is raised. When the reactor power is raised and whenthere isa balance between the heat generation and heat removal, then reactor is said to be in steady state. In case, if there is any imbalance between the heat generation and heat removal, then the reactor is said to be in transient condition. In a nuclear reactor, there can be a overpower transient (where the heat generation is more than the heat removal) or under cooling event (heat removal capacity is less than the heat generation). Unprotected over power transient makes the power to increases continuously and results in fuel melting. In a working reactor, there are inherent safety features available in the design to control the transient. In addition, there are engineered safety features to arrest the transient and accident and also to mitigate the radioactive release to the public. If the engineering safety features failed to protect the reactor against any over power transient, it is called Unprotected Transient Over Power Accidents (UTOPA). In case of under cooling event, if the flow is disrupted, it is called Unprotected Loss of Flow Accident (ULOFA), and if the coolant is not available then it is called Unprotected Loss of Coolant Accident (ULOCA). If the unprotected transients are not addressed and mitigated it may lead to coolant boiling and fuel melting. The saturation temperature of coolant is far less than melting temperature of fuel and clad material. After coolant boiling, it is possible for the fuel and clad to melt and the molten corium can form into a bubble kind of structure.

3.2 Safety Concerns of Sodium

In a fast reactor,coolant enters through the core bottom and it removes the heat which is produced in the fuel pin and comes out through the core top. Suppose if there is primary pump failure due to offsite power failure and if there is unexpected delay in starting the backup emergency power supply, then the coolant flow will start coasting down, as the primary sodium pumps are designed with flywheels. This coast-down further aids core cooling under unexpected power failure condition. Under this condition, the heat removal capacity of the reactor is less than its heat generation. This will initiate coolant boiling at the top of the core, and with time it may slowly propagate in to the core centre. When the liquid coolant is changed into vapor, it makes the fission neutrons to remain in the higher energy; otherwise it may lose some energy through scattering with liquid sodium. In fast reactor, the importance of the neutron increases as the neutron energy increasesin the core centre. With the rise in neutron energy, number of neutrons produced per neutron absorption (η) increases. So, boiling of coolant in the core centre accelerate the fission process. On the other hand, void in the periphery of the reactor allow this high energy neutron to leak out of the system, which will decelerate the fission process. The removal worth of sodium, i.e. changes in fission reaction after removing sodium from a given reactor location is positive around the core centre and negative near the periphery. This can be explained more through term 'reactivity'. Removal of sodium near the core centre gives positive reactivity feedback due to spectral hardening, and near the core periphery negative reactivity feedback due to leakage. Overall feedback due to the whole core voiding depends on the core size. Smaller the reactor size, leakage contributes more and makes the void reactivity negative and bigger the reactor size, reactivity due to spectral hardening in the core centre contributes more than the negative leakage and makes the void co-efficient positive. So, sodium boiling in a medium or a larger sized reactor gives positive reactivity, which is a safety concern.

There are studies taken up, to reduce the positive void co-efficient in future reactors. However, optimizing the fast reactor with lowsodium void co-efficient affects the neutron economy. With negative void co-efficient, if the number of neutron leaking out of the system is more, it reduces the number of neutrons available for breeding and increases the fissile requirement. So, void co-efficient optimization results in reducedbreeding and higher fuel inventory.

3.3 Issues of Fast Reactor Core Not in the Most Reactive Configuration

Higher enrichment and volume fraction of fuel in fast reactor makes the reactor not in most reactive

configuration. Under gross melting of fuel, it would slump and change the reactor configuration. Slumping of fuel further accelerates the neutron production and may take the reactor to Core Disruptive Accident (CDA). So, higher fissile enrichment is a safety concern in fast reactors. But, in a fast reactor there are inherent safety feedbacksavailable to protect the reactor against any untoward incidents, and there are also engineered safety features to enhance the safety. These aspects are discussed below:

3.3.1 Expansion Feedbacks

Important feedbacks which evolve during the transients are feedbacks due to (a) Fuel and clad axial expansion (b) Doppler Effect of U-238 capture resonances (c) Coolant expansion and (d) Core radial expansion. In fast reactors, removal worth of fuel is negative, whereas it is positive for steel and coolant. Feedbacks from fuel axial expansion and Doppler Effect give negative reactivity feedback upon rise in power (fuel temperature). Similarly, the steel and coolant expansion gives positive feedback in medium and large sized fast reactors upon rise in power as well as drop in coolant flow. Core radial expansion feedback is due to grid plate expansion and core flowering. It gives negative feedback upon rise in coolant temperature. Among the above said feedbacks, fuel axial expansion and Doppler feedbacks are prompt feedback and the other feedbacks are delayed with their time constants. Other than the above said feedback, some more feedbacks are available to protect the reactor under transients. They are the control rod drive line expansion feedback [Chenu et al, 2012, Sathiyasheela,2015] and vessel expansion feedback.

Upon rise in outlet coolant temperature, there is an expansion of control rod drive line which passes through the annular space between drive mechanism and the protective shroud tube. Expansion of drive mechanism causes apparent insertion of the control rod in to the core which results in negative reactivity. Similarly, heat transport system of the reactor is tuned to transfer the optimized heat corresponding to nominal full power. Any excess heat produced during the transient would result in increase in coolant temperature at the reactor inlet. Rise in inlet coolant temperature causes expansion of the grid plate on which the reactor sub-assemblies are loaded. Grid plate expansions allow more neutrons to leak out of the reactor, which results in negative reactivity feedback. Rise in inlet coolant temperature also causes thermal expansion of reactor vessel which is hanging from the roof slab in the downward direction. Expansions of the reactor vessel in the downward direction introduce an apparent expulsion of control rod and a positive reactivity feedback. The overall feedback based on the apparent insertion/expulsion is merely negative. When the coolant temperature rises during a transient, there is flowering of sub-assemblies. These flowerings of sub-assemblies are due to the temperature profile in the radial direction due to the power profile. So, thermal expansion of the sub-assembly is more on the side which is facing a higher temperature (core centre) than the one which is facing a lower temperature. This results in bending of subassemblies. When the sub-assembly top is not clamped and space pad locations are arranged in such a way that bending of sub-assembly leads to flowering, which results in leakage of neutron and negative reactivity feedback. As the core radial expansion is a combination of both grid plate expansion and flowering feedback, core radial expansion feedback contribution is more in the top than at the bottom.

3.3.2 Fuel Extrusion or Squirting Feedbacks

If the reactivity insertion rate is more than the feedback capacity, and if there is fuel melting, then there isa molten fuel motion within the pin from the central region to the axial periphery of the core. This pre-clad failure in pin fuel motion is called fuel squirting or extrusion. Extrusion of molten fuel introduces negative reactivity feedback and this negative reactivity feedback takes the reactor to a new steady state, or to sub-critical state. Use of annular oxide pin is expected to provide inherent shutdown mechanism during the hypothetical LMFBR accidents by providing pathway for molten fuel to be ejected from the active core region to the top and bottom blanket. This mechanism is found to be effective for higher ramp rates of a few $/s [Smith,1985]. For lower ramp rates of the order of a few cents/s, this mechanism also works if there is a central hole with a radius of 0.069 to 0.143 cm [Tentner,1985]. For PFBR,an inner central hole of radius 0.08 cm is provided. In Transient Reactor Test Facility (TREAT) experiments with a reactivity insertion rate of 5 cents/sec were conducted for fresh fuel pins and irradiated fuel pins [Pitner,1985]. Pre-failure axial molten fuel relocation was observed in fresh fuel pin (TS-1 experiment) and irradiated fuel pin (TS-2 experiment).The later PINEX series experiments also verified the concept of axial internal motion within the annular pin, representing an inherent shutdown for LMFBR during accidents[Porten, 1981]. By quoting the

results of HUT-52A experiments also, it is stated that due to high fuel temperature in the reactor fuel pins compared to an experimental pin, this mechanism is expected to be active even with low reactivity insertion rates. From the experimental results, it is interpreted that at least 15 % of the total fuel inventory from the melt region underwent 'fuel squirting' and gave a negative reactivity feedback. This extrusion feedback can take the reactor to a steady state or a sub-critical state.

3.4 Issues of Lower Delayed Neutron Fraction

Higher enrichment of plutonium fuel reduces the effective delayed neutron fraction (β_{eff}) to almost half of the thermal reactor value. This implies a lower safety margin to achieve super prompt criticality. It is a safety concern in fast reactor. But, in fast reactors, the fissile breeding is more. This implies, a reactivity swing due to burn up is small and this practically reduces the excess reactivity load. Due to that the frequency of control rod withdrawal is reduced. The excess reactivity load is more in thermal reactor for the same reason. This higher excess reactivity in thermal reactor compels the designer to go for different kind of reactivity management such as mixing the soluble poison with coolant in order to reduce the reactivity load on the control rods. So, feedback due to rise in coolant temperature gives positive reactivity due to loss of absorption through soluble poison and due to higher fuel utilization factor *f*. But, there is negative reactivity due to spectral hardening. This makes the operator to manipulate between the control rod speed and flow to maintain the stable reactor operation. But, in fast reactors, control rod withdrawal is the only mode of reactivity addition, and the reactivity co-efficients doesn't change its sign during the course of the operation. So, manipulation of control rod under transient is straight forward. This reduces the probability of manual error, while managing unprotected transients. Similarly, reactivity contribution due to the fission products such as Xe and Sm will create reactivity oscillations across the core in thermal reactors and the operator need to consider all these while fixing the power flattening. But, this is not a problem in fast reactors as their cross sections are very small in this energy range. As fast reactor is a tightly coupled core, insertion of unknown reactivity perturbation will be felt by all part of the reactor and change in temperature also happen uniformly throughout the reactor, with that perturbation can be managed by feedbacks. Thus, tightly coupled core reduces the possibility of local boiling and melting etc. All these factors, makes the control rod management easy for the operator and reduces the probability of reactor achieving super prompt criticality, makes small delayed neutron fraction is not a safety concern.

3.5 Advantages of Sodium as the Coolant

Sodium isnot onlyremovingthe heat effectively from the compact reactor core, it also remains in the liquid state over a fairly broad temperature range. Sodium exhibits the best combination of required characteristics as compared with other possible coolants, namely excellent heat transfer properties, low pumping power requirements, low system pressure requirements (one can use virtually atmospheric pressure), the ability to absorb considerable energy under emergency conditions (due to its operation well below the boiling point), a tendency to react with or dissolve (and thereby retain) many fission products that may be released into the coolant through fuel element failure, and finally, good neutronics properties(low absorption cross section). Not only that, as the core is operating closer to the ambient pressure, it makes the possibility of a loss-of-coolant accident as remote event. In a pool type fast reactor, entire reactor core such as the heat exchangers and primary pumps are immersed in a pool of liquid sodium, which makes the loss of primary coolant is an extremely unlikely event. The coolant loops are designed and placed in an elevation such that the natural convection is possible under unexpected reactor shutdown, the heat from the reactor core would be sufficient to keep the coolant circulating even if the primary cooling pumps were to fail. So, it is possible to remove the decay heat under natural circulation without fuel melting temperature. On the other hand there are unfavorable characteristics of sodium such asits chemical reactivity with air and water, its activation under irradiation, its optical opacity and its positive void co-efficient in core neutronics. But, these disadvantages are considered in practice to be outweighed by the merits of sodium as a coolant.

3.5.1 Possibility of Inherent Decay Heat Removal

When the reactor is brought to shutdown under unexpected emergency conditions, it is possible that the fission power will reduce to zero, and even the contribution of delayed neutron will die out within about half an hour. But, the contribution of decay power will persist for months and years. Main contribution of decay powerin a nuclear reactor arises from radioactive decay of fission products.

Thousands of fission products are formed during fission, and they have a wide range of half life from fraction of seconds to thousands of year. Other than that, alpha, beta, gamma radiations from the higher actinides such as U-239 and Np-239 and activation of sodium and stainless steel materials also contribute to the decay heat [Sridharan,2003]. If the decay poweris not removed, then the slow heating of core due to decay power will lead to fuel melting and coolant boiling. But, with sodium as a coolant it is possible to set up a sodium-to-air heat transfer loop, based on buoyancy induced natural circulation flow. All that it requires is a heat flow path with a proper elevation difference between heat source and heat sink. Better thermal conductivity of sodium exhibit good convective heat transfer even under low flow condition. In fast reactors, it is possible to remove the decay heat through inherent safety mechanism, under off site power failure and the unavailability of onsite emergency power supply. At the maximum, it may require a manual opening of damper to create a natural circulation flow path.

3.6. Engineered Safety Features

Other than the above said inherent safety features of fast reactors, there are several engineered safety features provided in the designto avoid the reactor goes to a state where the reactor is damaged due to core heating which leads to a threat to the public due to radioactivity release. The important engineered safety features are: (a) Core monitoring systems to detect the reactor parameters which when goes beyond the SCRAM threshold provide signals for safety action (b) Shut down system to shut the reactor down under untoward situation (c) Decay heat removal system to remove the decay heat after shut down (d) Core catcher to collect the molten corium and spread itso that the possibility of re-criticality is excluded (e) A strong vessel to withstand the shock in case of CDA and (f) Containment system to contain the radio-toxic elements by withstanding CDA and the pressure developed due to sodium fire.

3.6.1 Core Monitoring Systems

Fast reactor is designed with core monitoring systems to detect and provide signal for safety actions. The SCRAM parameters from core monitoring systems and heat transport systems are connected to the plant protection system to automatically shutdown the reactor under unexpected core behavior. Neutron detectors monitor the flux and provide signals for safety action on neutron power, period and reactivity when they cross the threshold value. To avoid spurious SCRAM, 2/3rdlogic is used while crediting the safety actions. Similarly, there are thermo couples provided to determine the coolant inlet, outlet, centre sub-assembly outlet temperatures and difference of temperature across the core. There are flow meters to determine the coolant flow, power to flow ratio etc. So, there are many SCRAM parameters available to protect the reactor. There are delayed neutron detectors placed at various locations to find out the clad rupture. Based the core monitoring signals, reactor can be brought to shutdown and decay heat may be removed when the reactor shows an unexpected behavior.

3.6.2 Reactor Shutdown System

In a typical fast reactor, shutdown mechanisms that adopt absorber rods are provided to protect the reactor against any untoward incident. The shutdown mechanisms are classified into two major categories, viz., control and safety rod mechanism and diverse safety rod mechanism. The diverse safety rods are intended to SCRAM the reactor under emergency conditions and the control and safety rods are for control and safety action. Under emergency condition, control and safety rods also used to SCRAM the reactor and bring the reactor to a safe shut down. In fact in a smaller experimental fast reactor, only one type of control rods are used to control and SCRAM the reactor. Both the shutdown mechanisms are designed in such a way that each system can independently take the reactor to safe shutdown even if one of the most efficient rods is stuck and the other control system is completely unavailable. Before the reactor achieves criticality, diverse safety rods are withdrawn to their top most positions. Criticality and full power is achieved by raising the control and safety rods based on a recommended procedure. Control rods are banked at a particular height, when the reactor reaches full power. However, there is a possibility of uncontrolled withdrawal of control rod, in case if the motor fails to stop the rod withdrawal. Then the control rod withdrawal may happen till the control rod come completely out of the reactor. This leads to Unprotected Transient Over Power Accident (UTOPA). Fuel melting and fuel pin failure is the possible consequence of this kind of transients. To avoid this, of late control rods are provided with a mechanical device known as stroke limiting deviceto reduce the probability of uncontrolled withdrawal of control rods. This will allow only limited control rod withdrawal. Similarly, under pump failure due to offsite power failure conditions, the control rods are

expected to fall under gravity. Likelihood of both systems unavailable is 10^{-6}/y. So, loss of flow and simultaneous failure of shut down system comes under Beyond Design Basis Events (BDBE).

However, IAEA has adopted "Design Extension Condition" (DEC) to further improve safety by enhancing the plant's capability to withstand accidents that are more severe than design basis accidents [IAEA, 2012]. The DEC is to provide practicable solution to prevent or mitigate some of the BDBE. In this regard to achieve DEC for some of the chosen BDBE, additional passive safety mechanisms are envisaged to strengthen the reactor safety and also to practically eliminate core melting and slumping and hence the probability of CDA. Some of the chosen passive safety mechanisms are Hydraulically Suspended Absorber Rods (HSAR) and Ultimate Shutdown Systems (USS) [Vijayashree, et al, 2015]. The HSAR is a passive system which is optimized to fall when the flow is reduced to below the prescribed value. It provides passive safety to the fast reactors under Unprotected Loss of Flow Accidents (ULOFA). However, HSAR may not be efficient in mitigating UTOPA. The lithium-6 injection system is recommended to protect the reactor against both UTOPA and ULOFA. Lithium-6 injection is kept within the fuse plug. When the outlet temperature goes above the prescribed temperature limit, fuse will melt and allows the lithium to pass through the allowed gap and bring the reactor to safe shut down. So, BDBE also addressed through HSAR and Lithium injection system. So, when an unprotected transient is not controlled through inherent safety mechanism, passive way of mitigating the events is made possible in a fast reactor.

3.6.3 Decay Heat Removal System

When the reactor parameter crosses the threshold value, then there is a SCRAM action to bring the reactor to cold shut down. The residual fission power is available for short span of time but the decay power will exist. The decay power is about 6-7% in the beginning then it drops to 1 % in about one hour. In fast reactors, there are decay heat exchangers available to transfer the decay heat with the available pony motors and with the emergency onsite power supply such as diesel generator, battery backup etc. to remove the decay heat. In case if there is off site power failure and unavailability of onsite power supply, decay heat is partially removed with the flow available due to coast down of fly wheel mounted on the pump. Then the rest of the decay heat is removed through natural circulation flow as explained earlier. In PFBR, two types of systems, viz. OGDHR and SGDHR systems, are used for decay heat removal.

3.6.4 Core Catcher

In addition to the inherent safety of fast reactors and available shut down systems to protect the reactors based on reliable SCRAM parameters, there is a possibility (Beyond design basis event) of total internal blockage (TIB) of coolant flow, where the balance of heat generation and heat removal get affected which results in fuel melting and slumping. When there is fuel slumping, it may slump into more reactive configuration as the enrichment and fuel volume fraction is more in fast reactor and there is a possibility of re-criticality. To avoid re-criticality, molten corium is spread in a tray called core catcher and the heat is removed through natural circulation.

3.6.5 Reactor Containment

There are many safety systems available in fast reactor to contain the radioactive materials and fission products such as fuel, the first barrier to hold them within the fuel matrix, clad, the second barrier to contain it, primary coolant the third barrier which holds the fission products which are released because of clad failure. Under beyond design bases accident when the above said barriers are broken, to avoid the radioactive release to the public, reactor containment is provided in the design which acts as the final barrier. Actually, in fast reactors when there is CDA due to fuel melting and slumping, the entire core will be formed like a bubble and the pressure exerted during its expansion to the surrounding sodium and the vessel results some leakage of sodium to the containment and starts burning. Containment is designed to withstand this pressure, so that radioactive release to the public is avoided. So, even in extreme case, when there is accident, the public is not exposed with radioactive release. It is contained within the containment because of this engineered safety feature.

4. Fast Reactor Stability

The stability of a nuclear reactor with respect to internal and external perturbations is to be ensured for its safe and reliable operation. The compact small size core and fast spectrum of fast reactors makes it more stable compared to thermal systems. The core is neutronically tightly coupled unlike thermal reactor which means that power disturbance at any point of core instantaneously manifests the same way at all points in core. Thus a tightly coupled fast reactor

core is more stable compared to a loosely coupled thermal core. The neutron spectrum in the fast range makes FBRs free from instabilities induced by fission product poisons (like Xe) due to its lower absorption cross section with fast neutrons. In case of BWRs the two phase flow instabilities is a serious safety concern while in fast reactor the coolant is always maintained at liquid state without any pressurization.

Reactor power depends on the system temperatures through various reactivity feedback mechanisms. Thermal inertia of fuel, clad and coolant results in a time lag between power change and temperature changes and give rise to a delayed feedback loop of reactivity. By design it is ensured that the reactivity feedback is negative for an increase in power but there is a delay time. Various methods have been applied to study the stability characteristics of FBRs, each method has its own advantages and are complementary to each other [Hetrick, 1971]. The equations governing fast reactor dynamics are nonlinear in nature because of the reactivity dependent power change and generation of reactivity feedbacks with power change. Stability analysis is carried out considering all the nonlinearities using bifurcation theory and Lyapunov second method. The stability analysis for the linearised system is done by using Nyquist criteria [Anuraj, 2015] and root locus method. The response of the system to reactivity and flow perturbations are also studied with a transient analysis code ensuring stability.

5. Conclusions

Fast reactors have attractive neutronics properties which provide higher fuel utilization with closed fuel cycle. Higher fuel burnup and breeding is possible in a fast reactor. It has the capability to incinerate and transmute long-lived minor actinides and fission products, so that environmental burden of nuclear waste and its radio-toxicity can be reduced from 1000 years to 300 years. The advantages of using sodium as the coolant are significantly higher than its disadvantages which are manageable with proper design. The inherent safety features coupled with engineered safety features allows safe and reliable operation of fast reactors under various operating conditions and also during various protected and un-protected transients. The sodium-cooled systems have been selected as one of the systems under Generation-IV International Forum(GIF) to achieve a design to provide improved safety, sustainability,non-proliferation resistance, low nuclear waste and reduced economy. In India, metal FBRs with higher breeding ratio and low doubling time is considered for the future because of its higher breeding potential and inherent safety characteristics. The advances in the FBR design with improved safety are briefly discussed.

Acknowledgement

The authors would like to acknowledge Dr. A. Riyas RND/IGCAR and Dr. G. Pandikumar RSDD/ IGCAR for the useful comments and discussions.

REFERENCES

1. Anuraj,V. L. , SrinivasanG. S. and DevanK., 'Stability Characteristics of the 500 MW Indian PFBR', Nuclear Technology and radiation protection, Vol. 30, No. 2,pp 113-123, (2015).
2. Chenu, A., Mikityuk, K., Chawla, R., Analysis of selected Phenix EOL tests withthe FAST code system—Part II: Unprotected phase of the natural convection test.Ann. Nucl. Energy 49, 191–199 (2012).
3. Chetal, S.C., et al.," a perspective on the future development of FBRs in India",Proceedings of an International Conference Fast Reactors and Related Fuel Cycles: Challenges and Opportunities FR09Kyoto, Japan, 7–11 (2009).
4. David L. Hetrick, Dynamics of Nuclear Reactors, University of Chicago press, Chicago, (1971).
5. IAEA Safety Standards Safety of Nuclear Power Plants: Design for protecting people and the environment No. SSR-2/1, International Atomic Energy Agency Vienna (2012).
6. Jacques Bouchard, "The GEN IV Roadmap: The Way Towards Sustainable Development of Nuclear Energy", International Energy Agency Workshop on Energy Technology Roadmaps Paris, May 15-16 (2008).
7. Pitner, A. L., et al, "TS-1 and TS-2 Transient Over Power Tests on FFTF Fuel" Tran. Am. Nucl. Soc. USA, Vol 5, p 351-352 (1985).
8. Porten, D. R. et al, "Internal Fuel Motion as an Inherent Shutdown Mechanism", Topical meeting on reactor safety aspects of fuel behavior, Sun Valley ID, USA, (1981).
9. Smith, D. E., "Internal Fuel motion in Annular Fuel for 50 cents and 10 cents TOP Accidents", Transaction of ANS, Vol 49, p 276 (1985).
10. Sathiyasheela,T. , Riyas, A., Sukanya R., Mohanakrishnan, P. , Chetal, S.C.," Inherent Safety Aspects of Metal fuelled FBR", Nuclear Engineering and Design, 265 1149-1158, (2013).
11. Sathiyasheela,T., Natesan,K. , Srinivasan, G. S. , Devan, K., Puthiyavinayagam, P.,Analysis of unprotected transients with control and safety rod drive mechanism expansion feedback in a medium sized oxide fuelled fast breeder reactor, Nuclear Engineering and Design, 291, 1–9 (2015).
12. Sridharan,M. S., Indira,R., and Om Pal Singh, "Total Decay Heat Estimate in PFBR", PFBR/01115/DN/1118, Rev. A (2003).
13. Tentner , A. M., and Hill, D. J. , A Mechanistic Model for the Analysis of In-Pin Fuel Relocation Under LOF and TOP conditions for SAS4A, Tran. Am. Nucl. Soc.USA, Vol 49, p 275-276 (1985).
14. Walter, A., Reynolds, A., Fast Breeder Reactors, Pergamon Press, Inc., New York(1981).
15. Vijayashree R. et al., Shutdown Systems, FBR1&2/31000/ DN/1015, Rev-B (2015).

Life Cycle Reliability and Safety Engineering
Vol.4 Issue 4(2015) 11-21

Overview of Reactor Core Level Calculation by Nodal and Finite Difference Methods

Tej Singh*, Tanay Mazumdar, Paritosh Pandey, P. V. Varde

Reactor Physics & Nuclear Engineering Section, Research Reactor Services Division, Bhabha Atomic Research Centre, Mumbai, Maharashtra, PIN-400085, India.
**Corresponding author: Email: t_singh@barc.gov.in*

Abstract

In general, reactor core parameters like reactivity, neutron flux, power etc. are calculated in two steps. In first step, neutron transport equation is solved for a lattice (usually made of a fuel assembly and associated coolant, moderator and structural material) to generate few group (2 to 5 group) homogenized cross section from multigroup cross section library (69 or 172 group). This step is known as lattice level calculation. It is followed by core level calculation (in 2nd step) in which neutron diffusion equation is solved using few group homogenized cross section (calculated in lattice level) to calculate the reactor core parameters. Nodal Expansion Method (NEM) and Finite Difference Method (FDM) are two techniques which are frequently used to carry out the core level calculation. Here we will briefly discuss about the methodology, development of computer codes, benchmarking, limitation etc. of NEM and FDM.

Keywords: *Lattice; Assembly; Node; Mesh; Homogenization*

1.0 Introduction

Reactor core consists of lots of heterogeneities in a sense that there are varieties of materials used as fuel, clad, coolant, moderator, reflector and other structural components in core. So, the reactor physics calculation of core parameters viz. reactivity, neutron flux, power etc. is not at all straightforward. In principle, neutron transport equation, which gives neutron distribution in a core as a function of space, time and angle, should be used for the reactor physics calculation in heterogeneous medium. But, considering the amount of heterogeneities involved in a typical reactor core and large number (69 or 172 group) of neutron energy group cross section data to be used in the calculation, it is impractical to solve neutron transport equation for the entire reactor core. Hence, the calculation is divided into two levels; (i) lattice level calculation and (ii) core level calculation. In lattice level calculation, reactor core is divided into a number of regions called "lattice" which contains one fuel assembly and associated coolant, moderator and structural material. For a lattice, neutron transport equation is solved using 69 or 172 group cross section data and few group (2 to 5 group) homogenized cross section data is generated. Thus, keeping reaction rate conserved, materials of fuel, clad, coolant etc. in the lattice are replaced with an equivalent material having few group homogenized cross section data set. Since, heterogeneities are removed computationally in lattice level, neutron diffusion equation is now solved for the whole reactor core using few group homogenized cross section data in core level calculation.

Several numerical methods such as Finite Difference Method (FDM) (K. L. Derstine, 1984), Nodal Method (R. D. Lawrence, 1983; R. D. Lawrence, 1986) etc. have been developed to solve the diffusion equation. In FDM, reactor core is divided into a number of meshes. Then, the diffusion equation is integrated over a mesh volume and applying Green's theorem, volume integral is converted into surface integral. Finally, the diffusion equation is discretized to obtain finite difference equation. Solution of the finite difference equation gives neutron flux in each mesh. FDM is a straightforward method to solve the diffusion equation though it invariably requires the mesh size to be equal to diffusion length of the material. Hence, large number of mesh is required in case of light water reactor and subsequently computational time becomes quite long. NEM is a suitable alternative in this regard. In this method, mesh size (here mesh is termed as "node") could be taken as large as a fuel assembly since neutron flux in each mesh is expanded in terms of suitable basis function (Polynomial, Bessel etc.). In NEM, three dimensional diffusion equation is converted into a set of three one dimensional equations by integrating the diffusion equation over two directions transverse to each coordinate axis. The set of one dimensional equations, thus obtained, is then solved to calculate node averaged neutron flux.

This paper is written in following way. In section 2.0, NEM and FDM are briefly described. The next section is dedicated to various benchmark problems available in literature and solution of the problems by various NEM and FDM based computer codes.

2.0 Methodology

2.1 Nodal Expansion Method (NEM)

Nodal expansion method (NEM) for square geometry proposed by R. D. Lawrence (R. D. Lawrence, 1986) is briefly described here. In this method, reactor is divided into a number of homogeneous, rectangular nodes within which cross sections are assumed to be constant. For k-th node ($-\Delta xk/2<x<\Delta xk/2$, $-\Delta yk/2<y<\Delta yk/2$, $-\Delta zk/2<z<\Delta zk/2$ where Δxk, Δyk and Δzk are node dimensions along x, y and z directions respectively as shown in Fig.1), 3-D, multigroup, steady state neutron diffusion equation is integrated over two transverse directions (say y and z) to obtain 1-D (say x) diffusion equation as given below.

$$\frac{d}{dx}J^k_{gx}(x)+\frac{1}{\Delta y_k}L^k_{gy}(x)+\frac{1}{\Delta z_k}L^k_{gz}(x)+\Sigma^k_{rg}\phi^k_{gx}(x) = Q^k_{gx}(x) \quad (1)$$

where $J^k_{gx}(x)$ is x directed current averaged over y and z, $L^k_{gy}(x)$ and $L^k_{gz}(x)$ are average net leakage currents along transverse directions y and z respectively, $\Sigma^k_{rg}(x)$ is g-th group removal cross section of material in k-th node, $\phi^k_{gx}(x)$ and $Q^k_{gx}(x)$ are x dependent neutron flux and source of g-th group in k-th node respectively. Now, $\phi^k_{gx}(x)$ is expanded in terms of polynomials upto fourth order as following.

$$\phi^k_{gx}(x)\approx\overline{\phi^k_g}f_0(x)+\sum_{i=1}^{4}a^k_{gxi}f_i(x) \quad (2)$$

where $\overline{\phi^k_g}$ is node averaged flux, a^k_{gxi} is expansion coefficient and $f_i(x)$ (i=0,1,…,4) is polynomial of x defined as $f_0(x)=1$, $f_1(x)=x/\Delta x_k=\xi$, $f_2(x)=3\xi^2-1/4$, $f_3(x)=\xi(\xi^2-1/4)$ and $f_4(x)=(\xi^2-1/20)(\xi^2-1/4)$. By setting $\Phi^k_{gx}(\Delta x_k/2)=\Phi^{+k}_{gx}$ and $\varphi_{gx}{}^k(-\Delta x_k/2)=\phi_{gx-}{}^k$, first two expansion coefficients a^k_{gx1} and a^k_{gx2} $a_{gx2}{}^k$ are obtained respectively as $a_{gx1}{}^k=\varphi_{gx+}{}^k-\varphi_{gx-}{}^k$ and $a_{gx2}{}^k=\Phi^k_{gx\cdot}+\varphi_{gx-}{}^k-2\varphi^k_g$. Other two expansion coefficients a^k_{gx3} and a^k_{gx4} are determined by applying Galerkin method, which is a kind of weighted residual method, with weights $f_1(x)$ and $f_2(x)$ respectively to Eq.(1). Finally, outgoing partial currents through both x-directed surfaces of k-th node are expressed in terms of these four expansion coefficients which are functions of incoming partial currents, source and its moments and leakage moments. Similar expressions are obtained for y and z directed outgoing partial currents. All these equations are clubbed together to form a single matrix equation as following.

$$\left[J^k_{g,out}\right]_{6\times1}=\left[P^k_g\right]_{6\times7}\left[Q^k_g-L^k_g\right]_{7\times1}+\left[R^k_g\right]_{6\times6}\left[J^k_{g,in}\right]_{6\times1} \quad (3)$$

where $[J^k_{g,out}]_{6x1}$ and $[J^k_{g,in}]_{6x1}$ are outgoing and incoming partial current matrix respectively, $[Q^k_g]_{7x1}$ and $[L^k_g]_{7x1}$ are source and leakage moment matrix respectively, $[P^k_g]_{6x7}$ and $[R^k_g]_{6x6}$ are matrices containing node dimension and removal cross section, diffusion coefficient of material in node. Like $\Phi^k_{gx}(x)$, transverse leakage is also expanded in terms of polynomials, but here it could be restricted upto second order (e.g. $L^k_{gy}(x) = L^k_{gy'}+ b^k_{gy1}\ f_1(x) + b^k_{gy2}\ f_2(x)$) as the accuracy achieved in calculation is insignificant with respect to computation effort involved in higher order expansion. In order to find out two expansion coefficients b^k_{gy1} and b^k_{gy2}, average leakage of two neighbouring nodes on either side are calculated for inner nodes while for boundary nodes, calculation is done for next and second next neighbor situated on the side opposite to boundary. Finally, leakage moments are expressed in terms of these coefficients. Eq.3 is solved for incoming current zero boundary condition.

In conventional core calculation, homogenization error is caused due to preservation of only reaction rate (K. S. Smith, 1986). Discontinuity factor $f_{gs}{}^k$ for s-th surface of k-th node in g-th energy group, which is the ratio of heterogeneous flux to homogeneous flux of the node, is introduced to preserve both reaction rate and surface averaged current simultaneously and thereby avoid this homogenization error. These factors are included in the relation between outgoing and incoming partial currents through one surface of a node and incoming partial current through the same surface of neighbouring node. These factors are to be calculated by some lattice code, prior to diffusion calculation.

Effective multiplication factor (k_{eff}) is calculated by doing a number of inner and outer iterations. In inner iteration, keeping fission source constant, neutron flux is calculated from partial currents which are obtained from Eq.(3) and in outer iteration, fission source (F) is updated with these flux values and k_{eff} is calculated from $k_{eff}{}^n=k_{eff}{}^{n-1}(F_n/F_{n-1})$ where n and (n-1) are present

and previous outer iterations respectively.

A computer code NEMSQR (T. Singh, T. Mazumdar, P. Pandey, 2014) is developed based on the methodology described above. Apart from reactivity and neutron flux/power, this code is capable to calculate integral kinetics parameters viz. effective delayed neutron fraction and prompt neutron lifetime (or generation time) by calculating both direct and adjoint flux. Adjoint flux calculation is same as direct flux with differences in fission and scattering source terms and in iteration process which, in adjoint case, starts from lowest energy group and proceeds towards highest energy group.

For hexagonal geometry similar recipe is given by

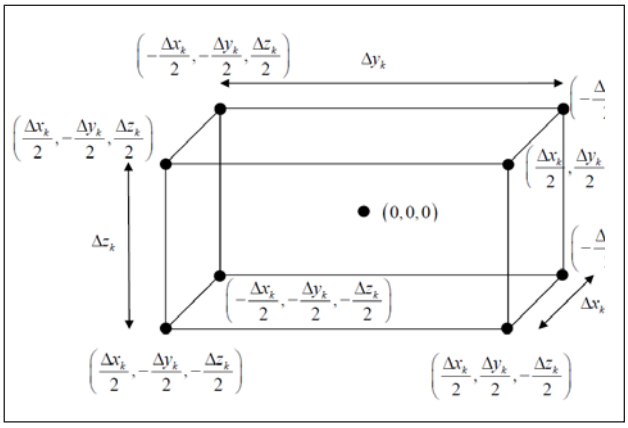

Figure 1: (0,0,0) centred k-th node of dimension Δxk×Δyk×Δzk, considered in nodal expansion method

R. D. Lawrence (R. D. Lawrence, 1983; R. D. Lawrence, 1986). A computer code NEMHEX (T. Singh, T. Mazumdar, P. Pandey, *Unpublished Manuscript*) is developed based on the methodology described in above references.

Another type of nodal method based on finite Fourier transform technique has been developed to solve the steady state, multigroup neutron diffusion equation for reactor core calculations in 2D and 3D rectangular Cartesian geometry (Singh and Sengupta, 1999). A similar method for Hex-Z geometry has also been developed (Singh and Jagannathan, 1993). In this method, the neutron source in a node is approximated by a 5 point quadratic in X-Y plane and a quadratic in axial direction. The partial currents on the surfaces of the node have been assumed to be constant and equal to their average values. The equations cast in response matrix form are solved by standard fission source iterative approach. The outer iterations are accelerated using a coarse mesh rebalancing scheme. The algorithm has been implemented in computer codes FINFOR-SQR (Square geometry) and FINFOR-HEX (Hexagonal geometry).

2.2 Finite Difference Method (FDM)

The reactor core is spatially divided into a number of discrete meshes. It is assumed that each mesh is having constant nuclear properties i.e. multi group homogenized cross sections which are available from lattice cell calculations. For the sake of simplicity, a square 2D (X-Y) core of side L is considered. Let the core be divided into n×n square meshes of side h; there will be (n+1)grid lines (including the core boundaries) with h=L/n. if the mesh point is designated to be at the centre of each mesh, the mesh point (i, j), will have coordinates xi = (i-1/2)h, y_j = (j-1/2)h and the mesh will be bounded between the lines x = xi ± h/2 and y = y_j ± h/2. Now, the diffusion equation is integrated over the mesh (i,j) and applying Green's theorem and assuming the flux and the cross sections in the mesh to be constant, one gets

$$\begin{aligned}&\frac{D_{ij}}{h^2}\left(4\phi_{ij}-\phi_{i+1,j}-\phi_{i-1,j}-\phi_{i,j+1}-\phi_{i,j-1}\right)+\Sigma_{ij}\phi_{ij}=S_{ij}\\&\Rightarrow a_{i,j-1}\phi_{i,j-1}+a_{i-1,j}\phi_{i-1,j}+a_{ij}\phi_{ij}+a_{i+1,j}\phi_{i+1,j}\\&+a_{i,j+1}\phi_{i,j+1}=S_{ij}\end{aligned} \tag{4}$$

where $a_{i,j} = 4D_{i,j}/h^2 + \sum_{ij}$ and all other a's are equal to $-D_{i,j}/h^2$. In the above equation, the group subscript g has been dropped for clarity even though the equation is valid for any energy group. For the core, appropriate boundary conditions are to be applied. For the time being it is assumed that the flux, $\phi_{i,j}$ will be zero for i,j equal to 0 or n+1. Eq.4 is the 5 point finite difference equation for mesh (i,j) linking the flux in the mesh with the fluxes in the four adjoining meshes. The right hand side is the group source in the mesh accounting for contributions from fissions in all the groups and scattering from all other groups. The diffusion equation for each group has been converted into a set of n×n simultaneous equations with n×n unknown fluxes. In matrix form, the above system of equations can be written as

$$A\Phi = S \tag{5}$$

where A is a $n^2 \times n^2$ matrix, Φ is a column vector of order n^2 and S is the source vector of order n^2.

It may be noted that similar sets of equations can be derived for 1D and 3D (X-Y-Z) cases; for 1D cases, it will be a 3-point difference equation and for 3D cases, it will be a 7-point FD equations. Further, it should be

appreciated that for purpose of illustration, a simple square core broken into meshes of equal size has been considered though the treatment is equally applicable to any convex core (including cases where triangular/ hexagonal meshes are applicable) divided into meshes of different sizes. With respect to above, the matrix elements will be different but the basic structure of the matrix will remain similar.

Iterative scheme for solution of the FD equations for the fluxes and the eigenvalue (λ) is similar to the scheme (Inner-Outer iteration) described in previous section. Without going too much into the mathematical aspects, it is noted that the matrix A has certain properties (like it is sparse, block tri-diagonal etc.) which makes the iterative approach for solving them more efficient. It should also be mentioned that the numerical approach leads to the largest eigenvalue or keff value of the system with real non-negative eigenfunctions or fluxes which are acceptable from physical considerations as far as steady state reactor behaviour is concerned.

3.0 Benchmarking of Computer Codes

3.1 Square Geometry

Three static benchmark problems are selected for square geometry. First problem is a three dimensional IAEA PWR benchmark problem. Second one is static version of a three dimensional LRA BWR kinetics benchmark problem and third one is a three dimensional LMFBR benchmark problem which is a simplified model of MARK I core design of SNR 300 prototype LMFBR. Description of the benchmark problems and their results are given below.

3.1.1 3D IAEA Two Neutron Energy Group PWR Benchmark Problem:-

The 3D IAEA PWR benchmark problem was introduced in 1971 by Micheelson and Neltrup (Micheelson and Neltrup, 1971) and later included in ANL-7416 (BSS-11, page no. 277 of ANL-7416, supplementary 2, June, 1977). In the problem, reactor core consists of 177 fuel assemblies including 108 type-I fuel assemblies (Fuel 1), 56 type-II fuel assemblies (Fuel 2), 15 rodded fuel assemblies (Fuel 2+Rod) out of which 9 are fully rodded and 4 are partially rodded fuel assemblies. The quarter symmetric core is surrounded by 64 reflector assemblies both in axial and radial directions. Reflector elements at top of the rodded assemblies (Reflector+Rod) are different from rest of the reflector elements (Reflector). All assemblies are arranged in a square lattice of pitch 20 cm. Active height of a fuel assembly is 340 cm. Thickness of both axial and radial reflector is 20 cm. Fig.2 shows horizontal and vertical cross sections of full reactor core. Two group homogenized lattice parameters of different materials of the core, used in the calculation, are given in ANL-7416. Fission spectrum is taken as 1.0 (χ1) and 0.0 (χ2). The calculation is performed for two different spatial meshes to show the dependence of mesh size on results. The coarse mesh solution (i.e. 20×20×20) uses a 20 cm spatial mesh both in radial as well as axial directions whereas the fine mesh solution (i.e. 10×10×20(10)) uses a 10 cm radial mesh and a 20 cm axial mesh except in the axial reflectors where a 10 cm axial mesh is used. In Fig.3, radial power distribution of quarter core, keff value and their relative errors, as obtained from NEMSQR for fine mesh structure, are presented along with reference value. Reference keff value and power distribution are taken from benchmark solution given by Finnemann (11-A1-3, page no. 373, ANL-7416, supplementary 2, June, 1977) for 10×10×20(10) mesh structure using nodal method based code IQSBOX where flux is expanded in each node up to fifth order. keff value for coarse mesh is 1.0296 and

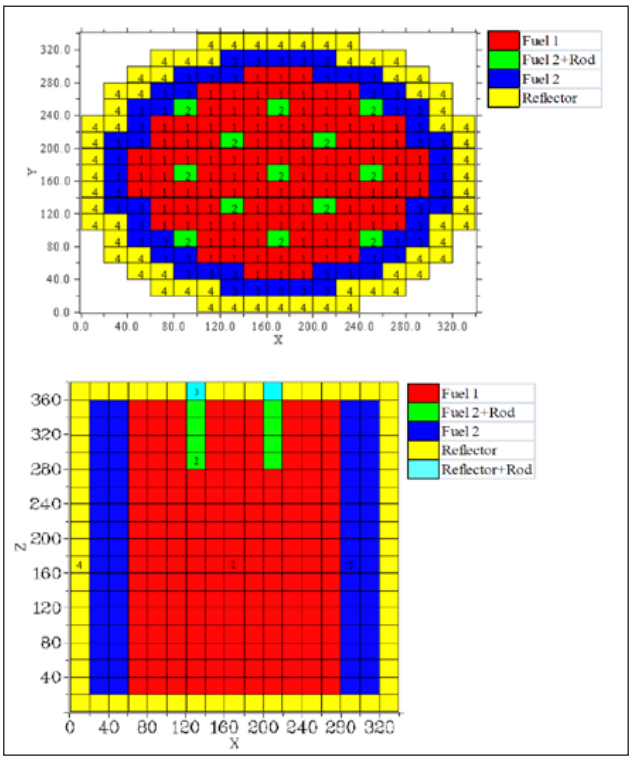

Figure 2: Horizontal (Top) and vertical (Bottom) cross sections of 3D IAEA two neutron energy group PWR benchmark core

$\lambda_{cal} \rightarrow$ 1.0293
$\lambda_{ref} \rightarrow$ 1.02904
$\varepsilon_\lambda \rightarrow$ 0.03

0.0000 0.0000 0.00	0.0000 0.0000 0.00	0.0000 0.0000 0.00	0.0000 0.0000 0.00					
0.7846 0.7730 1.50	0.7652 0.7530 1.62	0.7143 0.7070 1.03	0.0000 0.0000 0.00	0.0000 0.0000 0.00	0.0000 0.0000 0.00			
0.9664 0.9580 0.88	0.9802 0.9740 0.64	1.0073 0.9970 1.03	0.8707 0.8640 0.78	0.6148 0.6080 1.12	0.0000 0.0000 0.00	0.0000 0.0000 0.00		
0.9586 0.9540 0.48	1.0573 1.0550 0.22	1.0929 1.0880 0.45	0.9271 0.9230 0.44	0.7094 0.6990 1.49	0.5938 0.5970 0.54	0.0000 0.0000 0.00	0.0000 0.0000 0.00	
0.6058 0.6100 0.69	1.0762 1.0720 0.39	1.1852 1.1810 0.36	0.9770 0.9720 0.51	0.4733 0.4750 0.36	0.7079 0.6990 1.27	0.6091 0.6080 0.18	0.0000 0.0000 0.00	
1.1950 1.1950 0.00	1.2876 1.2920 0.34	1.3095 1.3110 0.11	1.1767 1.1790 0.20	0.9749 0.9720 0.30	0.9239 0.9230 0.10	0.8644 0.8640 0.05	0.0000 0.0000 0.00	0.0000 0.0000 0.00
1.4233 1.4230 0.02	1.4273 1.4320 0.33	1.3618 1.3690 0.53	1.3084 1.3110 0.20	1.1838 1.1810 0.24	1.0882 1.0880 0.02	1.0015 0.9970 0.45	0.7055 0.7070 0.21	0.0000 0.0000 0.00
1.2807 1.2830 0.18	1.3912 1.3980 0.49	1.4274 1.4320 0.32	1.2865 1.2910 0.35	1.0734 1.0720 0.13	1.0535 1.0550 0.14	0.9750 0.9740 0.10	0.7583 0.7530 0.70	0.0000 0.0000 0.00
0.7205 0.7290 1.17	1.2813 1.2830 0.13	1.4219 1.4230 0.08	1.1947 1.1950 0.03	0.6047 0.6100 0.87	0.9561 0.9530 0.33	0.9610 0.9580 0.31	0.7792 0.7730 0.80	0.0000 0.0000 0.00

Figure 3: Comparison of quarter core power distribution, keff value as given by NEMSQR and IQSBOX for 3D IAEA two neutron energy group PWR benchmark problem

for fine mesh is 1.0293 while the reference value is 1.02904. Therefore, accuracy of solution increases as mesh size decreases.

3.1.2 3D LRA Two Neutron Energy Group BWR Benchmark Problem:-

The 3D LRA BWR benchmark problem was introduced by Langenbuch and Werner in ANL-7416 (BSS-14, page no. 548 of ANL-7416, supplementary 2, June, 1977). Initial static part of this full core kinetics benchmark problem is considered here. BWR core of the problem consists of 312 fuel assemblies including 160 controlled fuel assemblies of type-I (Fuel 1 with rod), 36 uncontrolled fuel assemblies of type-I (Fuel 1 without rod), 112 controlled fuel assemblies of type-II (Fuel 2 with rod) and 4 controlled fuel assemblies of type-II (Fuel 2 without rod). Like 3D IAEA PWR, this

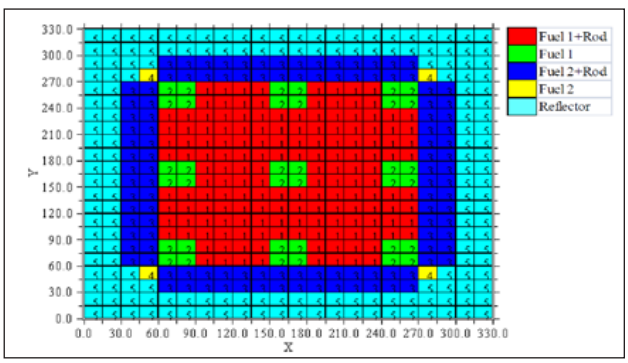

Figure 4: Horizontal cross section of 3D LRA two neutron energy group BWR benchmark core

core also has quarter symmetry and it is surrounded by 169 reflector assemblies both in axial and radial directions. Active height of a fuel assembly is 300 cm. Thickness of both axial and radial reflector is 30 cm. Horizontal cross section of full reactor core is given in Fig.4. Two group homogenized lattice parameters of different materials of the core, used in the calculation, are given in ANL-7416. Fission spectrum is taken as 1.0 ($\chi 1$) and 0.0 ($\chi 2$) and average number of neutrons released per fission (ν) is 2.43. The calculation is performed for three different spatial meshes. The coarse mesh solution (i.e. 15×15×25(15)) uses a 15 cm radial mesh and a 25 cm axial mesh except in the axial reflectors where a 15 cm axial mesh is used. The fine mesh solution (i.e. 7.5×7.5×12.5(7.5)) uses a 7.5 cm radial mesh and a 12.5 cm axial mesh except in the axial reflectors where a 7.5 cm axial mesh is used. The very fine mesh solution (i.e. 5×5×12.5(7.5)) uses a 5 cm radial mesh keeping axial mesh size same as in fine mesh. In Fig.5, radial power distribution of quarter core, keff value and their relative errors, as obtained from NEMSQR for very fine mesh structure, are presented along with reference value. Reference keff value and power distribution are taken from solution given by Zerkle (page no. 114, Phd thesis by Zerkle, 1992) for 5×5×12.5(7.5) mesh structure using nodal method based code QUAGMIRE where quartic flux expansion with quadratic transverse leakage approximation in core and flat transverse leakage

$\lambda_{cal} \rightarrow$ 0.99669
$\lambda_{ref} \rightarrow$ 0.99638
$\varepsilon_\lambda \rightarrow$ 0.03

0.9247 0.9241 0.0649	0.8682 0.8671 0.1269	0.8273 0.8267 0.0726	0.8529 0.8527 0.0235	0.9318 0.9321 0.0322	0.9699 0.9711 0.1236	0.8431 0.8457 0.3074	0.0000 0.0000 0.0000	0.0000 0.0000 0.0000
1.4839 1.4811 0.1890	1.2846 1.2811 0.2732	1.1741 1.1729 0.1023	1.2215 1.2212 0.0246	1.4220 1.4212 0.0563	1.6767 1.6787 0.1191	1.6188 1.6204 0.0987	1.3247 1.3271 0.1808	0.0000 0.0000 0.0000
1.6691 1.6606 0.5119	1.1544 1.1510 0.2954	0.9690 0.9670 0.2068	1.0234 1.0225 0.0880	1.3390 1.3391 0.0075	2.0520 2.0499 0.1024	2.1608 2.1596 0.0556	1.6189 1.6204 0.0926	0.8429 0.8457 0.3311
1.3934 1.3851 0.5992	0.9442 0.9401 0.4361	0.7856 0.7830 0.3321	0.8452 0.8436 0.1897	1.1528 1.1520 0.0694	1.8537 1.8512 0.1350	2.0517 2.0499 0.0878	1.6765 1.6787 0.1311	0.9698 0.9711 0.1339
0.7947 0.7906 0.5186	0.6756 0.6706 0.7456	0.6221 0.6184 0.5983	0.6815 0.6784 0.4570	0.8676 0.8643 0.3818	1.1526 1.1520 0.0521	1.3388 1.3391 0.0224	1.4217 1.4212 0.0352	0.9316 0.9321 0.0536
0.5157 0.5123 0.6637	0.4947 0.4907 0.8152	0.4963 0.4923 0.8125	0.5564 0.5527 0.6694	0.6814 0.6784 0.4422	0.8450 0.8436 0.1660	1.0230 1.0225 0.0489	1.2210 1.2212 0.0164	0.8526 0.8527 0.0117
0.4170 0.4134 0.8708	0.4110 0.4070 0.9828	0.4283 0.4243 0.9427	0.4963 0.4923 0.8125	0.6220 0.6184 0.5821	0.7853 0.7830 0.2937	0.9685 0.9670 0.1551	1.1736 1.1729 0.0597	0.8270 0.8267 0.0363
0.4451 0.4406 1.0213	0.4044 0.3998 1.1506	0.4110 0.4070 0.9828	0.4947 0.4907 0.8152	0.6754 0.6706 0.7158	0.9438 0.9401 0.3936	1.1539 1.1510 0.2520	1.2840 1.2811 0.2264	0.8678 0.8671 0.0807
0.6199 0.6124 1.2247	0.4452 0.4406 1.0440	0.4170 0.4134 0.8708	0.5157 0.5123 0.6637	0.7946 0.7906 0.5059	1.3930 1.3851 0.5704	1.6683 1.6606 0.4637	1.4832 1.4811 0.1418	0.9242 0.9241 0.0108

$P^f_{cal} \rightarrow$
$P^f_{ref} \rightarrow$
$\varepsilon^f_P \rightarrow$

Figure 5: Comparison of quarter core power distribution, K_{EFF} value as given by NEMSQR and QUAGMIRE for 3D LRA two neutron energy group BWR benchmark problem

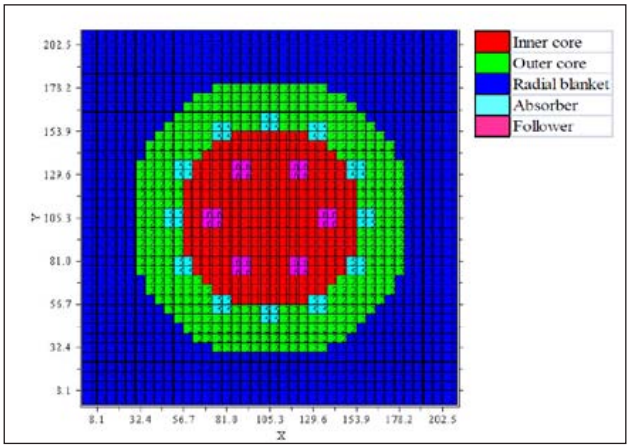

Figure 6: Horizontal cross section of 3D four neutron energy group LMFBR benchmark core

approximation in reflector is used. keff value for coarse mesh is 0.997437 which is improved quite significantly to 0.996786 for fine mesh and 0.996686 for very fine mesh where the reference value is 0.996381.

3.1.3 3D LMFBR Four Neutron Energy Group Benchmark Problem

The 3D LMFBR benchmark problem was introduced by Buckel, Kuefner and Stehle in ANL-7416 (18-A2, page no. 810 of ANL-7416, supplementary 3, December, 1985). It is a challenging problem since it involves four energy group calculation. In the problem, quarter symmetric reactor core is divided into two concentric regions; inner and outer core region. Active height of these two core regions are 95 cm each. Reactor core is surrounded by blanket regions both radially (Radial blanket region) and axially (Axial blanket region). Thickness of radial blanket is variable and ranges from 29.7 cm to 72.55 cm (approx.) while axial blanket is 40 cm thick both at top and bottom. There are several locations in core where two types of absorber assemblies are placed. Absorber region of one type of assembly is extended from core top to bottom of top axial blanket and of second type of assembly is extended from core top to an elevation of height 87.5 cm. Rest of the region below absorber is filled with follower region. Fig.6 shows horizontal cross section of full reactor core. Four group homogenized lattice parameters of different materials of the core, used in the calculation, are given in (page no.158-159, Phd thesis by Zerkle, 1992). Fission spectrum is taken as 0.768 (χ1), 0.232 (χ2), 0.0 (χ3) and 0.0 (χ4). The calculation is performed for four different mesh sizes. First one is 5.4(8.1)×5.4(8.1)×9.5(10) which implies a mesh structure of a 5.4 cm radial mesh except at the end of radial blanket where a 8.1 cm radial mesh is used and a 9.5 cm axial mesh except in the axial blanket where a 10 cm axial mesh is used (38×38×18 mesh points for full core). keff value of the problem, as obtained from NEMSQR for the mesh structure explained above, is 1.015299 whereas the reference value is 1.013746 ($\varepsilon\lambda$ = 0.15). Reference keff value is taken from solution given by Finnemann (18-A2-3, page no. 821 of ANL-7416, supplementary 3, December, 1985) for the identical mesh structure using nodal method based code NEMBOX where quartic flux expansion is used. keff value from the code QUAGMIRE is 1.013695 for the same mesh structure, which may be considered to be the reference value for this benchmark problem (page no. 117, Phd thesis by Zerkle).

Stability problem may be encountered if axial and radial mesh sizes are taken to be very different. As reported by Zerkley and in 3D LMFBR problem, if axial mesh size is more than three times of radial mesh size, then such instability will be experienced. This problem will not exist if the mesh sizes in axial and radial direction are comparable.

3.2 Hexagonal Geometry

Five static benchmark problems are selected for hexagonal geometry. First problem is a three dimensional VVER-440 benchmark problem. Second one is another VVER-440 benchmark problem which is a modified version of the first one. Third is a three dimensional LMFBR benchmark problem which is derived from triangular-z model of SNR-300 prototype LMFBR by modifying its core outer boundary. Fourth and fifth problems are related to two three dimensional VVER-1000 reactors. Description of the benchmark problems and their results are given below.

3.2.1 3D, 30° Symmetric, Two Energy Group VVER-440 Benchmark Problem

The 3D VVER-440 benchmark problem, listed as AER-FCM-001 in AER benchmark test set, was introduced by Seidel et al. (Seidel et al., 1985). In the problem, reactor core consists of 349 fuel assemblies out of which 114 are type-I fuel assemblies (Fuel 1), 126 type-II fuel assemblies (Fuel 2), 102 type-III fuel assemblies (Fuel 3) and 7 partially rodded assemblies (Control rod+Fuel 2). It is a 30° symmetric core which is reflected axially by 25 cm thick axial reflector at top and bottom of the core and radially by 72 reflector assemblies (Radial reflector). Active height of a fuel assembly is 250 cm. All assemblies are arranged in a hexagonal lattice of pitch 14.7 cm. Fig.7 shows horizontal and vertical cross sections of full reactor core respectively. Two group homogenized lattice parameters of different materials of the core, used

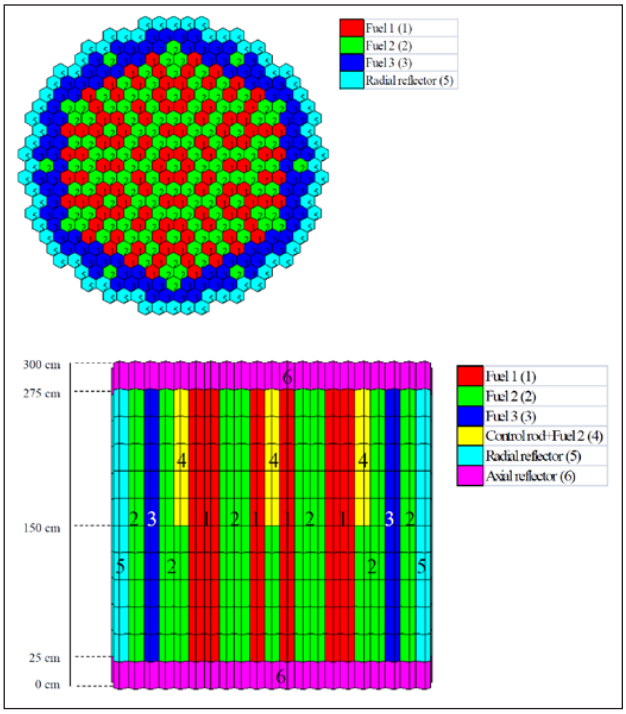

Figure 7: Horizontal (Top) and vertical (Bottom) cross section of 3D, 300 symmetric, two energy group VVER-440 benchmark core

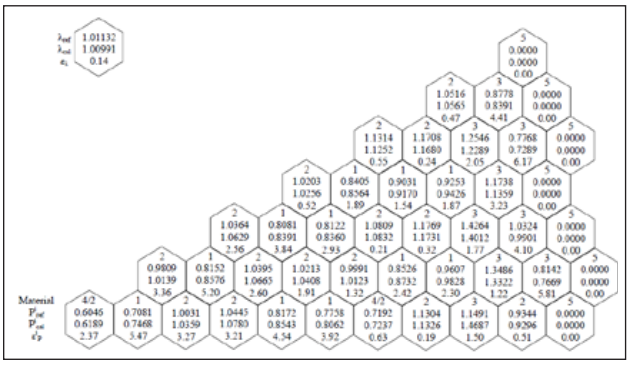

Figure 8: 1/12 th core power distribution, k_{eff} value, as given by NEMHEX, of 3D, 30^0 symmetric, two energy group VVER-440 benchmark problem and relative errors as compared to reference values given by Maráczy

in the calculation, are given in (*E-reference*: AER benchmark problem - FCM001). Fission spectrum is taken as 0.768 (χ1) and 0.232 (χ2). The calculation is performed taking radial mesh size equal to size of an assembly and axial mesh size equal to 25 cm. In Fig.8, radial power distribution of 1/12-th core, keff value and their relative errors, as obtained from NEMHEX, are presented along with reference value. Reference keff value and power distribution are taken from solution given by Maráczy (Maráczy, 1995), which is also available in (Grundmann, 1999). Relative percentage error of NEMHEX for keff value is 0.14% and maximum relative percentage error for assembly power is 6.17%.

3.2.2 3D, 180° Symmetric, Two Energy Group VVER-440 Benchmark Problem

This 3D VVER-440 benchmark problem, listed as AER-FCM-002 in AER benchmark test set, was introduced by Hegyi et al. (Hegyi et al., 1998). It has been derived from previous benchmark problem by replacing one type-II fuel assembly on the symmetry line with a partially rodded assembly. Rest of the problem remains same. Fig.9 shows horizontal cross section of full reactor core. Two group homogenized lattice parameters of different materials of the core, used in the calculation, are given in (*E-reference*: AER benchmark problem - FCM002). The calculation is performed adopting the same mesh size as taken in earlier problem. For obtaining reference solution, finite difference code DIF3D (Derstine, 1984) was used with various mesh size out of which finest mesh size was 1.212436 cm radially and 3.571429 cm axially and then the result of finest mesh was extrapolated to generate the result of zero mesh size with the help of Richardson's method (Richardson, 1911) i.e. assuming the calculated values are functions of even powers of mesh size (Maráczy, 1995). All the results are listed in Table-1. keff value of the problem, as obtained from NEMHEX, is 1.031713 whereas the reference value is 1.032487 which suggests only 0.075% relative error.

3.2.3 3D 60° Symmetric, Four Energy Group SNR-300 Benchmark Problem

This 3D SNR-300 benchmark problem was introduced by R. D. Lawrence in ANL-7416 (18-A6, page no. 871 of ANL-7416, supplementary 3, December, 1985) after modifying core outer boundary of a triangular-z model of SNR-300 prototype LMFBR (already described in section 3.1.3) so that the problem can be solved by both triangular geometry

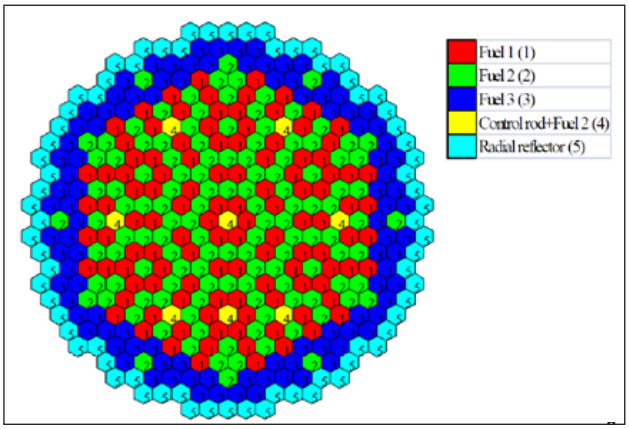

Figure 9: Horizontal cross section of 3D, 180º symmetric, two energy group VVER-440 benchmark core

Table-1: k_{eff} Value of 3D, 180° Symmetric VVER-440 Core for Different Mesh Sizes

Name of Code	Mesh Size (cm)		k_{eff} Value
	Radial	Axial	
DIF3D	2.829016	8.333333	1.031998
	2.121762	6.250000	1.032145
	1.697410	5.000000	1.032244
	1.414508	4.166667	1.032311
	1.212436	3.571429	1.032357
DIF3D (Richardson's method)	0.0	0.0	1.032487 (Ref. solution)
NEMHEX	=Assembly size	25.0	1.031713

and hexagonal geometry codes. Unlike 3D LMFBR problem, core in this problem is 60° symmetric. Rest of the core description remains same. Sidelength of a hexagonal assembly is 6.4665 cm. Fig.10 shows horizontal and vertical cross sections of full reactor core respectively. Four group homogenized lattice parameters of different materials of the core are same as used in the 3D LMFBR benchmark problem (section 3.1.3). Fission spectrum is taken as 0.768 (χ_1), 0.232 (χ_2), 0.0 (χ_3) and 0.0 (χ_4). The calculation is performed taking radial mesh size equal to size of an assembly and axial mesh size equal to 9.5 cm in active core region and 10 cm in axial reflector region. In Table-2, four group region averaged neutron flux, as obtained from NEMHEX, are presented along with reference value and their relative errors. Neutron flux is calculated by making total core power equal to 3.0 W. Reference k_{eff} value and neutron fluxes are taken from solutions submitted by R. D. Lawrence (18-A6-1 and 18-A6-2, page no. 874-879 of ANL-7416, supplementary 3, December, 1985) using finite difference code DIF3D (Extrapolated solution) and nodal method based code DIF3D(NODAL) (Lawrence, 1983; Solution with 18 axial mesh planes). Relative percentage error of NEMHEX in k_{eff} value (=1.01140) is 0.15% when compared to DIF3D results (k_{eff}=1.00989) and 0.014% when compared to DIF3D(NODAL) results (k_{eff}=1.01125). Maximum relative percentage error in neutron flux calculation is 6.23% when compared to DIF3D results and 4.23% when compared to DIF3D(NODAL) results. Though neutron flux differs more than 4-5% from benchmark value at few regions/energy groups, overall a good agreement is observed between NEMHEX results and benchmark solution.

Table-2: Comparison of Four Group Region Averaged Neutron Fluxes for 3D, 60° Symmetric SNR-300 Core

Energy group	Region	Average flux (n/cm^2/sec) by			Relative % error with respect to	
		DIF3D	DIF3D (NODAL)	NEMHEX	DIF3D	DIF3D (NODAL)
1	Inner core	4.0569×10^{6}	4.0442×10^{6}	4.1785×10^{6}	3.00	3.32
	Outer core	2.4870×10^{6}	2.5004×10^{6}	2.5834×10^{6}	3.88	3.32
	Radial blanket	3.0649×10^{5}	3.0528×10^{5}	3.1520×10^{5}	2.84	3.25
	Absorber	1.2640×10^{6}	1.2600×10^{6}	1.3017×10^{6}	2.98	3.31
	Follower	2.3688×10^{6}	2.3557×10^{6}	2.4352×10^{6}	2.80	3.37
	Axial blanket	3.6273×10^{5}	3.6266×10^{5}	3.7560×10^{5}	3.55	3.57
2	Inner core	1.9072×10^{7}	1.9039×10^{7}	1.9675×10^{7}	3.16	3.34
	Outer core	1.0594×10^{7}	1.0612×10^{7}	1.0966×10^{7}	3.51	3.34
	Radial blanket	2.2209×10^{6}	2.2421×10^{6}	2.3171×10^{6}	4.33	3.35
	Absorber	6.1898×10^{6}	6.1669×10^{6}	6.3704×10^{6}	2.92	3.30
	Follower	1.2375×10^{7}	1.2360×10^{7}	1.2786×10^{7}	3.32	3.45
	Axial blanket	3.4705×10^{6}	3.4652×10^{6}	3.6004×10^{6}	3.74	3.90
3	Inner core	1.7579×10^{6}	1.7568×10^{6}	1.8156×10^{6}	3.28	3.35
	Outer core	9.2860×10^{5}	9.2696×10^{5}	9.5798×10^{5}	3.16	3.35
	Radial blanket	3.0960×10^{5}	3.1550×10^{5}	3.2630×10^{5}	5.39	3.42
	Absorber	4.6361×10^{5}	4.5690×10^{5}	4.7088×10^{5}	1.57	3.06
	Follower	1.3897×10^{6}	1.3978×10^{6}	1.4475×10^{6}	4.16	3.56
	Axial blanket	5.2703×10^{5}	5.2667×10^{5}	5.4887×10^{5}	4.14	4.22
4	Inner core	3.2706×10^{5}	3.2758×10^{5}	3.3883×10^{5}	3.60	3.43
	Outer core	1.5343×10^{5}	1.5295×10^{5}	1.5823×10^{5}	3.13	3.45
	Radial blanket	9.0518×10^{4}	9.2870×10^{4}	9.6160×10^{4}	6.23	3.54
	Absorber	5.3702×10^{4}	5.1321×10^{4}	5.3273×10^{4}	0.80	3.80
	Follower	3.4029×10^{5}	3.4488×10^{5}	3.5651×10^{5}	4.77	3.37
	Axial blanket	1.9564×10^{5}	1.9770×10^{5}	2.0607×10^{5}	5.33	4.23

3.2.4 3D, 30° Symmetric, Two Energy Group VVER-1000 Bench-Mark Problem:-

The 3D VVER-1000 benchmark problem, listed

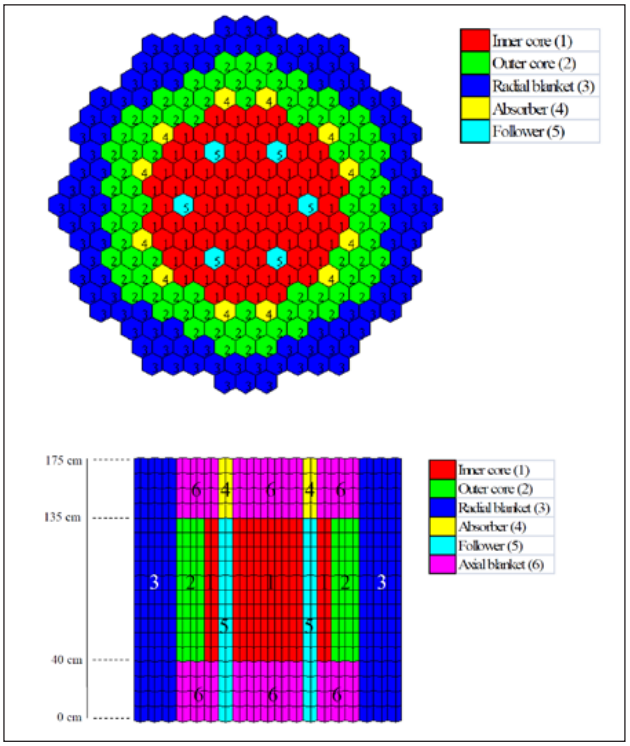

Figure 10: Horizontal (Top) and vertical (Bottom) cross section of 3D, 60º symmetric, four energy group SNR-300 benchmark core

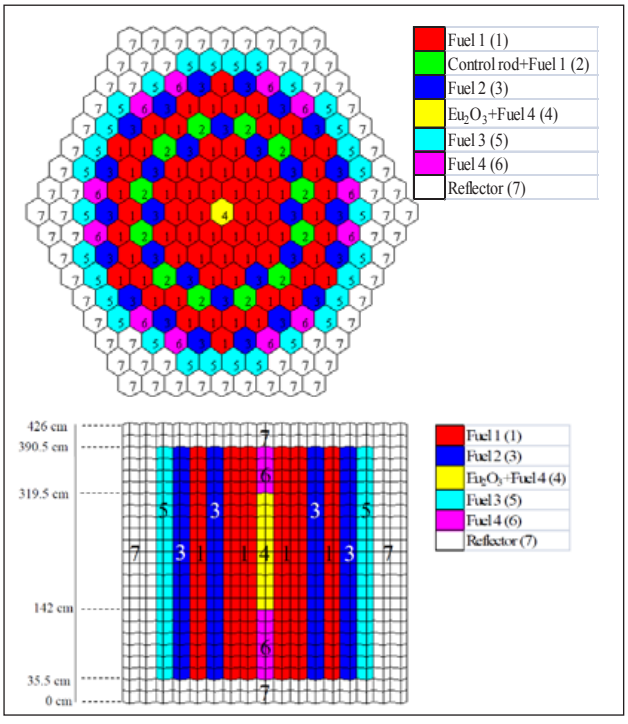

Figure 11: Horizontal (Top) and vertical (Bottom) cross section of 3D, 30º symmetric, two energy group VVER-1000 benchmark core

as AER-FCM-101 in AER benchmark test set, was introduced by Schulz (Schulz, 1996). In the problem, reactor core consists of 151 fuel assemblies out of

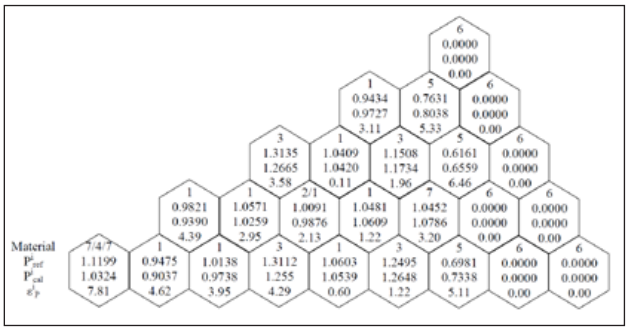

Figure 12: 1/12 th core power distribution, keff value, as given by NEMHEX, of 3D, 30º symmetric, two energy group VVER-1000 benchmark problem and relative errors as compared to reference values given by Kolev et al.

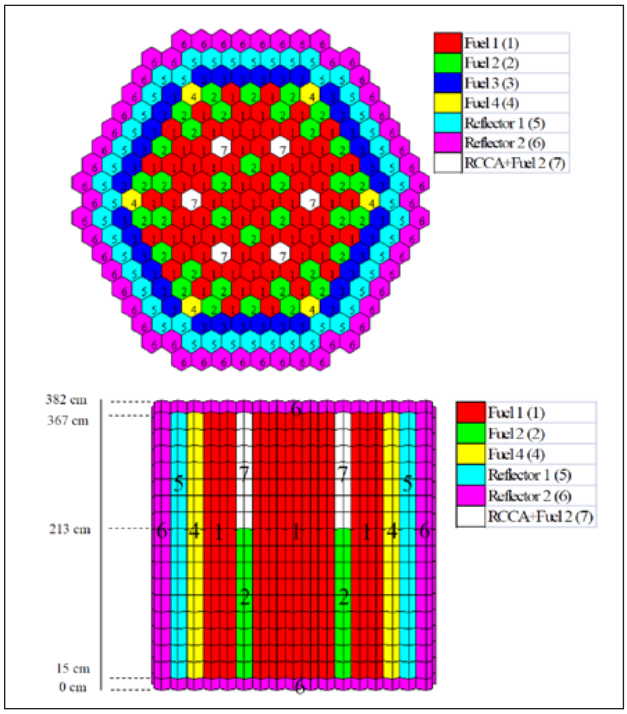

Figure 13: Horizontal (Top) and vertical (Bottom) cross section of 3D, 60º symmetric, two energy group VVER-1000 benchmark core

which 66 are type-I fuel assemblies (Fuel 1), 12 partially rodded assemblies (Control rod+Fuel 1), 30 type-II fuel assemblies (Fuel 2), 30 type-III fuel assemblies (Fuel 3), 12 type-IV fuel assemblies (Fuel 4) and 1 central assembly which consists of Eu2O3 and Fuel 4 (Eu2O3+Fuel 4). It is a 30º symmetric core which is reflected axially by 35.5 cm thick reflector at top and bottom of the core and radially by 66 reflector assemblies. Active height of a fuel assembly is 355 cm. All assemblies are arranged in a hexagonal lattice of pitch 24.1 cm. Fig.11 shows horizontal and vertical cross sections of full reactor core respectively. Two group homogenized lattice parameters of different materials of the core, used in the calculation, are given

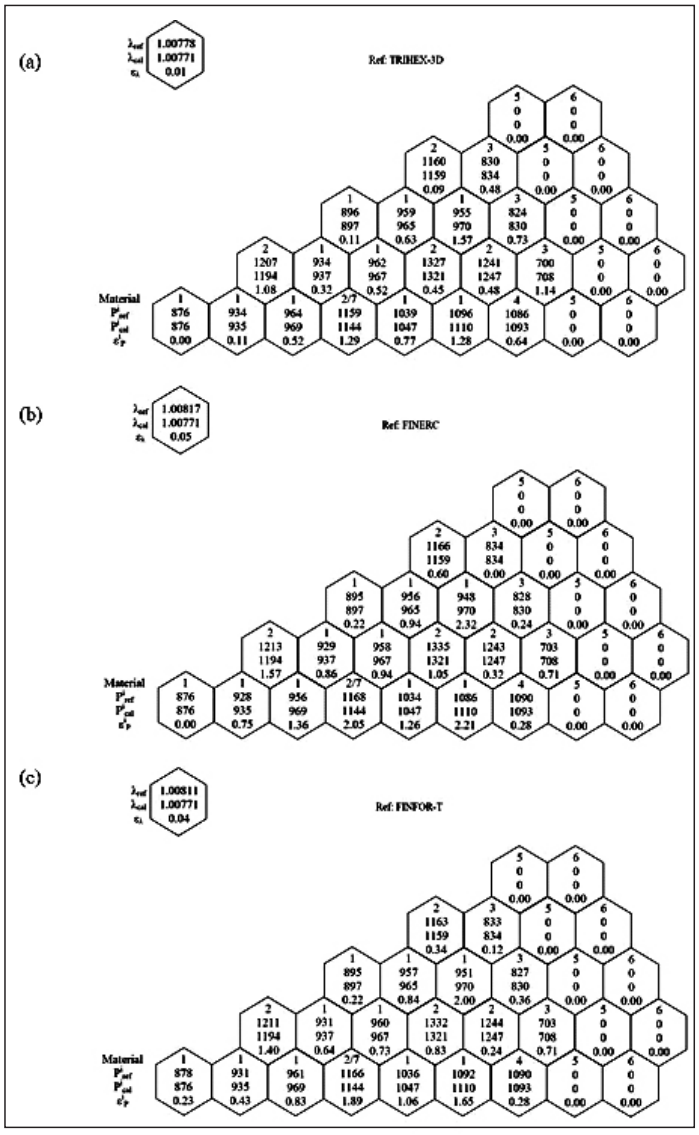

Figure 14: 1/12 th core power distribution, keff value, as given by NEMHEX, of 3D, 60° symmetric, two energy group VVER-1000 benchmark problem and relative errors as compared to reference values generated by (a) TRIHEX-3D, (b) FINERC, (c) FINFOR-T.

in (*E-reference*: AER benchmark problem – FCM101). Fission spectrum is taken as 1.0 (χ1) and 0.0 (χ2). The calculation is performed taking radial mesh size equal to size of an assembly and axial mesh size equal to 17.75 cm. In Fig.12, radial power distribution of 1/12 th core, keff value and their relative errors, as obtained from NEMHEX, are presented along with reference value. Reference keff value and power distribution are taken from solution given by (Kolev et al., 1997), which is also available in (Grundmann, 1999). Relative percentage error of NEMHEX for keff value is 0.09% and maximum relative percentage error for assembly power is 7.81%. Since bigger pitch length, as compared to VVER-440 benchmark problem, is dealt in this problem, error in power distribution is found to be slightly more.

3.2.5 3D, 60° Symmetric, Two Energy Group VVER 1000 Bench Mark Problem :-

This 3D VVER-1000 benchmark problem was formulated by Singh and Jagannathan (Singh and Jagannathan, 1993). In the problem, reactor core consists of 163 fuel assemblies out of which 79 are type-I fuel assemblies (Fuel 1), 36 type-II fuel assemblies (Fuel 3), 36 type-III fuel assemblies (Fuel 3), 6 type-IV fuel assemblies (Fuel 4) and 6 partially rodded assemblies (RCCA+Fuel 2). It is a 60° symmetric core which is reflected axially by 15 cm thick reflector (Reflector 2) at top and bottom of the core and radially by two layers of reflectors comprising of 48 Reflector 1 assemblies and 54 Reflector 2 assemblies. Active height of a fuel assembly is 352 cm. All assemblies are arranged in a hexagonal lattice of pitch 23.6 cm. Fig.13 shows horizontal and vertical cross sections of full reactor core respectively. Two group homogenized lattice parameters of different materials of the core, used in the calculation, are given in (Singh and Jagannathan, 1993). Fission spectrum is taken as 1.0 (χ1) and 0.0 (χ2). The calculation is performed taking radial mesh size equal to size of an assembly and axial mesh size equal to 22 cm in active core region and 15 cm in top and bottom reflector region. Radial power distribution (1/12 th core power distribution is given since it, upon reflection on 30° inclined edge, represents 1/6 th rotational symmetric core) and keff value, as obtained from NEMHEX, are compared with the results of three codes, viz. TRIHEX-3D (Jagannathan and Jain, 1990), FINERC (Jagannathan, 1983) and FINFOR-T (Singh and Jagannathan, 1993), available in the literature where this problem is given. TRIHEX-3D is a finite difference method based diffusion code which divides one hexagon into 6n2 number of equitriangular meshes where n is number of subdivisions per side of the hexagon. For the present problem, each hexagon was divided into 54 triangles (n=3) and 36 axial meshes were considered. FINERC is a finite element method based computer code which divides each hexagon into 6 triangles and the solution is approximated using polynomials of different order. The solution of present problem was obtained using quadratic polynomial and 18 axial meshes. In FINFOR-T, multigroup diffusion equation is solved for triangular-z geometry using finite fourier transformation. For solving present

problem, mesh structure, identical to that taken in FINERC, was adopted. In Fig.14, comparison of results between the codes is presented. Relative percentage error of NEMHEX for keff value are 0.01% (TRIHEX-3D), 0.05% (FINERC), 0.04% (FINFOR-T) and maximum relative percentage error for assembly power are 1.57% (TRIHEX-3D), 2.32% (FINERC), 2.00% (FINFOR-T).

4.0 Conclusion

It is important to note that the mesh size taken for calculation plays the key role in dictating the accuracy of calculation. In heavy water moderated reactor, FDM based code can take mesh size as large as equal to an assembly like NEM based code. But, for light water moderated reactor, mesh size cannot be taken more than 2-3 cm for FDM based code while for NEM based code, we could use assembly sized mesh by exploiting the flux expansion feature of NEM. Though reactor physics calculation is normally done in two steps, in recent years, due to the phenomenal increase in computing power, attempts have been made to develop computer codes for solving the neutron transport equation directly in full reactor core i.e. without the need for a separate lattice calculation for obtaining homogenized cross sections.

Acknowledgement

Authors would like to thank Shri R. C. Sharma, Director, Reactor Group for his constant support and encouragement to carry out computer code development work for core level calculation.

References

1. AER benchmark problems, Available online at http://aerbench.kfki.hu/aerbench/
2. Argonne Code Center, June, 1977. Benchmark Problem Book, Report ANL-7416, Suppl. 2. Argonne National Laboratory, Argonne, IL.
3. Derstine, K.L., 1984. DIF3D: a code to solve one-, two-, and three-dimensional finite-difference diffusion theory problems.[LMFBR] (No. ANL-82-64). Argonne National Lab., IL (USA).
4. Grundmann, U., 1999. New 3D nodal method HEXNEM for improving the accuracy of the hexagonal version of the code DYN3D. Institute of Safety Research, 9.
5. Hegyi, G., Makai, M., Maraczy, C., 1998. Diffusion benchmark calculations of a VVER-440 core with 180 symmetry. In Proceedings of the eighth Symposium of AER (p. 123).
6. Jagannathan, V., 1983. Evaluation of the finite-element-synthesis model using the 3-D finite-element technique. Annals of nuclear energy, 10(11), 569-578.
7. Jagannathan, V., Jain, R. P., 1990. TRIHEX-3D: A multigroup diffusion theory code for hexagonal lattice core analyses with auto-triangularisation. Bhabha Atomic Research Centre, Bombay (India).
8. Kolev, N. P., Lenain, R., Fedon-Magnaud, C., 1997. CRONOS Solutions of the AER 3D Benchmark for VVER-1000. CEA Internal Report, Saclay.
9. Lawrence, R.D., 1983. DIF3D Nodal Neutronics Option for Two-and Three-dimensional Diffusion Theory Calculations in Hexagonal Geometry. Argonne National Laboratory.
10. Lawrence, R.D., 1986. Progress in nodal methods for the solution of the neutron diffusion and transport equations. Progress in Nuclear Energy, 17(3), pp.271-301.
11. Maraczy, C., 1995. A Solution of Seidel's 3D Benchmark for VVER-440 with the DIF3D-FD Code. In Proceedings of 5th Symposium of AER (pp. 287-296).
12. Micheelson, B., Neltrup, H., 1973. The 3-D IAEA Benchmark Problem, Report RISO-M-1572.
13. National Energy Software Center, December, 1985. Benchmark Problem Book, Report ANL-7416, Suppl. 3. Argonne National Laboratory, Argonne, IL.
14. Richardson, L. F., 1911. The approximate arithmetical solution by finite differences of physical problems including differential equations, with an application to the stresses in a masonry dam. Philosophical Transactions of the Royal Society A 210 (459-470).
15. Schulz, G., 1996. Solutions of a 3D VVER-1000 Benchmark. In Proc. 6-th Symposium of AER on VVER Reactor Physics and Safety, Kirkkonummi, Finland.
16. Seidel, F., 1985. Diffusion calculations for VVER-440 2D and 3D test problem. In Proc. of the 14th Symp. of Temporary International Collective (TIC), Warsaw, Poland (Vol. 1, p. 216).
17. Singh, K., Jagannathan, V., 1993. Solution of the multigroup diffusion equation in triangular-< i> z</i> geometry using finite Fourier transformation. Annals of Nuclear Energy, 20(10), 667-677.
18. Singh, K. and Sengupta, S.N., 1999. A finite fourier transform method for three dimensional steady state reactor core calculations. Annals of Nuclear Energy, 26(6), pp.533-541.
19. Singh, T., Mazumdar, T., Pandey, P., 2014. NEMSQR: A 3-D multi group diffusion theory code based on nodal expansion method for square geometry. Annals of Nuclear Energy, 64, 230-243.
20. Singh, T., Mazumdar, T., Pandey, P. NEMHEX: A 3-D multi group diffusion theory code based on nodal expansion method for hexagonal geometry, Unpublished Manuscript.
21. Smith, K. S., 1986. Assembly homogenization techniques for light water reactor analysis. Progress in Nuclear Energy, 17(3), 303-335.
22. Zerkle, M. L., 1992. Development of a Polynomial Nodal Method with flux and current discontinuity factors, Phd thesis, Massachusetts Institute of Technology.

Life Cycle Reliability and Safety Engineering
Vol.4 Issue 4(2015) 22-28

Development of Adiabatic Doppler Feedback Model in 3D Space Time Analysis Code ARCH

D. K. Dwivedi, Anurag Gupta
Reactor Physics Design Division, Bhabha Atomic Research Centre, Mumbai, Maharashtra, PIN-400085, India
Email: ddwivedi@barc.gov.in

Abstract

Integrated 3D space-time neutron kinetics with thermal-hydraulic feedback code system is being developed for transient analysis of Compact High Temperature Reactor (CHTR) and Advanced Heavy Water Reactor (AHWR). ARCH (code for Analysis of Reactor transients in Cartesian and Hexagon geometries) has been developed with IQS module for efficient 3D space time analysis. Recently, an adiabatic Doppler (fuel temperature) feedback module has been incorporated in this ARCH-IQS version of the code. In the adiabatic model of fuel temperature feedback, the transfer of the excess heat from the fuel to the coolant during transient is neglected. The viability of Doppler feedback in ARCH-IQS with adiabatic heating has been checked with AER benchmark (Dyn002). Analyses of anticipated transient without scram (ATWS) case in CHTR as well as in AHWR have been performed with adiabatic fuel temperature feedback. The methodology and results have been presented in this paper.

Keywords: *Neutronic, Feedback, Thorium fueled Reactor, Safety, ATWS*

1. Introduction

Indian three stage reactor program envisages the generation of power from thorium to sustainable, safe and clean way of energy production [1]. The compact high temperature reactor (CHTR) is being designed as a technology demonstrator for comprehensive high temperature reactor program for hydrogen production by thermo-chemical splitting of water [2]. The 100 kWth CHTR is ^{233}U-Th fueled, BeO moderated, Pb-Bi eutectic cooled prismatic block type vertical reactor [3]. The major core design parameters of CHTR [2] in given in Table-1.The Advanced Heavy Water Reactor (AHWR) has also been designed to meet the objectives of sustainable and safe nuclear power production from thorium based fuel. The 300 MWe AHWR is LEU-Th fuelled, boiling light water-cooled and heavy water-moderated vertical pressure-tube type reactor, as one of its design variant [1]. The major core design parameters of LEU-Th fueled core of AHWR [1] are given in Table-2.

The new conceptual core design of CHTR and AHWR are in advanced stages which necessitates sophisticated safety and anticipated transient analyses. The current International trend is to perform integrated Neutronic-Thermal-hydraulic studies under larger multi-physics multi-scale framework. In view of that, a program to develop multi-physics capability has been initiated for envisaged design and safety analysis of these nuclear reactors. In this regard, a computationally efficient Improved Quasi Static (IQS) model [4] has been incorporated in the 3D space-time analysis code ARCH [5] and subsequently an adiabatic fuel temperature feedback model has been included in the IQS module. The rationale for inclusion of adiabatic fuel temperature feedback module in ARCH-IQS is that it can be considered as step further to the analysis of neutron kinetics without feedbacks. The assumption of adiabatic fuel temperature heating does not take into account the heat transfer mechanisms from the fuel to the coolant. Therefore, in the adiabatic approximation, the excess heat generated in the power excursion transient is deposited in the heat generating fuel itself.

The transient predictions of the code ARCH-IQS have been validated with well known AER benchmarks [4]. The adiabatic Doppler (fuel temperature) feedback capability of the code has been benchmarked with AER benchmark problem (Dyn002) for VVER-440 [6, 7]. The adiabatic feedback scheme has also been adopted in ARCH-IQS for the analyses of anticipated transient without scram (ATWS) scenario in hexagon latticed core of CHTR as well as square latticed core of AHWR. For the transient analyses of CHTR and AHWR with fuel temperature feedback, the variation of condensed few-group (i.e. > 2 group) homogenized cross-sections data with fuel temperature was found impractical to be defined by a single mathematical

relation. Therefore, an approach of linear interpolation of multi-group parameters with change in fuel temperature distribution during transient has been considered for CHTR and AHWR [8]. A set of multi-group cross-section data at various fuel temperature points is generated at small temperature intervals (i.e. 50 °C) by lattice simulation transport theory code ITRAN [9]. For Doppler feedback, the values of multi-group cell homogenized cross-sections/ parameters at instantaneous fuel temperature are predicted with linear interpolation of respective parameters (at preceding and following temperature points) provided as input data-set in code ARCH-IQS. The objectives of the present work is the validation of ARCH-IQS for a rod ejection accident with a simple Doppler feedback mechanism which is the most important feedback mechanism and its use for simulation of postulated ATWS case in CHTR and AHWR. The ATWS case in CHTR has been carried out by ARCH-IQS with adiabatic fuel temperature feedback and the results have been compared with point kinetics model [10]. The ATWS case in LEU fuelled core of AHWR with adiabatic Doppler feedback has also been simulated and presented in this paper.

Table 1: Major Core Design Parameters of CHTR

Reactor power	100 kWth
Core configuration	prismatic block type vertical
Fuel	^{233}U-Th based TRISO fuel
Fissile (^{233}U) content in the heavy metal	33.75%
Core life cycle	15 effective full power years
Core burnup	68000 MWd/t of heavy metal
Moderator	BeO
Reflector	BeO and graphite
Coolant	LBE (44.5% Pb + 55.5% Bi)
Coolant inlet/outlet temperature	900 °C/ 1000 °C
Core diameter	1.27 m
Core height	1.0 m
Power regulation	12 control rods in outer coolant channel
Primary SDS	6 shut-off rods
Secondary shutdown system	12 axial movable BeO blocks

Table 2: Major Core Design Parameters of LEU-Th Fueled AHWR

Reactor power	920 MWth, 300 MWe
Avg. fissile content	4.21% in $LEUO_2$-ThO_2 fuel
Core configuration	pressure tube type vertical
Coolant	Boiling light water
Moderator	Heavy water
Total coolant channels	444
Lattice pitch	225 mm (square pitch)
No. of pins in fuel cluster	54
Average discharge burnup	64,000 MWd/t
Active fuel length	3.5 m
Primary shut down system	45 shut off rods
Secondary shut down system	Liquid poison injection in moderator
No. of control rods	24 :ARs-8, RRs-8, SRs -8
Passive Poison Injection	Poison injection through a passive valve actuated by steam pressure
Doppler coefficient	-2.82 x 10^{-5}(k/°K)

2. Adiabatic Fuel Temperature Feedback Model

The adiabatic fuel heating assumes no transfer of the excess heat generated in the fuel during transient. Therefore, this model does not require a detailed thermal-hydraulic calculation to be performed in the neutron kinetic code. The change in the fuel mesh temperature during transient in adiabatic model is considered as follow [8],

$$M_f\, C_f\, \frac{dT_f}{dt} = \gamma_p N(t) - \gamma_p N(0) \qquad (1)$$

where, M_f is the mass of the fuel in the mesh, C_f is specific heat, T_f is mesh temperature, $\gamma_p N(t)$ is the power being produced in the fuel mesh at time 't'. The eqn. (1) has been solved with fully implicit method for every spatial mesh independently. No excess heat is considered to be transferred from the fuel meshes during transient.

Due to changes in fuel temperature of the meshes during transient, the variation of cross-section parameters for reactivity feedback is treated differently for hexagon lattice based core VVER-440 in AER benchmark [6] and in CHTR & AHWR, as discussed ahead.

2.1 Adiabatic Fuel Temperature Feedback Model for AER Benchmark

For AER benchmark problem (Dyn-002) [6, 7], the adiabatic feedback is described by the following dependence for the fission cross section of the second neutron energy group on fuel temperature,

$$\Sigma_{f,2}^{n}(t) = \Sigma_{f,2}^{n,0}(t)\left[1 + \gamma\left(\sqrt{T_f^n(t)} - \sqrt{T_{f,0}}\right)\right] \quad \ldots (2)$$

with $T_f(0) = 260°C$ & $T_f(0) = 260°C$ & $\gamma = -7.228 \times 10^{-4}\ (°C)^{-\frac{1}{2}}$. $\Sigma_{f,2}^{n,0}$ is the fission cross section of the thermal energy group for mesh number 'n' and provided as inputs. It is assumed that the value of the Doppler constant γ and the reference temperature $T_{f,0}$ is independent from the type of fuel. The instantaneous fuel temperature $T_f(t)$ in each mesh containing fuel has been calculated from eqs.(1) and for fuel temperature feedback, The second-group fission cross-section, $\Sigma_{f,2}^{n}(t)$ are updated according to eqn. (2).

2.2 Adiabatic Fuel Temperature Feedback Model for CHTR and AHWR

For adiabatic fuel temperature feedback of reactivity for the design analysis of reactor i.e. CHTR and AHWR, the variation in multi-group parameters due to change in temperature has been tackled by following interpolation scheme [5]:

$$\Sigma_g^{n,m}(t+\Delta t) = \Sigma_g^{n,m}(t) + \frac{[\Sigma_g^m(i+1) - \Sigma_g^m(i)]}{[T_f^m(i+1) - T_f^m(i)]} \times [[T_f(t+\Delta t') - T_f^m(i)] \quad \ldots\ldots (3)$$

where $\Sigma_g^{n,m}$ is the cross-section/parameter for 'g' energy group, 'm' type of fuel material present in the 'n' index of the mesh, when fuel mesh temperature is $T_f(t)$ at time the moment 't'. In the interpolation process, $\Sigma_g^m(i)$ is input cross-section/parameter at $T_f^m(i)$ fuel temperature, which is generated input data-set through lattice simulation, 'm' is the index for number of cross-section data point provided in the input for given material 'm'. It is suggested to prepare data-set library for the whole range of transient fuel temperature at small intervals to have more points in the range of temperature variation for better predictions. In the case of data-set generated at small temperature intervals, the present scheme of linear interpolation for the instantaneous value of multi-group cross-section data for reactivity feedback would be admissible for any reactor transient and could result similar predictions as in case of AER benchmark case.

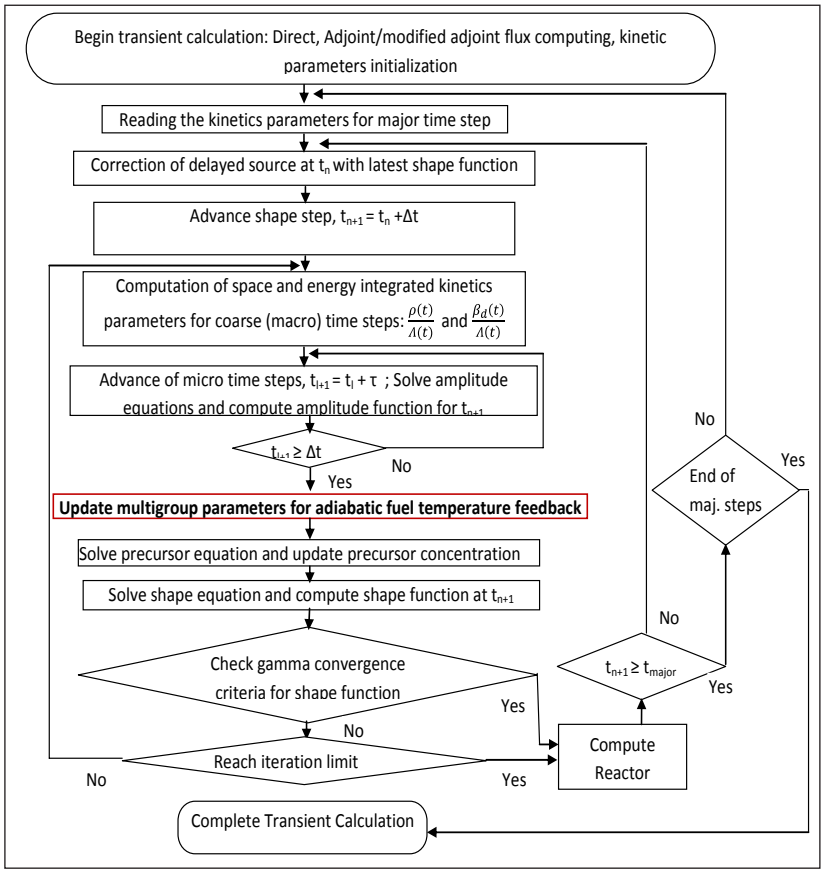

The flow diagram of IQS module in ARCH with adiabatic feedback module is given in Figure 1.

3. Results and Analyses

3.1 Validation of ARCH-IQS with AER Benchmark

The AER benchmark (Dyn001) analysis with IQS module in ARCH has been qualified to check the viability of the code for 3D space time analysis without feedback [4]. The adiabatic fuel temperature feedback module in ARCH-IQS has also been validated with AER benchmark (Dyn002) [6]. The rising power is arrested by fuel In the AER-Dyn002, the transient is initiated by the ejection of the eccentric rod (reactivity worth of 2$) in 0.16 s at hot zero power.

The control rod removal speed is taken 12.5 m/s. The initial reactor power is 1.375 kW. The feedback mechanism is based on the adiabatic increase of fuel temperature from the initial value of 260 °C. The rising power is arrested by fuel temperature feedback only. The transient is

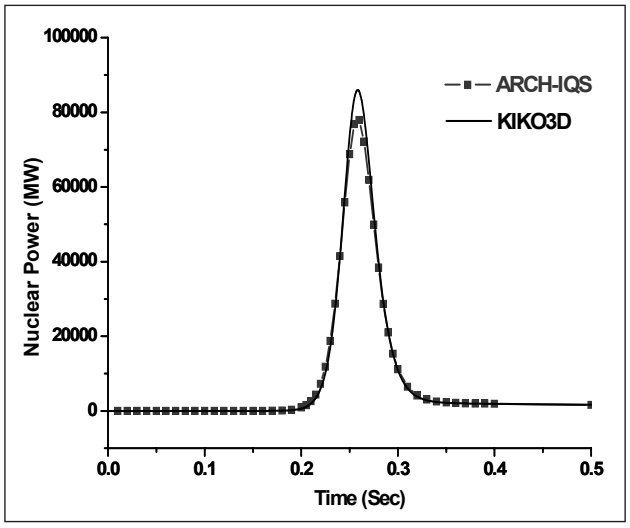

Figure 2: Nuclear Power variation with time in AER-Dyn002

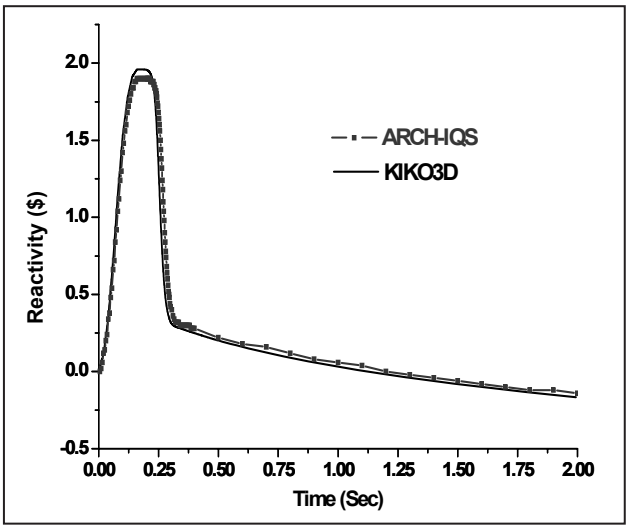

Figure 5: Core reactivity variation with time in AER-Dyn002

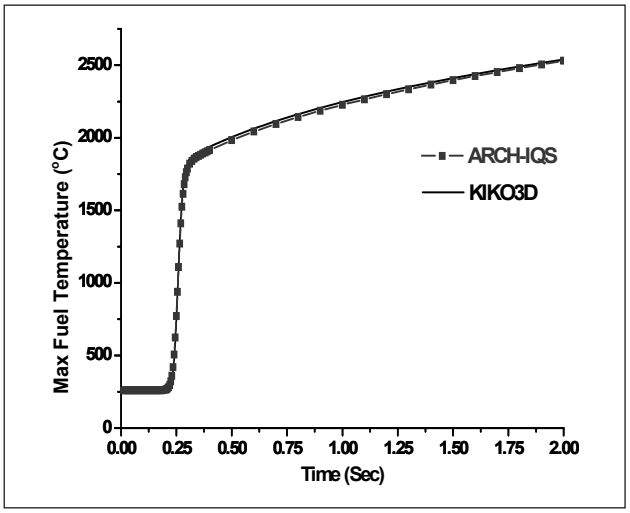

Figure 3: Maximum fuel temperature variation with time in AER-Dyn002

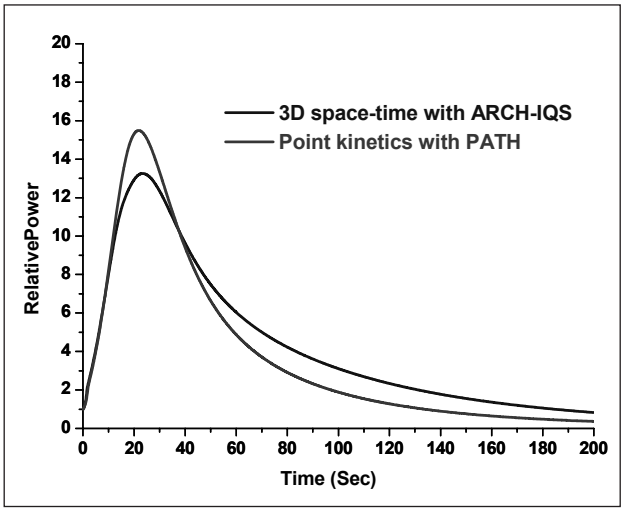

Figure 6: Variation of relative power with time in case of ATWS in CHTR

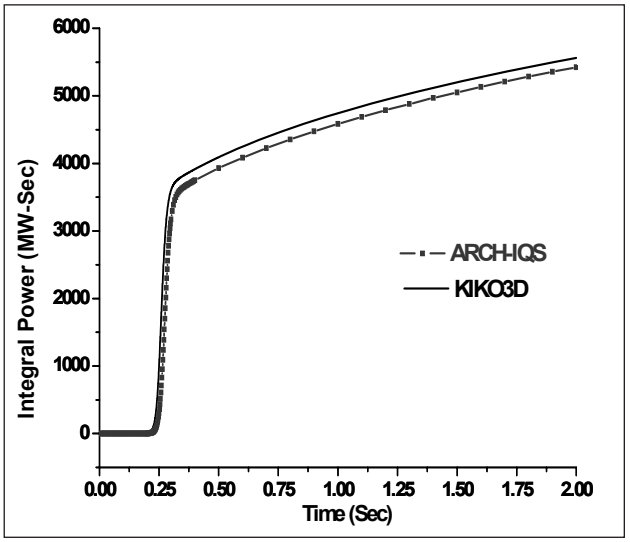

Figure 4: Integral power variation with time in AER-Dyn002

simulated up to t = 2 s. The results of ARCH-IQS (Fig.2-5) shown are be found to be in good agreement with the KIKO3D results [6].

3.2 ATWS Analysis During Core Start-Up of CHTR

3D space time analysis of ATWS case in CHTR has been carried out with Doppler feedback of reactivity from adiabatic rise of fuel temperature. In ATWS case, inadvertent withdrawal of single control rod in critical configuration of CHTR core at the reactor startup condition has been simulated. During start-up of reactor, core temperature is assumed to be 200 °C. After the ejection of control rod of 3.52 mk reactivity within 1.5 sec (with a positive insertion rate of 25 cents/sec), transient was followed up to 200 sec. It is seen that the power rise in the core was arrested by Doppler feedback due to adiabatic heating of

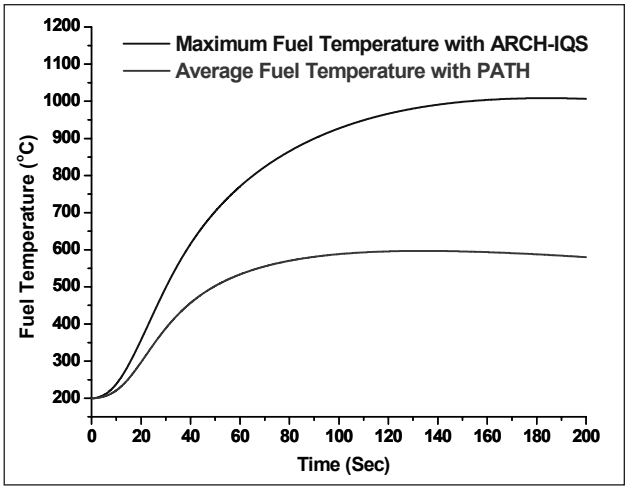

Figure 7: Maximum fuel temperature variation with time in case of ATWS in CHTR

the fuel (Fig.6). The fuel temperature coefficient in start-up core temperature condition of CHTR was computed as -1.58×10^{-5}/ °C. This case of anticipated transient without scram was also compared with point kinetics simulation. The variation of maximum fuel temperature predicted by ARCH-IQS which considers power peaking effect in the core, has been compared in Fig.7 with average fuel temperature predicted with point kinetics code PATH [10].

3.3 ATWS Analysis in Hot Zero Power Condition of AHWR

The AHWR-LEU core consists of total 69 reactivity devices comprising of 45 shut off rods (SORs) as part

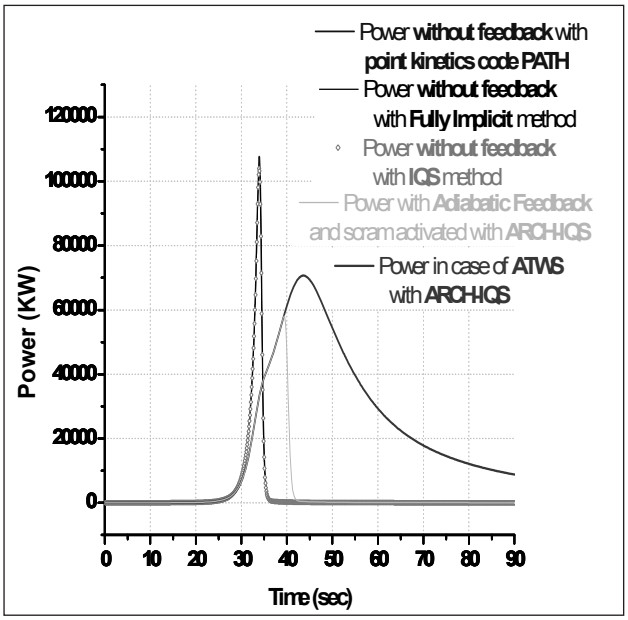

Figure 8: Power variation during transient with and without feedback in AHWR

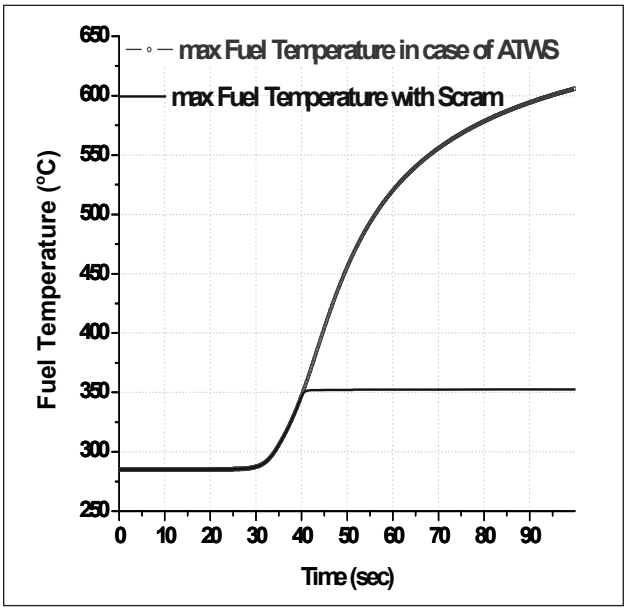

Figure 9: Variation of fuel temperature with and without scram in case of LORA in AHWR

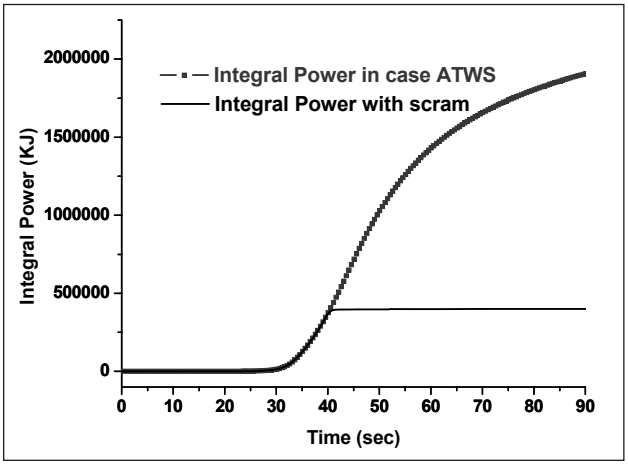

Fig 10: Variation of 'time integral power (in KJ)' with and without scram

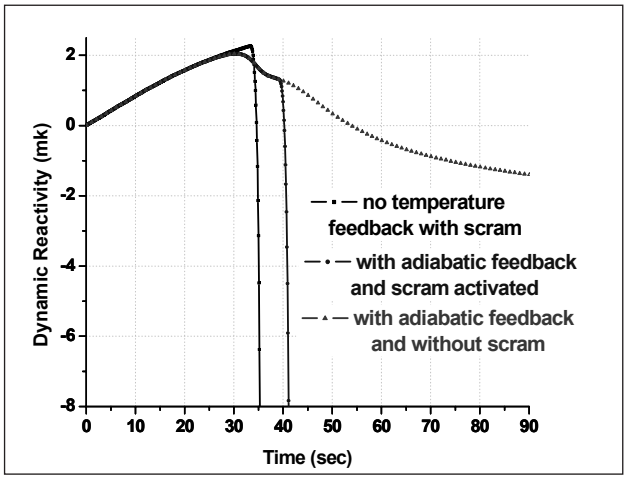

Figure 11: Variation of Dynamic reactivity of the core in case of with and without scram

of primary shut down system and 24 rods as a part of the Reactor Regulating System (RRS). The 24 rods of RRS system are divided into three types Absorbers Rods (ARs), Regulating Rods (RRs) and Shim Rods (SRs) to meet the reactor regulation requirements and they are uniformly distributed as 2 rods of each type per quadrant of the core. In normal operating configuration, the 8 ARs are fully IN, the 8 SRs are fully OUT and 8 RRs are at about 67% IN [11].The reactivity transient in case of loss of regulation accident (LORA), the uncontrolled withdrawal of reactivity devices could occur. The 3D space time analysis of LORA case (i.e. withdrawal of RRs of bank1 at speed of 2.6 cm/sec) in critical configuration of equilibrium LEU fuelled core of AHWR has been carried out with code ARCH-IQS. The initial nuclear power is considered to be at 9.2 KW (which is 10^{-5} times of the full operating power) and average fuel temperature is taken 285 ^{o}C. Due to ejection of regulating rods, positive reactivity being inserted in the core and power starts to rise. During the transient, as the power rise reaches over 55.2 MW (which is 6% of the full operating power), primary shut down system is activated (at an estimated insertion speed of 100.0 cm/sec) with 500 ms of time delay. This case has been simulated without temperature feedback with various simulation methods and has also been investigated for the scenario of Anticipated Transient Without Scram (ATWS) i.e. where the power rise in the core was arrested with Doppler feedback due to adiabatic fuel heating (Fig.8). The simulation of transient with adiabatic fuel temperature feedback shows that when scram is activated, maximum fuel temperature is reaching up to 350 ^{o}C, whereas in ATWS scenario, the maximum fuel temperature keeps on rising to quench the positive reactivity inserted in the core and stabilises at around 600 ^{o}C (Fig. 9). In adiabatic approximation in the simulation, the excess heat deposited in the fuel of the core during transient has also been estimated (Fig. 10). The net dynamic reactivity in the core with different postulated condition in simulation during transient is shown in Fig. 11.

Conclusion

The safety analyses of new advanced reactors require multi-physics multi-scale modeling. As a part of development of advanced code system, Doppler feedback capability has been incorporated in the 3-D space time analysis code ARCH and a new version of ARCH-IQS has been developed with adiabatic model of fuel heating. The use of the code with adiabatic Doppler (fuel temperature) feedback has been checked with AER benchmark (Dyn002). The results of ARCH-IQS are found to be in very good agreement with KIKO3D.

For the anticipated transient analysis with adiabatic fuel temperature feedback, the variation of few-group homogenized cross section parameters with transient fuel temperature has been incorporated with linear interpolation scheme in ARCH-IQS. Inadvertent withdrawal of single control rod (i.e. ATWS) in CHTR has been simulated in start-up critical core configuration with Doppler feedback. The variation of power and fuel temperature with 3D space time kinetics code ARCH-IQS have been compared with point kinetics code PATH. The maximum fuel temperature in the core in case of 3D space time analysis with ARCH-IQS, accounts the power peaking effect in CHTR. The postulated ATWS scenario in AHWR-LEU core has also been simulated with ARCH-IQS with adiabatic fuel temperature feedback. The comparison of ATWS in AHWR-LEU core has been carried out with different case of scram and feedbacks considered in the simulations. The capability of Doppler feedback in ARCH-IQS is with adiabatic fuel heating considers no transfer of excess heat deposited in the fuel during transient. The development of model of heat transfer from fuel to coolant through conduction with simple hydraulic model for the design and safety analyses of nuclear systems are under considerations and is going to be reported in coming future.

Acknowledgement

We express our acknowledgement to Dr. P.D. Krishnani, ex-Head RPDD, BARC. We are sincerely thankful to Dr. Umasankari Kannan, RPDD, BARC, for her critical review and remarks. We are very grateful to Dr. H.P. Gupta, Raja Ramanna Fellow, ThPD, BARC, for fruitful discussion and suggestions. The authors are sincerely thankful to Shri Amod K Mallick and Shri Indrajeet Singh, RPDD, BARC for providing details of AHWR-LEU core for simulation.

References:

1. Kumar Sinha, "Advanced Nuclear Reactor Systems – An Indian Perspective", Energy Procedia 7 (2011) 34–50, 2011
2. I.V. Dulera, R.K. Sinha, "High temperature reactors", *Journal of Nuclear Materials, vol. 383, 183–188, 2008*
3. D. K. Dwivedi, Anurag Gupta, P. D. Krishnani, "Challenges in core reactivity management and control optimization in

physics design of Compact High Temperature Reactor", *BARC Newsletter, 317, Nov. - Dec. 2010*

4. D. K. Dwivedi, Anurag Gupta, A.K. Srivastava and P. D. Krishnani, "Incorporation of Improved Quasi Static (IQS) scheme module in 3-D space-time analysis code ARCH", *ARP 2013 – Advance in Reactor Physics: Simulation Techniques and Analysis Methodologies, Anushakti Nagar, Mumbai, India, October 23-25, 2013*
5. Anurag Gupta, "ARCH: A 3D space time analysis code in Cartesian and Hexagon geometries", *NSRP-19, Mamallapuram, TN, 12-15, Dec. 2012*
6. http://aerbench.kfki.hu/aerbench/Dyn002.pdf, http://aerbench.kfki.hu/aerbench/dyn002_solaeki.txt, http://aerbench.kfki.hu/aerbench/ dyn002_solaeki.doc
7. Obadurrahman K. et al., 'Development and Validation of Coupled Dynamics Code 'TRIKIN' for VVER Reactors', *Nuc. Eng. and Tech., vol.42(3), 2010*
8. G. Kamelander, "RETRANS – A PROGRAM FOR CALCULATING REACTIVITY TRANSIENTS", *Computer Physics Communications 39, 105 – 125, 1986*
9. Krishnani P.D., "CLUB-A multi-group integral transport theory code for analysis of cluster lattices", *Ann. nucl. Energy, 9, p.255, 1982*
10. D. K. Dwivedi, Anurag Gupta and P. D. Krishnani, "PATH: A computational code for Point kinetics Analysis with lumped Thermal-Hydraulic feedback", *RPDD\HTR\57\ March 2014*
11. Indrajeet Singh et. al., "Reactivity Initiated Transient Analysis of Equilibrium AHWR-LEU Core with 3D Space Time Kinetics Code ARCH", *RPDD\AHWR\293 \4-May\2015*.

Life Cycle Reliability and Safety Engineering
Vol.4 Issue 4(2015) 29-36

Worth Measurement of Reactivity Devices Using Inverse Kinetics Method

Pandey Paritosh, Singh Tej*, Varde P.V.
RRSD, BARC, Mumbai, India
** Corresponding author: E-mail: t_singh@barc.gov.in*

Abstract:

There are different techniques to measure reactivity like dynamic and inverse kinetics. In the dynamic technique stable reactor period is measured and reactivity is determined from the in-hour formula but this is more accurate for positive reactor period only. In the inverse kinetics method, the variation in neutron density with time is used to determine the precursor concentration, $c_i(t)$ with time. The computation of $c_i(t)$ can be undertaken in two different ways. (i) $c_i(t)$ is computed in terms of n(t) by directly solving the differential equation of $c_i(t)$ (ii) direct integration of the differential equation assuming linear variation of $c_i(t)$. The process begins by assuming a functional form of the neutron concentration variation between two successive time intervals. This leads to an approximate estimate of the precursor concentration and thus the reactivity at the current time. The inverse kinetics method can be applied to obtain reactivity worth of any reactivity device using critical or subcritical method. In the critical method i.e. rod drop method, reactor is initially maintained in the steady and critical state, while in the subcritical method, the reactor is initially maintained in the steady and subcritical state. Care must be taken while using the method in low reactor power regime and subcritical regime where the contribution from source term becomes important. In the paper, different cases have been discussed wherein standard methods have been applied to measure reactivity of shut off rods under different conditions, bringing out the importance of the source term, wherever it arises.

Key words: Inverse point kinetics, shut off rod worth, source term

1.0 Introduction

Determination of reactivity worth of reactivity devices like shut off rods (SORs) is important aspect of operation of a nuclear reactor. There are different techniques to measure the reactivity of nuclear reactor like static, dynamic and kinetic [1]. In static technique, the reactivity change is balanced by known equivalent reactivity change so that reactor is maintained in the critical state at the same operating power. In the dynamic technique, the reactivity change is introduced, resulting in the change in reactor power. The measurement of stable reactor period in this case will give information about the inserted reactivity. The reactivity worth can also be estimated using inverse point kinetics with recorded power profile with time when initially the reactor is in equilibrium and is in: i) subcritical state, ii) critical state (as in rod drop method).

The inverse kinetics procedure discussed here is based on methodology as given in [1] and [2]. The method can be used as a tool in calibration of control rods devices in the reactor. The inverse kinetic method offers direct indication of the worth of the control devices under any operating condition, and hence can be utilized for calibration of the reactivity control devices.

The point kinetics equations tell us about how neutron population (or reactor power) varies with time when reactivity changes are induced in the core:

$$\frac{dn}{dt} = \frac{(\rho - \beta)n}{\Lambda} + \sum_i \lambda_i c_i + S \tag{1}$$

$$\frac{dc_i}{dt} = \frac{\beta_i n}{\Lambda} - \lambda_i c_i \tag{2}$$

where, the terms used in eq-1 and eq-2 are as follows; n(t) is time dependent neutron density, ρ is time dependent reactivity, β_i is delayed neutron fraction of i^{th} group, β is total delayed neutron fraction, c_i is neutron precursor concentration of i^{th} group, λ_i is decay constant of precursor group i, S is independent neutron source term and Λ is prompt neutron generation time.

The above equations can be rearranged to solve for reactivity. There are standard methods for solving above equations numerically for reactivity. Knowing that reactor power is measured as discrete variable, in the solution method, above equations are combined into one, solved for reactivity ρ assuming some functional form of neutron density between two successive time intervals.

There are instances like low power critical operation regime and subcritical operation regime where explicit mention of source term becomes a necessity. Often the value of source term is not known. Different methodology exists to estimate reactivity as well as the source term under these conditions. For example, [3] describes a method to estimate reactivity and source term valid for subcritical measurement of reactivity using inverse point kinetics. Reference [4] describes a method to determine reactivity worth of shut off rods (SORs) using rod drop method under low power operation where effect of source term cannot be neglected.

We describe each of the above methods in brief and show our calculation where we used the above mentioned methodologies under appropriate conditions.

2.0 Numerical Solution of Inverse Point Kinetics Equations

Eq-1 and 2 can be rearranged as:

$$\frac{\rho(t)}{\beta} = 1 + \frac{\Lambda}{\beta}\frac{1}{n}\left(\frac{dn}{dt} - \sum_i \lambda_i c_i - S\right) \tag{3}$$

$$c_i(t) = \int_{-\infty}^{t} \frac{n}{\Lambda}\beta_i e^{-\lambda_i(t-\tau)}d\tau \tag{4}$$

Where, in deriving eq-4, eq-2 was integrated upto present time t.

Eq-2 can also be written as

$$c_i(t) = c_i(0)e^{-\lambda_i t} + \int_0^t \frac{\beta_i}{\Lambda} n(\tau) e^{-\lambda_i(t-\tau)}d\tau \tag{5}$$

where $c_i(0)$ is precursor concentration at time t=0.

Further, precursor concentration at an later time instance t+Δ can be related to that at previous time t:

$$c_i(t+\Delta) = e^{-\lambda_i\Delta}\left[c_i(t) + \int_0^{\Delta} \frac{\beta_i}{\Lambda} n(\tau+t) e^{-\lambda_i(-\tau)}d\tau\right] \tag{6}$$

In one approach, integral in above eq-6, denoted by I, is solved using different neutron density variations:[2]. Here, expression for reactivity is determined assuming change in neutron flux in time interval t to t+Δ as: i) exponential, ii) linear, iii) function depending on linear and exponential terms:

$$n(t+\tau) = n(t)e^{\alpha\tau}$$

$$n(t+\tau) = n(t)(1+a\tau)$$

$$n(t+\tau)e^{\lambda_i\tau} = n(t)(1+b\tau)$$

The parameters α, a and b can be determined by using the neutron concentration value at time t and t+Δ. Further, if it is assumed that there is linear variation in precursor concentration in the time interval t to t+Δ, along with the assumed form of neutron concentration variation as given in (i) and (ii) above, [2] gives two additional expressions of reactivity.

The method proposed in [1] is briefly discussed below. Eq-3 and 4 can be combined as

$$\frac{\rho}{\beta} = 1 + \frac{l}{\beta kn}\left[\frac{dn}{dt} - \beta\sum_i \frac{\beta_i}{\beta}\lambda_i \int_{-\infty}^{t} k\frac{n}{l}e^{-\lambda_i(t-\tau)}d\tau - S\right] \tag{7}$$

Where l is prompt neutron lifetime related to neutron generation time, Λ and k_{eff}, k as:

$$\Lambda = \frac{l}{k}$$

Eq-7 permits determination of instantaneous reactivity from the knowledge of the reactor power history. Reactor power is measured at discrete time interval. Eq-7 is converted into a discrete expression that can be solved by numerical techniques. Measured reactor power can be related to an integral of neutron absorption rate over a short time interval:

$$P(m) = A\int_{(m-1)\Delta t}^{m\Delta t} \frac{n}{l}\mathrm{d}\tau \approx \mathrm{A}\frac{n(t)}{l}\Delta\mathrm{t} \tag{8}$$

Where, P(m) is power at time t=mΔt, m is discrete time interval index and A is a proportionality constant.

The derivative term dn/dt can be approximated as

$$\frac{dn}{dt} = \frac{n(t+\Delta t)\text{-}n(t)}{\Delta t}$$
$$\approx \frac{l}{A\Delta t}\left[\frac{P(m+1)-P(m)}{\Delta t}\right] \tag{9}$$

The functional form of neutron concentration between successive time interval Δt can be taken as linear. Going through the details as in [1], the expression of reactivity can be readily derived. The final expression of reactivity is given below, where m is current time index (starting from j=0, i.e. steady state; to j=m, current time), P(m) is reactor power at current time.

$$\frac{\rho(m)}{\beta} = 1 + \frac{\left[\frac{l}{\beta\Delta t}\{P(m+1)-P(m)\} - \sum_i \frac{\beta_i}{\beta}\left\{A + \sum_{j=1}^{m} k(j)(B+C)e^{-\lambda_i(m-j)\Delta t}\right\} - \frac{S}{\beta}\right]}{k(m)P(m)}$$

where (10)

$$A = k(0)P(0)e^{-\lambda_i m\Delta t}$$

$$B = P(j)\left(1-e^{-\lambda_i\Delta t}\right)$$

$$C = \frac{P(j+1)-P(j)}{\Delta t}\left(\Delta t - \frac{1-e^{-\lambda_i\Delta t}}{\lambda_i}\right)$$

3.0 Calculation Methodology for Reactivity Worth Measurement From Critical State in Presence of Source

Calculation of reactivity from inverse kinetics requires estimation of the source term. But, if the reactor is operating at high power, we can use the method just discussed, with contribution from source term neglected. At low power, however, proper estimation of source term is necessary to get correct value of reactivity. We were particularly interested in estimation of shut off rods reactivity worth at low power. If the source term is unknown, we proceed using the method developed in [4].

Once full worth of the shut off rods, ρ_d is realized, its relationship with constant source term is given by:

$$\rho_d = \rho_j - \Lambda S / n_j \quad (11)$$

Here, ρ_j is reactivity calculated from inverse point kinetics with source term taken as zero, and n_j is reactor power or equivalent.

Above equation is linear in form. To estimate ρ_d, least squares approximation for ρ_j and n_j can be made. This method for determining the post-scram reactivity is called Least Squares Inverse Kinetics Method (LSIKM). Eq-11 can be rearranged to get different fitting models. In total 4 models were used as given in Table-1.

Table-1: Fitting Models

Case	Fitting Model
1	$\rho_j = \Lambda S / n_j + \rho_d$
2	$1/n_j = \rho_j / \Lambda S - \rho_d / \Lambda S$
3	$n_j = \rho_j n_j / \rho_d - \Lambda S / \rho_d$
4	$\rho_j n_j = \rho_d n_j + \Lambda S$

4.0 Calculation Methodology of Subcritical Method

As described in [3], the standard point kinetics equation in presence of source is used; since low power measurement was involved. For a subcritical reactor at constant power P, the reactivity ρ is given by

$$\rho = -\frac{\Lambda S}{P} \quad (12)$$

Here S is the source strength.

When the reactivity device (say SOR) is brought inside the core, the power changes (see illustrative Fig-1). The reactivity after the insertion of SOR can be written as

$$\rho(t) = \beta - \frac{g(t)}{P(t)} - \frac{\Lambda S}{P(t)} \quad (13)$$

Where g is a function proportional to total decay rate of precursor concentration, which inturn depends on the reactor power history. Thus g is obtained from observed power history. Plot of g v/s P (power) will be linear after the reactivity insertion is realized. From the slope of the resulting line on g-P plane, the reactivity inserted can be obtained.

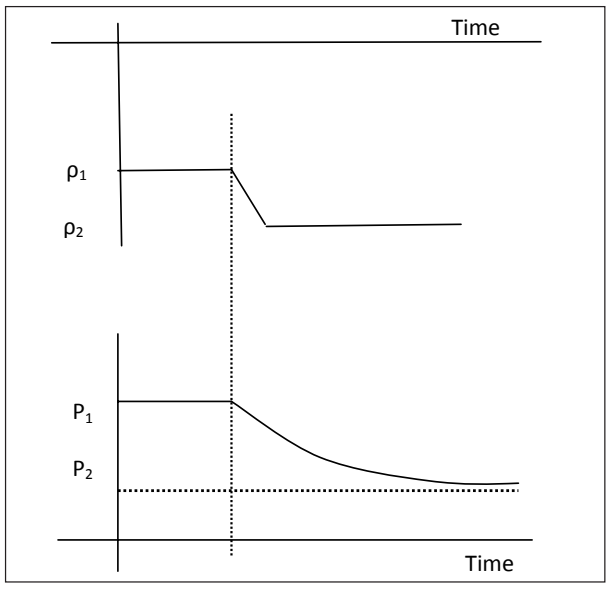

Figure 1: Schematic of change in reactor power with insertion of negative reactivity in subcritical reactor

5.0 Reactivity Worth Calculation In Different Conditions

A Fortran 90 based computer code IK based on inverse point kinetic method was developed and

validated. Here, we give some application of above mentioned methods.

5.1 Total Reactivity Worth Measurement of all SORs for Dhruva Reactor

Dhruva is a heavy water cooled, moderated and reflected, 100 MW_{th} research reactor fuelled with natural uranium [5]. The shutdown system is comprised of 9 shutoff rods with cadmium as absorbing material. Experiment for reactivity worth measurement of nine shut off rods with adjuster rod fully in was carried out. The reactor was initially made critical at low power (LP) with adjuster rod down. Fast recorder with scan time of 1 msec was connected to record log power signal from log rate safety channel A, linear power signal of Campbell channel A and MRDC channel (multi range DC channel). Recording was started and reactor was scrammed. It may be noted that dump override switch was actuated to trip the reactor without moderator dumping. From the recorded power v/s time profile, using the inverse kinetics equations, the reactivity worth is readily obtained. Fig-2 shows the reactor power profile as a function of time before and after manual scram from LP. Here, the reactor was scrammed from steady state and the precursor concentration (including 6 group delayed neutron and 8 group photoneutron) correspond to their steady state value. Moreover, the steady state power at LP was about 450 KW (from log rate safety channel), which is large enough to neglect the source term to determine the reactivity worth of all SORs. Fig-3 shows the reactivity worth profile of shut off rods as obtained by inverse point kinetics technique.

It can be seen from the figure that worth of nine shut off rods is about 120 mk.

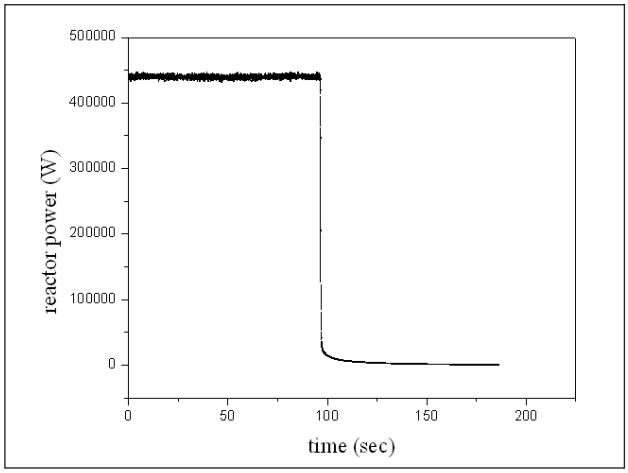

Figure 2: Reactor power profile when reactor was scrammed from LP

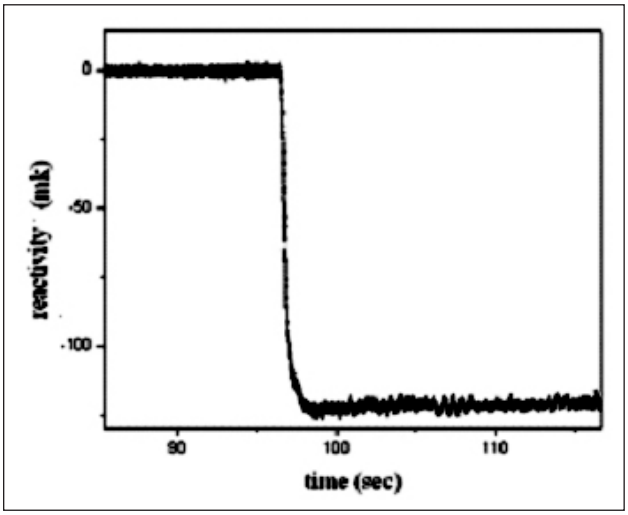

Figure 3: Reactivity v/s time profile of nine SORs with time

5.2 Total Reactivity Worth Measurement of all SORs for Critical Facility (CF)

The Critical Facility has been designed to facilitate study of three types of cores using heavy water as moderator and reflector [6]. The three cores are based on different fuel types. Among them, the reference core consists of 19-pin natural uranium metal fuel cluster. The rated power of the reactor is 100 W. The fast shutdown of the reactor (reference core) on a trip signal is achieved by gravity fall of the set of six cadmium shut off rods into the core. After the reactor trip is initiated the shut off rod completes 90% of the total travel in less than 1.5 sec. The remaining 10% drop is damped and the total time taken for the 100 % drop is about 6 sec. To estimate the reactivity worth of SORs, Reactor was tripped on manual scram. The power variations with time during reactor trip at 100 Watt for 6 shut off rod were measured using the fast recorder system. The reactivity worth of 6 shutoff

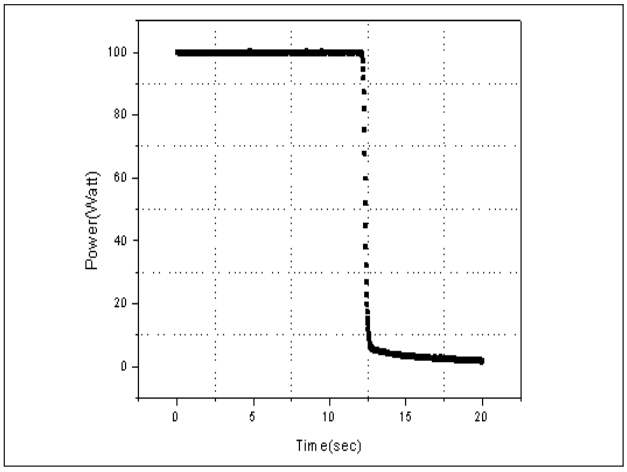

Figure 4: Power profile for 6 SOR (sampling time 20 ms)

rods was estimated using the inverse kinetic method.. The worth computed using inverse kinetic method was about 105 mk. The measured power profile for 6 shut off rods during tripping is shown in Fig-4 and reactivity worth profile for it is shown in Fig-5.

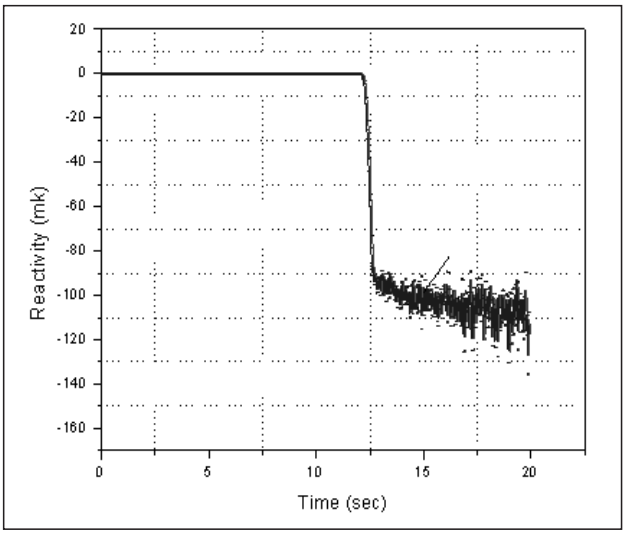

Figure 5: Reactivity profile for 6 SOR (sampling time 20 ms)

5.3 Total Reactivity Worth Measurement of All SORs for Cirus Reactor.

Cirus reactor is 40 MW research reactor that operated upto 2010. The reactor has been since permanently shutdown. In Cirus, the fast shutdown of the reactor on a trip signal was achieved by gravity fall of a set of a six boron carbide shut off rod into the reactor vessel.

For the reactivity worth measurement of all SORs following may be noted. After the reactor trip is initiated, the shut off rods drop completely into reactor vessel in less than 2 sec. Normally on a reactor trip, control and dump valves open within 2 sec and the moderator level in the reactor vessel drops to dump level within 3 minutes but in this case VOT (valve over-ride time which defeat dumping trip circuit) was actuated to lock the heavy water in the reactor vessel and reactor was tripped only by shut off rods.

Fast recorder was connected to Average log power channel and Multi Range Recorder (MRR) to measure power variation with time during the falling of Shut off rods. The recording frequency of fast recorder was 100 milli seconds. The reactor was tripped at LP (324 KW) for checking the total worth of SORs. The changes in Multi Range Recorder (MRR) power with time due to insertion of all six SORs as recorded by the fast recorder is given in Fig-6.

The estimated reactivity worth of six shut off rods from inverse kinetic method is about 54 mk which is shown in Fig-7. The measured value of 54 mk meets the requirement of Clause 5.1.1 of Technical Specifications for Cirus which states that the total worth of all SORs shall not be less than 50 mk.

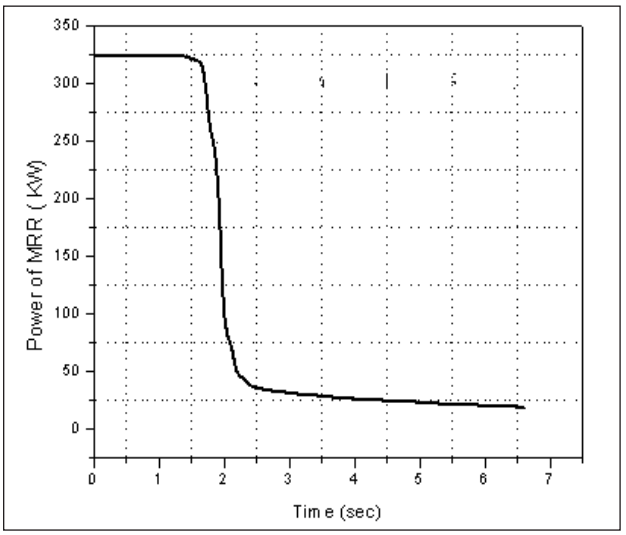

Figure 6: Change in MRR power with time as recorded by fast recorder

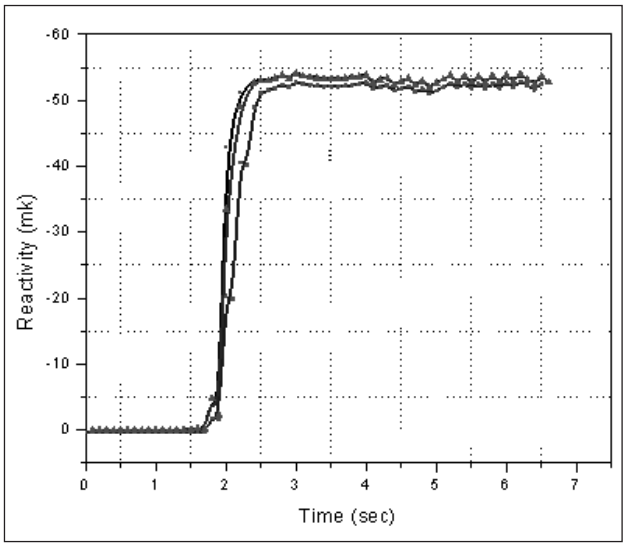

Figure 7: The estimated reactivity worth of six shut off rods from inverse point kinetics method

5.4 Total reactivity Worth Measurement of All SORs for Dhruva Reactor when Photoneutron Concentration is Not in Steady State

Here, as an initial condition, reactor was operating at LP, but the photoneutron had not reached the steady state value corresponding to LP. Thus for reactivity worth measurement, method as given in section 3.0 was used. As an initial condition, the photoneutron concentration too was assumed to

be in steady state along with the delayed neutron precursor concentration. Hence it is assumed that extra photoneutron concentration (over and above its steady state value at LP) is absorbed in the source term.

Initially the reactivity was calculated using the inverse point kinetics method considering the source term to be zero. Fig-8 shows the power profile when the reactor was scrammed from LP. Thereafter, the fitting models given in Table-1 were used to obtain the reactivity worth, ρ_d, of the shut off rods. Results are given in Table-2. Calculated reactivity worth of shut off rods was closest to the true value of -120 mk from the second model.

Table-2: Reactivity Worth of Shut-off Rods From Different Fitting Models

Fitting model no.	Reactivity, ρ_d (mk)	Source, ΛS (W)
1	-104.7	1077
2	-110.0	1230
3	-103.5	1040
4	-101.6	983

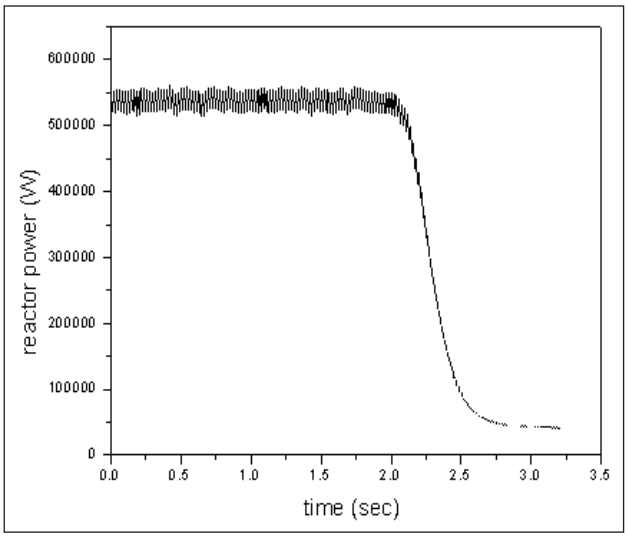

Figure 8: Reactor power profile when reactor was scrammed from LP

5.5 Reactivity Worth Measurement of a SOR for Dhruva Reactor from Subcritical Method

The measurement of reactivity worth of individual shut off rod was done with adjuster rod placed i) fully out and ii) fully in. The two SOR was selected for this, which lie nearest to the adjuster rod position. The reactivity worth of these two SORs (call it SOR#1 and #3) will be affected most by the movement of the adjuster rod. Measurement for reactivity worth of SOR#1 and 3 was carried out using subcritical count method. In this method, reactor is initially held in subcritical state at constant power. The reactivity device is introduced in the core, thereby; reactor goes further subcritical resulting in the lowering of the reactor power. Using the recorded power profile, before and after lowering of reactivity device, the reactivity worth was estimated. For the measurement of the power, fast recorder with scan time of 1 msec was connected to record log power signal from log rate safety channel A, linear power signal of Campbell channel A and MRDC channel. Due procedure was followed for the measurement.

Fig-9 shows the reactor power profile as recorded from the log rate safety channel for the condition i) adjuster rod up and SOR#1 brought inside the core,

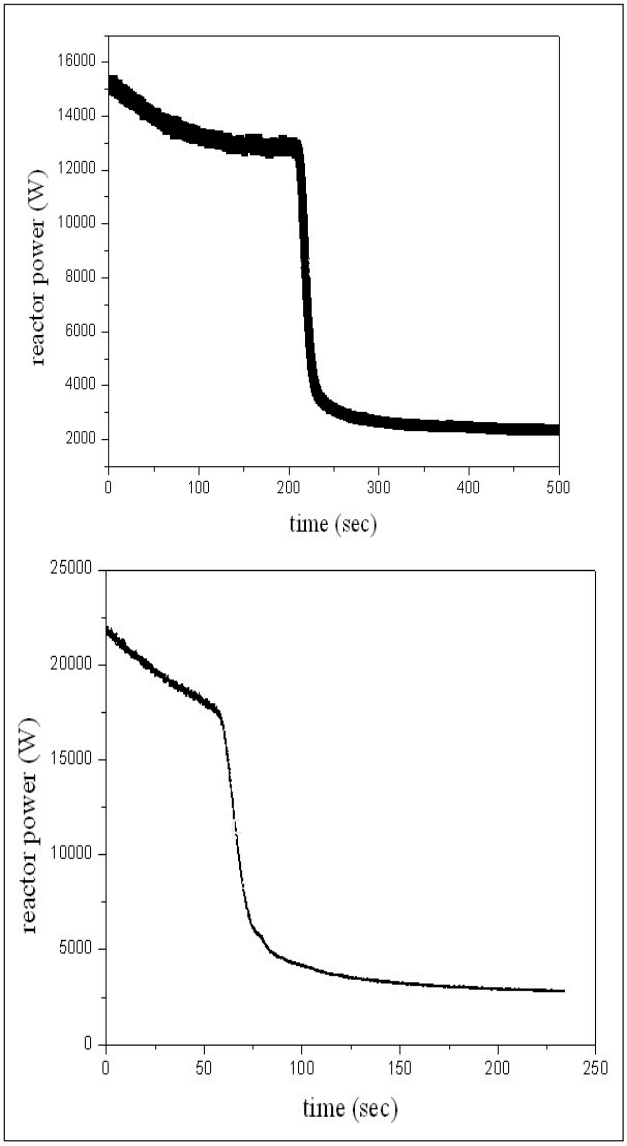

Figure 9: Reactor power profile as recorded from the log rate safety channel while SOR#1 was brought inside the core and i) adjuster rod fully out, ii) adjuster rod fully in

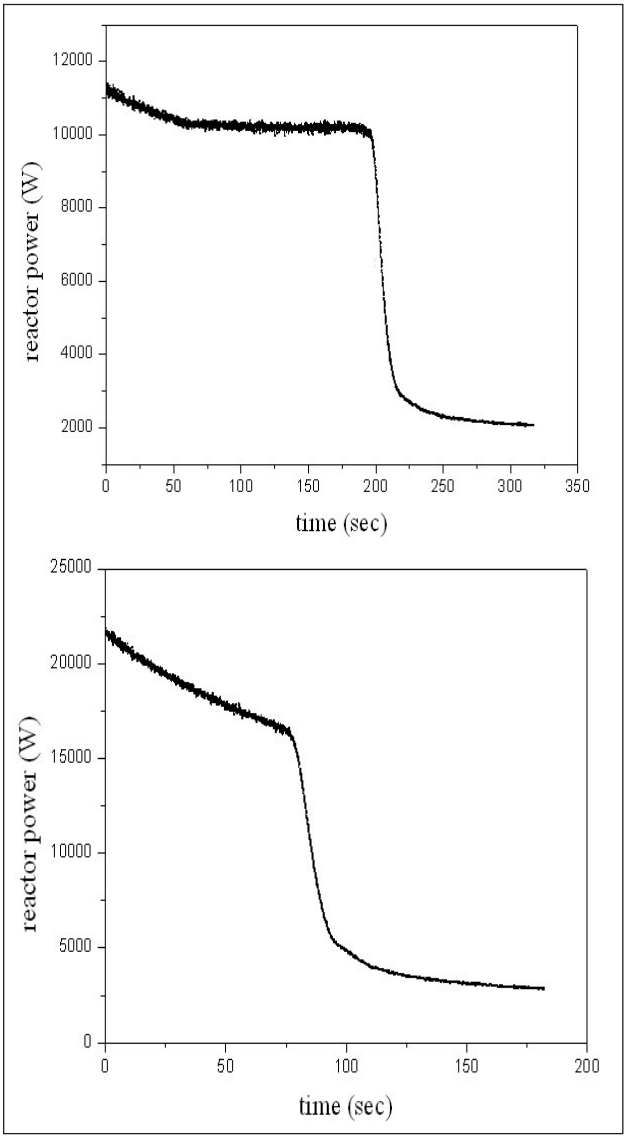

Figure 10: Reactor power profile as recorded from the log rate safety channel while SOR#3 was brought inside the core and i) adjuster rod fully out, ii) adjuster rod fully in

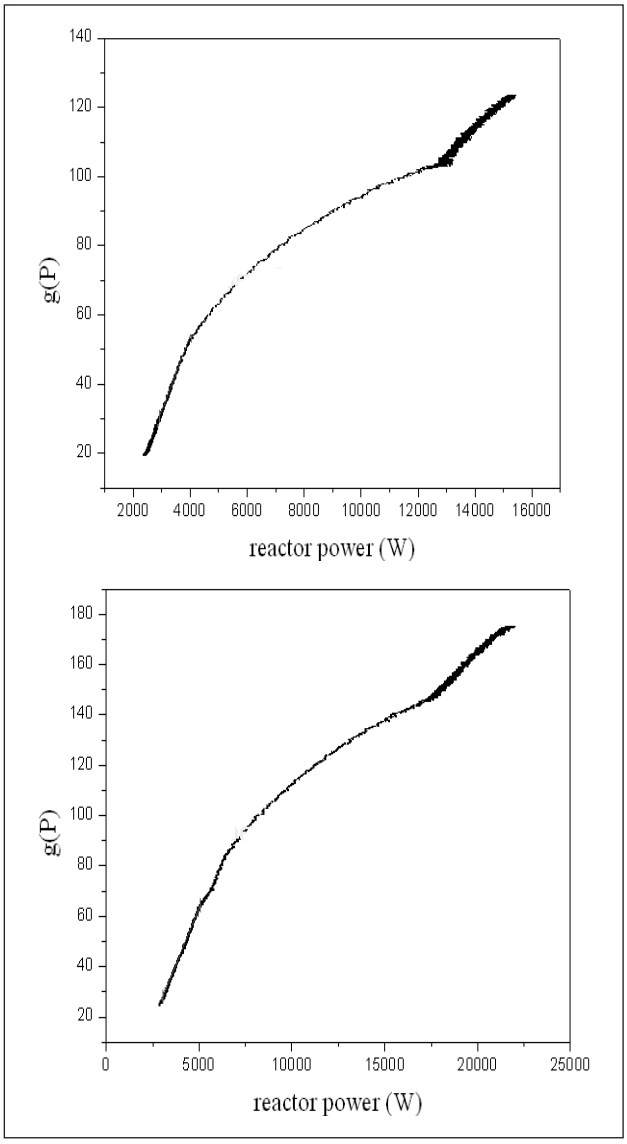

Figure 11: g(P) v/s reactor power plot for SOR#1 with i) adjuster rod fully up, ii) adjuster rod fully down

and ii) adjuster rod down and SOR#1 brought inside the core. Fig-10 shows the reactor power profile as recorded from the log rate safety channel for the condition iii) adjuster rod up and SOR#3 brought inside the core, and iv) adjuster rod down and SOR#3 brought inside the core.

For the estimation of reactivity worth of individual SORs, the g(p) parameter is calculated using the power profile. Fig-11 shows the g v/s P plot for the condition corresponding to Fig-9, while Fig-12 shows the g v/s P plot for the condition corresponding to Fig-10. From the plots it can be seen that value of g reduces as the power is reduced. The straight line portion of the curve can be fitted to obtain the slope which gives the reactivity.

Table-3 gives the reactivity worth as estimated from the slope of g v/s P plot. From the Table it is clear that the worth of individual SOR reduces when the adjuster rod is fully in. Also worth of individual SOR is 12 mk with adjuster rod out. The slope of the fitted line for SOR#1 with adjuster rod up and down is 0.0216 and 0.0183 respectively. The slope of the fitted line for SOR#3 with adjuster rod up and down is 0.0216 and 0.0182 respectively.

Table-3: Reactivity worth of SOR#1 and 3 with Adjuster Rod Fully Out and Fully In

Adjuster rod position	Worth (mk) of SOR#1	Worth (mk) of SOR#3
Fully in	8.8	8.6
Fully out	12.0	12.0

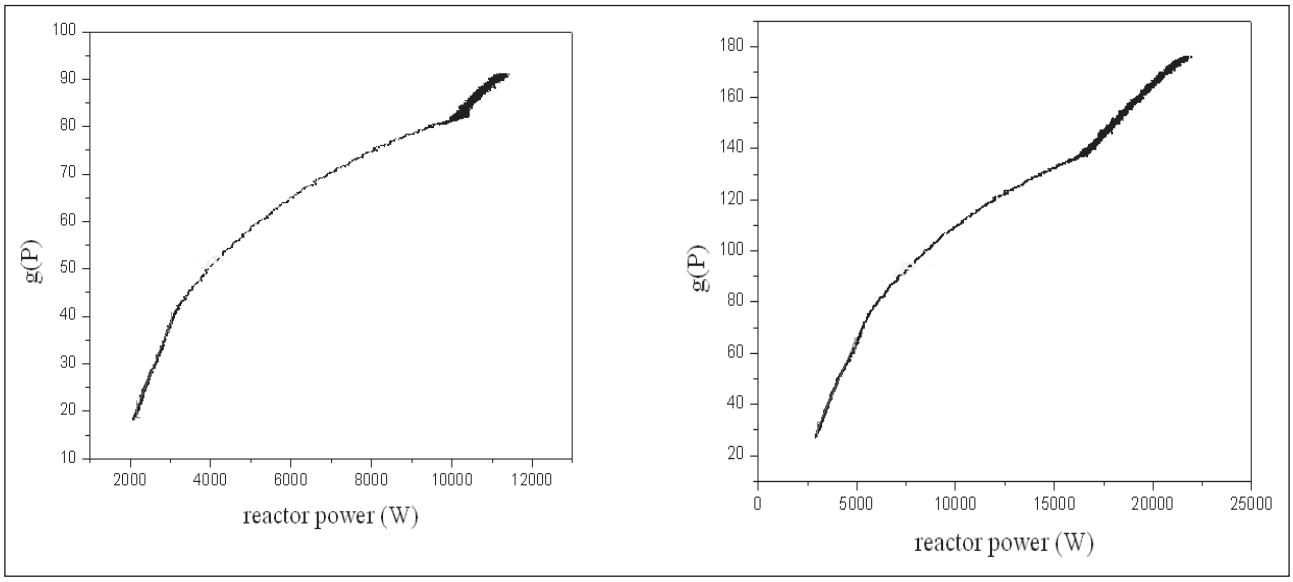

Figure 12: g(P) v/s reactor power plot for SOR#3 with i) adjuster rod fully up, ii) adjuster rod fully down

6.0 Conclusion

The IK computer code based on inverse point kinetic method can be used to measure the reactivity worth of control cum shut off rods, shut off rods, regulating rods and core sub-criticality. The source term can also be estimated wherever required.

References

1. Stephen E.Binney & Alla J.M. Baker, Design and development of a PC based reactivity meter for research reactor, Nuclear Technology, vol 85, April 1989.
2. B. J. Jun, IAEA TECDOC-1004, pp. 59-78, 1998.
3. J.E. Hoogenboom and A.R. van der Sluus, Neutron source strength determination for on-line reactivity measurements, Annals of nuclear energy, vol. 15, pp 553-559, 1988.
4. Seiji Tamura, Signal fluctuation and neutron source in inverse kinetics method for reactivity measurement in the subcritical domain, Journal of nuclear science and technology, 40:3, 153-157, 2003.
5. S.K. Agarwal, C.G. Karhadkar et al., Dhruva: Main design features, operational experience and utilization, Nuclear engineering and design, 236 (2006), 747-757.
6. V. K. Raina, R. Srivenkatesan, et al., Critical Facility for lattice physics experiments for the advanced heavy water reactor and the 500 MWe pressurized heavy water reactor, Nuclear engineering and design, 236 (2006), 758-769.

Life Cycle Reliability and Safety Engineering
Vol.4 Issue 4(2015) 37-43

Reactor Noise and its Role in Safety of Critical and Accelerator Driven Sub-critical Systems

Y. S. Rana, Tej Singh*, P.V. Varde
Reactor Physics & Nuclear Engineering Section, Research Reactor Services Division,
Bhabha Atomic Research Centre Mumbai, Maharashtra, PIN-400085. India
** Corresponding Author email t_singh@barc.gov.in*

Abstract

Reactor noise methods are important due to their passive nature i.e. one can obtain dynamic information from measurements at steady state. The methods have successfully been utilized for diagnostics of faults in different components of research and power reactors. The recent interest in accelerator driven sub-critical systems (ADS) and the necessity of monitoring their degree of sub-criticality has created a renewed interest in noise methods. Due to statistical properties of the external source, theoretical treatment of reactor noise in ADS is different from that of critical reactors. For such sources, we have developed a new theoretical approach. In this paper, we review the subject of noise in critical reactors and ADS. We also present salient features and some results of the theory developed by us.

Key Words: *Noise, Accelerator Driven Systems, Poisson.*

1.0 Introduction

The origin of the subject of reactor noise goes back to 1944 when Bruno Rossi first made experimental observations [1] on statistical fluctuations in neutron population in a nuclear reactor at Loss Alamos. Around the same period, Fermi, Feynman and de Hoffman developed theoretical formulations for studying reactor noise in nuclear systems. Since then, considerable developments have been made in the subject both on experimental and theoretical fronts [2,3,4,5]. The methods have successfully been utilized for diagnostics of faults in different components of research and power reactors [6,7,8,9]. Srinivasan and Om Pal Singh [6] and John and Om Pal Singh [7] studied sodium boiling noise and steam generators leak noise of Liquid Metal Fast Breeder Reactors (LMFBRs) under poor signal to noise ratio conditions. Arzhanov and Pazsit [8] have developed a noise theory for diagnostics of core barrel vibrations and verified the formulas by measurement data on PWRs. Moorthy, Rao and Kakodkar [9] diagnosed vibrations in fuel rods of Dhruva reactor by analyzing Power Spectral Density (PSD) signal of the rods.

The recent interest in accelerator driven sub-critical systems (ADS) and the necessity of monitoring their degree of sub-criticality has created a renewed interest in noise methods. The statistical properties of the external source in an ADS are different from that in a critical reactor which requires a new theoretical approach. Such a theoretical approach was developed by Degweker [10] and was extended further by Rana [11]. In this paper, we present a brief review of the subject of noise in critical reactors and ADS. We also present salient features and some results of the theory developed by us.

2.0 Noise in Critical Reactors

Reactor noise can broadly be divided in two parts viz., zero power reactor noise and power reactor noise. The inherent random phenomena such as interactions of neutrons with nuclei and the fission chain multiplication produced correlations lead to zero power reactor noise which is used to measure important safety parameters like prompt neutron lifetime and reactivity. Power reactor noise, in addition to neutronic fluctuations, deals with fluctuations arising due to mechanical vibrations, voids and temperature, and is used for online monitoring of the health of the power plant. In this paper, we consider only zero power systems. A number of the oretical and experimental techniques [4,12] have been developed for studying reactor noise and are reviewed in the following section.

2.1 Rossi Alpha Technique

The method is based on measurement of the probability $P(t_2|t_1)dt_2$ of detecting a neutron between around time t_2 provided there was a detection at some earlier time t_1. In the point model [13],

$$P(t_2|t_1)dt_2 = N_0 + \frac{\varepsilon\overline{\nu(\nu-1)}}{2\bar{\nu}^2}\alpha\frac{k_p^2}{\left(1-k_p\right)^2}e^{-\alpha\tau} \quad (2.1)$$

where $\tau = t_2 - t_1$, k_p is the prompt neutron multiplication factor, α is prompt neutron decay constant, ε is detector efficiency, $\bar{\nu}$ and $\overline{\nu(\nu-1)}$ are first and second moments of number of fission neutrons respectively.

The first term on the right hand side of the above Eq. (2.1) is the average count rate (referred to as uncorrelated component) and remains constant. The second term (correlated count rate) accounts for fission chain correlations. By plotting the correlated count rate as a function of τ, one can obtain α which is related with the reactivity of the system. Based on the method of counting, different experimental procedures [13,14,15,16] have been proposed for Rossi alpha measurements.

2.2 Feynman Alpha (Variance to Mean Ratio) Technique

In Feynman alpha method [17], repeated measurement of number of counts in a time interval Δt is carried out. The data is then used to calculate the variance to mean ratio, v/m. The ratio is plotted as a function of Δt. By fitting the plot to the following expression [18], reactor kinetic parameters can be obtained.

$$\frac{\mathrm{v}}{m} = 1 + \frac{2\varepsilon\overline{\mathrm{v}(\mathrm{v}-1)}}{\bar{\mathrm{v}}^2}\sum_{i=1}^{J+1} Y_i\left(1 - \frac{1-e^{-\alpha_i t}}{\alpha t}\right) \quad (2.2)$$

where J is the number of delayed neutron groups and $Y_i = A_i G(\alpha_i)/\alpha_i$. $G(s)$ is the zero power transfer function and A_i and α_i are its residues and poles, respectively.

2.3 Correlation Function and Power Spectral Density Methods

Auto Correlation Function (ACF) and Power Spectral Density (PSD) methods are very commonly used in reactor noise analysis due to their easy applicability. The ACF of a fluctuating signal $N(t)$ is defined as:

$$\phi_{NN}(\tau) = \lim_{T\to\infty}\frac{1}{2T}\int_{-T}^{T} N(t)N(t+\tau)dt \quad (2.3)$$

For correlation between noise signals of different types such as neutron density and detector current, the above function is known as Cross Correlation Function (CCF). The ACF for zero power reactor noise[12] is expressed as:

$$\phi_{NN}(\tau) = \varepsilon\lambda_f\overline{N}\left[\delta(\tau) + \frac{1}{2}\sum_i Y_i\alpha_i e^{-\alpha_i|\tau|}\right] \quad (2.4)$$

where the first term is white noise due to the detector and the second term is due to fission chain correlations. Fourier Transform of ACF yields PSD which is a measure of the power of the noise signal per unit of frequency.

2.4 Other Methods

Bennett [18] proposed a variant of variance to mean ratio technique known as Bennett variance technique. The variance to mean ratio, based on calculation of variance from cross-correlation of count rates in two successive time intervals, which does not diverge as reactor approaches criticality. Other methods for measurement of prompt neutron decay constant include polarity correlation method [19], the interval distributions method [20] and the dead time method [21]. Mihalczo [22] developed the Cf^{252} method for measuring sub-criticality.

2.5 Noise Theory of Critical Reactors

In low power systems, the inherent neutron noise can be considered theoretically as a Markov process. If $P_1(X,t)$ is the probability of the system being in state X at time t and $P_{1|1}(X_2,t_2|X_1,t_1)$ is the transition probability of the system going from state X_1 at time t_1 to the state X_2 at time t_2, all other states for a Markov process can be determined as follows:

$$P_1(X_2,t_2) = \sum_{X_1} P_{1|1}(X_2,t_2|X_1,t_1)P_1(X_1,t_1) \quad (2.5)$$

Thus, the Markov processes are completely described by the two probability functions $P_1(X,t)$ and $P_{1|1}(X_2,t_2|X_1,t_1)$. These probabilities are related through the Chapman Kolmogorov equation:

$$P_{1|1}(X_2,t_2|X_1,t_1) = \sum_X \begin{bmatrix} P_{1|1}(X_2,t_2|X,t) \\ \times P_{1|1}(X,t|X_1,t_1) \end{bmatrix} \quad (2.6)$$

2.5.1 Kolmogorov Forward Equation

This approach was first used by Courant and Wallace [23] and later studied by Matthes [24], Norelli [25], Dalfes [26], Pazsit [27] and Degweker [28]. In the point model [29], one writes the probability equation for state of the reactor at time $t+\Delta t$ in terms of its state at time t.

We start with the Chapman-Kolmogorov equation:

$$P(n,t\,|\,m,s) = \sum_l P(n,t\,|\,l,\tau)P(l,\tau\,|\,m,s) \quad (2.7)$$

and set $\tau = t\text{-}dt$ for deriving the forward equation.

$$\begin{aligned} &P(N,t+dt) = \lambda_c (N+1)dtP(N+1) \\ &+\sum_{\nu} \lambda_f (N-\nu+1)dtp(\nu)P(N-\nu+1) \\ &+SdtP(N-1,t) \\ &+[1-\{(\lambda_f+\lambda_c)N+S\}dt]P(N,t) \end{aligned} \tag{2.8}$$

where S is the source strength, λ_c, λ_f are the capture, fission probabilities per neutron per unit time and $p(\nu)$ is the probability that a fission reaction produces ν neutrons. Expanding the term on the LHS up to first order in dt, we can obtain the following equation:

$$\begin{aligned} &\frac{dP(N,t)}{dt} = \lambda_c (N+1)P(N+1) \\ &+\sum_{\nu} \lambda_f (N-\nu+1)p(\nu)P(N-\nu+1) \\ &+SP(N-1,t)-\{(\lambda_f+\lambda_c)N+S\}P(N,t) \end{aligned} \tag{2.9}$$

Here we introduce what is known as probability generating function (pgf). The pgf for the probability $P(N,t)$ of having N particles at time t, is defined as:

$$F(x,t) = \sum_N P(N,t)x^N \tag{2.10}$$

If $P(n \mid i)$ is the probability of having n particles in the system due to emission of i source particles with probability $p(i)$, the probability of having n particles in the system can be written as:

$$P(n) = \sum_i P(n \mid i)p(i) \tag{2.11a}$$

In terms of pgf, we get

$$F(x) = \sum_i F(x \mid i)p(i) \tag{2.11b}$$

Similarly, for two mutually independent probabilities, it can be shown [11] that,

$$F(x,t \mid 1,t_1;1,t_2) = F(x,t \mid 1,t_1)F(x,t \mid 1,t_2) \tag{2.12}$$

which can be generalized to any number of times.

The forward equation in terms of the pgf, becomes:

$$\begin{aligned} \frac{\partial F(x,t)}{\partial t} &= \begin{bmatrix} \lambda_c(1-x) \\ +\lambda_f(f(x)-x) \end{bmatrix} \frac{\partial F(x,t)}{\partial x} \\ &+S(x-1)F(x,t) \end{aligned} \tag{2.13}$$

The basic advantage of pgf method lies in that the algebra gets simplified. Various moments can be obtained by successive differentiation with respect to x and setting $x=1$.

2.5.2 Kolmogorov Backward Equation

The backward equation approach was first used by Pal [30] and Bell [31] and has been significantly developed by Matthes [32], Munoz-Cobo and Verdu [33] and Pazsit [27]. In the point model [29], one writes the probability equation for state of the reactor at time t given its state at some earlier time s. The Chapman-Kolmogorov equation is written with the intermediate time point $\tau = s + ds$ considering all the possible processes in the interval ds.

$$\begin{aligned} &P(n,t \mid m,s) \\ &= \lambda_c mdsP(n,t \mid m-1,s+ds) \\ &+\lambda_f mds\sum_{\nu} \begin{bmatrix} p(\nu) \\ \times P(n,t \mid m+\nu-1,s+ds) \end{bmatrix} \\ &+SdsP(n,t \mid m+1,s+ds) \\ &+\begin{bmatrix} 1-\{m(\lambda_f+\lambda_c) \\ +S\}ds \end{bmatrix} P(n,t \mid m,s+ds) \end{aligned} \tag{2.14}$$

Assuming $m=1$ and $S=0$ i.e. a single initial neutron in a source free medium and using pgf method, we get the following equation:

$$\begin{aligned} &-\frac{\partial F(x,t \mid 1,s)}{\partial s} = \lambda_c + \lambda_f \sum_{\nu} p(\nu)F^{\nu}(x,t \mid 1,s) \\ &-(\lambda_f+\lambda_c)F(x,t \mid 1,s) \end{aligned} \tag{2.15}$$

where we have used the relation $F(x,t \mid m,s) = F^m(x,t \mid 1,s)$ due to of independence of chains.

2.5.3 The Bartlett Formula

For a multiplying medium with an external source of Poisson type, the usual procedure for deriving moments of any observable quantity such as detector counts is to either write forward Master equation with source or follow backward Master equation approach. In the latter approach, first the backward Master equation is solved to find the pgf due to a single particle. The pgf with external source is then obtained by using the Bartlett formula [34]. This formula relates the pgf in the presence of a source S with the pgf in the absence of a source due to a single neutron at time τ.

$$F_S(x,t \mid 1,\tau) = \exp\left[S\int_{-\infty}^{t} \{F(x,t \mid 1,\tau)-1\}d\tau \right] \tag{2.16}$$

3.0 Reactor Noise in ADS

3.1 Initial Studies on the Subject

The early studies [35,36,37] on reactor noise in ADS assumed that the ADS source was a continuous Poisson source with the main difference from critical reactors arising due to spallation reaction in which a large number of neutrons are produced having a multiplicity distribution with a large mean and a large second factorial moment. Theoretical treatment of such a source will be similar to that of a spontaneous fission source and has been studied in detail by Munoz Cobo and Difilippo [38]. However, the principal difference between critical reactor noise and ADS noise is due to the statistical properties of the source. Unlike the source due to radioactive decay present in ordinary reactors, the accelerator produced neutron source in an ADS cannot be assumed to be a Poisson process. Moreover, the source may be pulsed. The initial studies either neglected both the effects i.e. periodic nature of the source and its non-Poisson character [35,37] or did not account for non-Poisson nature of a periodic source [39,40].

3.2 Studies with Non-Poisson Sources

3.2.1 The Non-Poisson Nature of the ADS Source

It was pointed out by us [41] that small fluctuations in current in an accelerator can give rise to the non-Poisson distribution of number of particles in a pulse. Moreover, accelerators produce particles in short bunches at periodic intervals rather than at random. There may also be correlations introduced during production of protons. The measurements for number of protons per shot during the TARC experiment [42] showed a few percent fluctuations which is much larger than would be expected for a Poisson source. Based on the published experimental data [40] we deduced the asymptotic values of the Y function and plotted them against the inverse of alpha. The fitted curve, in addition to the quadratic term due to fission chain correlations, showed the presence of a linear term which indicates a non-Poisson source contribution. The Feynman alpha measurements carried out by Hiroshi Taninaka et al. [43] with a pulsed D-T source, indicate that instabilities in the accelerator current result in a divergent variance to mean ratio and the formula based on Poisson source assumption underestimates the value of alpha. Thus, an accelerator produced neutron source cannot be assumed to be a Stochastic Poisson Point Process.

3.3 Theory of Reactor Noise in ADS

It was pointed out by Degweker [10] that the usual procedure (described in section 2.5.3) for treating reactor noise in critical reactors is not valid in ADS due to non-Poisson nature of the source. For such sources, the following method was suggested by the author.

Let $G(z_1, z_2, t)$ be the pgf of detecting counts in a short interval around time 0 and counts in a short interval around time τ due to single neutron injected in a source free medium at time t. If it is assumed that bursts of neutrons appear at times t_n with a multiplicity distribution $\rho(\nu)$ and the last of these bursts occurs at t_0 then the ones prior to this will occur at $t_0 - 1/f$, $t_0 - 2/f$ and so on. Here f is the frequency of the accelerator. Using the multiplicative property of pgfs for different source events, the pgf for the case of an arbitrary source is obtained. This property is due to the independent propagation of chains initiated by different source neutrons and is a consequence of the linear character of the neutron transport and multiplication. The resultant pgf is:

$$\prod_{n=0}^{\infty}\sum_{\nu}\rho(\nu)G^{\nu}(z_1, z_2, t_0 - n/f) = \prod_{n=0}^{\infty}F_{\rho}\left(G(z_1, z_2, t_0 - n/f)\right) \tag{3.1}$$

Since measurement intervals are generally not synchronized with the source pulses, t_0 is a uniformly distributed (between $\tau - 1/f$ and τ) random variable. Averaging over t_0, the pgf becomes:

$$g = f\int_{\tau-1/f}^{\tau}\prod_{n=0}^{\infty}F_{\rho}\left[G\begin{pmatrix} z_1, z_2, \\ t_0 - n/f, \tau \end{pmatrix}\right]dt_0 \tag{3.2}$$

Rossi alpha formula can be obtained by differentiating with respect to z_1 and z_2, and setting $z_1 = z_2 = 1$. This involves expressions for, G_{z_1}, G_{z_2} and $G_{z_1 z_2}$ which can be obtained by solving the Kolmogorov backward equation with a single neutron in a source free medium:

$$-\frac{\partial G}{\partial t} = \lambda_c(1-G) + \lambda_d(z\chi[0,\tau] + 1 - \chi[0,\tau] - G) + \lambda_f(g(G) - G) \tag{3.3}$$

$g(x)$ is the pgf of the neutron number distribution in a fission event and $\chi[0,\tau]$ is 1 if t lies in the interval $[0,\tau]$ and zero otherwise. For a Poisson source, the solution of this equation is used in the Bartlett formula

to obtain source induced moments. Since the source is non-Poisson, we use the resultant pgf (defined above) in place of the Bartlett formula. The final Rossi alpha formula is as follows:

$$f_2(0,\tau)=\frac{f\lambda_d^2}{2\alpha}\left[\frac{m_1^2}{1-e^{-\alpha/f}}\left\{\begin{matrix}e^{-\alpha/f}e^{\alpha\left(\tau-\frac{[f\tau]}{f}\right)}\\+e^{-\alpha\left(\tau-\frac{[f\tau]}{f}\right)}\end{matrix}\right\}+(m_2-m_1^2+2m_1Y_1)e^{-\alpha\tau}\right] \quad (3.4)$$

Where, m_1 and m_2 stand for the first and second factorial moments of the multiplicity distribution of neutrons produced by a proton bunch, f is the pulse repetition frequency, α is prompt neutron decay constant and $Y_1=\lambda_f\overline{\nu(\nu-1)}/2\alpha$. In the above Eq. (3.4), the first term is the usual uncorrelated term except the periodic nature which arises due to source properties. In the second term, the first part accounts for the source correlations while the second part is the fission chain correlation term.

3.4 Subsequent Developments

The non-Poisson periodically pulsed source of neutrons was later on generalized to include the possibility of correlations between pulses [41]. An exponential correlation in intensity of the neutron source pulses was assumed. For such a situation, the resultant pgf described in section 3.3, gets modified as:

$$f\int_{\tau-1/f}^{\tau}\left[\begin{matrix}\sum_{\nu_1,\nu_2,\ldots,\nu_N}\rho(\nu_1,\nu_2,\ldots,\nu_N)\\G^{\nu_1}(z_1,z_2,t_0-1/f)\\G^{\nu_2}(z_1,z_2,t_0-2/f)\\\ldots G^{\nu_N}(z_1,z_2,t_0-N/f)\end{matrix}\right]dt_0 \quad (3.5)$$

Following the methodology described earlier, we obtain the following Rossi alpha formula:

$$f_2(0,\tau)=\frac{f\lambda_d^2}{2\alpha}\left[\frac{m_1^2}{1-e^{-\alpha/f}}\left\{\begin{matrix}e^{-\alpha/f}e^{\alpha\left(\tau-\frac{[f\tau]}{f}\right)}\\+e^{-\alpha\left(\tau-\frac{[f\tau]}{f}\right)}\end{matrix}\right\}+(m_2-m_1^2+2m_1Y_1)e^{-\alpha\tau}\right] \quad (3.6)$$

$$+\frac{f\lambda_d^2\Gamma'^2}{2\alpha}\left(\begin{matrix}\frac{e^{-(\alpha+\beta)/f}e^{\alpha(\tau-[f\tau]/f)}}{1-e^{-(\alpha+\beta)/f}}\\+\frac{e^{-\alpha(\tau-[f\tau]/f)}}{1-e^{-(\alpha-\beta)/f}}\end{matrix}\right)e^{-\beta[f\tau]/f}$$

$$+\frac{f\lambda_d^2\Gamma'^2}{2\alpha}\left(\begin{matrix}\frac{e^{-(\alpha+\beta)/f}}{1-e^{-(\alpha+\beta)/f}}\\-\frac{1}{1-e^{-(\alpha-\beta)/f}}\end{matrix}\right)e^{-\alpha\tau}$$

Where, Γ'^2 is the variance of the number of neutrons produced in a pulse and β is the decay constant of the source correlations. The last term accounts for the correlations between different source pulses. The above formula was analyzed for different values of the β. It was concluded that if α and β are of about the same magnitude or if $\beta<<\alpha$, it is likely that noise experiments might yield β which may be mistaken for α! Only in the case $\beta>>\alpha$, i.e. where the source fluctuations can be treated as white, do we get a variation of the Rossi alpha which will give the correct value of α.

The theory of reactor noise in ADS was extended further to include delayed neutrons [44]. The methodology followed for inclusion of delayed neutrons is described below.

The equation for G gets modified to:

$$-\frac{\partial G}{\partial t}=-\lambda_a G+\lambda_c+\lambda_d\sum_{i=1}^{2}(z_i-1)\chi_i(t)+\lambda_f f(G(z_1,z_2,t),I_i) \quad (3.7a)$$

Where

$$I_i=\int_t^{\tau}\mu e^{-\mu(t'-t)}G(z,t')dt'+e^{-\mu(\tau-t)} \quad (3.7b)$$

$f(x,y_1,\ldots y_N)$ is the pgf ;

$\sum_{n,m_1,\ldots m_N}x^n y_1^{m_1},\ldots y_N^{m_N}p(n,m_1,\ldots m_N)$ $p(n,m_i)$ being the probability of finding n neutrons and m_i delayed neutron precursors of the i[th] group at time t, μ is precursors decay constant of the i[th] group. $\chi_1(t)=1$, in an interval dt_0 around $t=0$ and, $\chi_2(t)=1$, in an interval $d\tau$ around $t=\tau$.

To demonstrate the importance of inclusion of delayed neutrons, we show variation of Rossi alpha for heavy and light water systems in Fig.-1(a) and (b), respectively. It is evident from the figures that the importance of the delayed neutron contributions will be most clearly felt in those situations where the prompt and delayed time scales are not very distinct (such as heavy water systems) and the formulae (with delayed neutrons) would serve as corrections even on prompt neutron time scales.

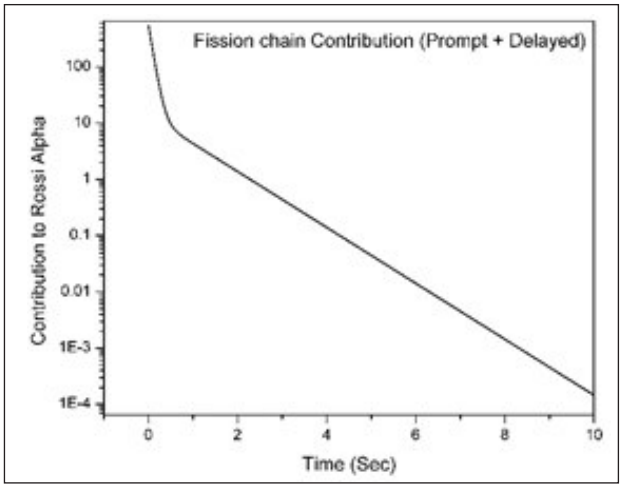

Figure 1 (a): Rossi alpha function for heavy water systems

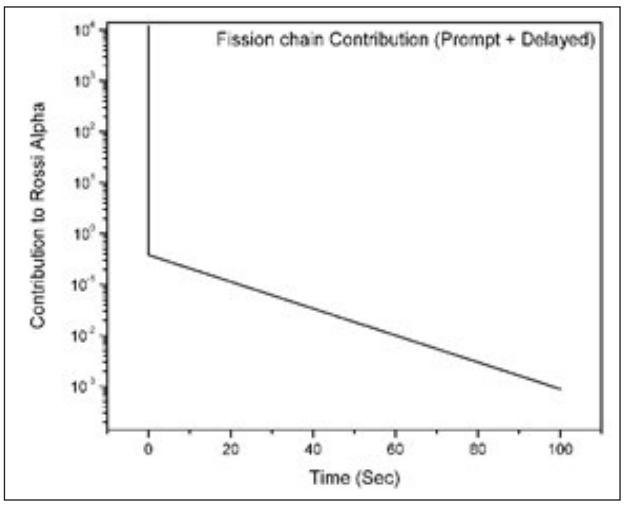

Figure 1 (b): Rossi alpha function for light water systems

4.0 Summary and Conclusions

Reactor noise methods have long been utilized for diagnostics of faults in different components of research and power reactors and measurement of various safety parameters. Well established recipes have been developed over the years for theoretical treatment of noise in traditional reactors. In recent years, accelerator driven systems have attracted worldwide attention due to their superior safety characteristics as compared to critical reactors and their potential to incinerate Minor Actinides (MAs) and transmute Long Lived Fission Products (LLFPs). Monitoring of sub-criticality in such systems will be an important safety requirement. Due to their passive nature, noise techniques are expected to be useful for the purpose.

The accelerator produced neutron source cannot be assumed to be a Poisson process and hence the traditional theoretical approach is not valid for such systems. A theory of reactor noise in ADS considering periodically pulsed source and its non-Poisson character has been developed by us. However, if noise methods are to be used for sub-criticality measurements, experimental studies on the statistical characteristics of the proton bunches should be carried out. It is also important to study the current fluctuation statistics of ion beams from accelerators, either theoretically or experimentally.

Acknowledgements

Author is thankful to Shri R.C. Sharma, Director, Reactor Group for his support and encouragement during preparation of this manuscript.

References

1. Pacilio et al. (1979), "The Analysis of Reactor Noise: Measuring Statistical Fluctuations in Nuclear Systems," *Advances in Nuclear Science and Technology, 11, 67*
2. Thie, J.A. (1981), "Power reactor noise," *American Nuclear Society*
3. Uhrig, R. E. (1970), "Random noise techniques in nuclear reactor systems," *The Ronald press company, New York*
4. Saito, K. (1979), "Source papers in reactor noise," *Prog. Nucl. Energy, **3**, 157*
5. Pazsit, I. and Pal, L. (2007), "Neutron fluctuations: a treatise on the physics of branching processes," *Elsevier Ltd.*
6. Srinivasan, G.S. and Om Pal Singh (1994), "Leak Noise detection in steam generator of Liquid Metal Fast Breeder Reactors using new statistical features," *Ann. Nucl. Energy, 21 (9), 571*
7. John, T.M. and Om Pal Singh (1985), "Coolant boiling noise in LMFBRs," *Ann. Nucl. Energy, 12 (1), 45*
8. Arzhanov, V. and Pazsit, I. (2003), "Diagnostics of Core Barrel Vibrations by In-Core and Ex-Core Neutron Noise," *Prog. Nucl. Energy 43, 151*
9. Moorthy, R.I.K., Rama Rao, A. and Kakodkar, A. (1991), "Diagnosis and cure of Dhruva fuel vibration," *Nucl. Engg. Design, 125, 259*
10. Degweker S.B. (2003) "Reactor Noise in Accelerator Driven Systems", *Annals of Nuclear Energy,* 30, 223
11. Rana, Y. S. (2013), "Theoretical studies on noise techniques for measuring physics parameters of accelerator driven systems," *Ph.D. Thesis, HBNI, Mumbai*
12. Williams, M. M. R. (1974), "Random Processes in Nuclear Reactors," *Pergamon Press, Oxford*
13. Orndoff, J. D. (1957), "Prompt neutron periods of metal critical assemblies," *Nucl. Sci. Eng., **2**, 450*
14. Brunson, G. S. et al. (1957), "Measuring the prompt period of a reactor," *Nucleonics, 15(11), 132*
15. Stribel, T. (1963), "Neutron lifetime and reactivity measurements in thermal reactors with the help of the Rossi-alpha method," *Nukleonik, **5**, 170*
16. Babala, D. (1967), "Point-reactor theory of Rossi-alpha experiment," *Nucl. Sci. Eng., **28**, 237*
17. Feynman, R. P. et al. (1956), "Dispersion of the neutron emission in U^{235} fission," *J. Nucl. Energy, **3**, 64*
18. Bennett, E. F. (1960), "The Rice formulation of pile noise," *Nucl. Sci. Eng., **8**, 53*

19. Veltman, B.P.T. and Kwakernaak, H. (1961), *Regelungstechnik* ***9****, 357*
20. Babala, D. (1966), "Neutron counting statistics in nuclear reactors," *Report KR-114*
21. Srinivasan, M. and Sahni, D. C. (1967), "Modified statistical technique for the measurement of alpha in fast and intermediate reactor assemblies," *Nukleonik,* ***9****, 155*
22. Mihalczo, J. T. et al. (1990), "Dynamic sub-criticality measurements using the Cf^{252}-source-driven noise analysis method," *Nucl. Sci. Eng.,* ***104****, 314*
23. Courant, E. D. and Wallace, P. R. (1947), "Fluctuations of the Number of Neutrons in a Pile", *Physical Review, 72(11), 1038*
24. Matthes, W. (1962), "Statistical Fluctuations and their correlation in reactor neutron distributions," *Nukleonik,* ***4****, 213*
25. Norelli, F. et al. (1975), "Stochastic kinetics: Analytical solutions of detailed probability balance equations," *Ann. Nucl. Energy,* ***2,*** *67*
26. Dalfes, A. (1966), "The random processes of a nuclear reactor and their detection," *Nukleonik,* ***8****, 94*
27. Pazsit, I. (1987), "Duality in transport theory," *Ann. Nucl. Energy,* ***14(1),*** *25*
28. Degweker, S. B. (1994), "A forward equation for stochastic neutron transport", *Ann. Nucl. Energy, 21(9), 531*
29. Arcipiani, B. and Pacilio, N. (1980), "A discussion of the forward and backward Kolmogorov equations for multiplying systems," *Ann. Nucl. Energy,* ***7,*** *553*
30. Pal, L. (1958) "On the theory of stochastic processes in nuclear reactors," *Il Nuovo Cimento, 7 (Suppl.)*, 25-42
31. Bell, G. I. (1965), "On the stochastic theory of neutron transport," *Nucl. Sci. Eng., 21, 390*
32. Matthes, W. (1966), "Theory of fluctuations in neutron fields," *Nukleonik,* ***8****, 87*
33. Munoz-Cobo, J.L. and Verdu, G. (1987), "Neutron stochastic transport theory with delayed neutrons," *Ann. Nucl. Energy, 14(7), 327*
34. Bartlett, M. S. (1955), "An introduction to stochastic processes," *Cambridge University Press, Cambridge*
35. Pazsit, I. and Yamane, Y. (1998), "The Variance-to-Mean Ratio in Subcritical Systems Driven by a Spallation Source," *Ann. Nucl. Energy, 25(9), 667*
36. Kuang, Z. F. and Pazsit, I. (2000), "A Quantitative Analysis of the Feynman- and Rossi-Alpha Formulas with Multiple Emission Sources," *Nucl. Sci. Eng., 136, 305*
37. Behringer, K. and Wydler, P. (1999), "On the Problem of Monitoring Neutron Parameters of the Fast Energy Amplifier," *Ann. Nucl. Energy, 26, 1131*
38. Munoz Cobo, J.L. and Difilippo, F. C. (1988), "Noise and Nonlinear Phenomena in Nucl. Systems," *Proc. NATO Adv. Res. Wksp. Plenum, NY*
39. Munoz Cobo J.L. et al. (2001), "Sub-critical Reactivity Monitoring in Accelerator Driven Systems," *Ann. Nucl. Energy, 28, 1519*
40. Pazsit, I. et al. (2005), "Calculation of the pulsed Feynman alpha formulae and their experimental verification," *Ann. Nucl. Energy,* ***32(9)****, 986*
41. Degweker, S. B. and Rana, Y. S. (2007), "Reactor Noise in Accelerator Driven Systems-II," *Ann. Nucl. Energy,* 34(6), *463*
42. Abanades, A. et al. (2002), "Results from the TARC experiment: spallation neutron phenomenology in lead and neutron-driven nuclear transmutation by adiabatic resonance crossing," *Nucl. Instr. Meth. A, 478(3), 577*
43. Hiroshi Taninaka et al. (2011), "Feynman-α analysis for a thermal sub-critical reactor system driven by an unstable 14 MeV neutron source," *J. Nucl. Sci. Tech., 48(9), 1272*
44. Rana, Y. S. and Degweker, S. B. (2009), "Feynman Alpha and Rossi Alpha Formulae with Delayed Neutrons for Sub-critical Reactors Driven by Pulsed Non-Poisson Sources," *Nucl. Sci. Eng., 162, 117*

Life Cycle Reliability and Safety Engineering
Vol.4 Issue 4(2015) 44-53

A Review of Neutronics and Thermal Hydraulics Coupled Codes SAC-RIT and RITAC

Jainendra Kumar, Tanay Mazumdar, Tej Singh* and P.V. Varde
Research Reactor Services Division, BARC, Mumbai-94
**corresponding author email ID: t_singh@barc.gov.in*

ABSTRACT

Safety analysis of a research reactor includes simulations of reactivity initiated accident (RIA), loss of coolant accident (LOCA) etc. For design and licensing of research reactors, computer codes with capability of analyzing those transients are needed. Many codes such as RELAP, RETRAN and ATHLET have been developed and widely used for safety analysis of power reactors operating under high temperature and high pressure conditions. Two computer codes namely SAC-RIT (Safety Analysis Code for Reactivity Initiated Transient)[1] and RITAC (Reactivity Initiated Transients Analysis Code)[2] based on coupling of point kinetics model with thermal-hydraulics model have been developed to analyze reactivity initiated transients related with upcoming projects like 2MW Upgraded Apsara and 30 MW HFRR being designed at BARC. The codes have been developed to carry out reactivity initiated transient analysis for nuclear research reactors with plate/pin type fuel assemblies. This paper is aimed at presenting a review of the two codes. In SAC-RIT point kinetics is solved using fourth order Runge-Kutta method while thermal hydraulics model is solved using explicit finite difference method. In RITAC point kinetics is solved using piece-wise constant approximation (PCA) method while thermal hydraulics is solved using finite difference along with Crank-Nicholson technique. Thermal hydraulic modeling is done using two phase homogeneous flow model of the coolant for two representative channels: average and the hottest channel. The average power channel provides the average core reactivity feedback, while hot channel is used to estimate the safety margins available during normal and accidental conditions. In the thermal hydraulics model, the wall to fluid heat transfer mode consists of liquid phase natural convection, liquid phase forced convection, nucleate boiling, sub-cooled nucleate boiling, saturated boiling, transition boiling, film boiling and vapor phase convection. Both codes have been benchmarked against the transient analysis of 10 MW MTR (IAEA-BENCHMARK)[3].

Introduction

Research reactors besides providing neutron beams to facilitating neutronic experiments are playing important role in the production of useful radioisotopes required for medical, agricultural and industrial applications. Different types of research reactors are being operated around the globe and many more are under design/commissioning phase. Prior to commissioning, safety analyses for various postulated initiating events (PIEs) including reactivity initiated accident (RIA), loss of flow accident (LOFA) etc. are required. Analysis of PIEs related with reactivity initiated transients is important to ensure adequate safety margin for the reactor under nominal and accidental scenario. The analysis involves modeling of time dependent neutronic behavior of the reactor core to predict power rise under simulated reactivity insertion along with feedback reactivity arising due to change in temperature distribution in the core, voiding in coolant channel etc. Reactivity feedbacks are estimated by thermal hydraulics modeling of fuel-coolant channels in the core. Plate and pin type fuel geometry are the most common fuel designs used in research reactors. Two computer codes namely SAC-RIT (Safety Analysis Code for Reactivity Initiated Transients) and RITAC (Reactivity Initiated Transients Analysis Code) have been developed to analyze postulated initiated events (PIEs) related with reactivity initiated transients for upcoming research reactor projects i.e. 2MW Upgraded Apsara Reactor and High Flux Research Reactor (HFRR). Thermal hydraulic modeling is done by considering two representative channels: average and the hottest channel. The average power channel provides the average core reactivity feedback, while hot channel is used to estimate the safety margins available during normal and accidental conditions.

In the SAC-RIT[1] computer code, point kinetics equations are solved numerically by fourth order Runge Kutta method based on the information about reactivity insertion and then its outcome i.e. the neutronic power information is supplied to the thermal hydraulic code where mass, momentum and energy conservation equations are solved identically to find out not only the transient temperatures of fuel, clad and coolant, but the temperature dependent reactivity feedback also which will dictate the trend of power and temperature in following time steps. In RITAC [2] point kinetics is solved using Piece-wise constant approximation (PCA) method while thermal hydraulics is solved using finite difference along Crank-Nicholson technique. The codes are benchmarked against the transient analysis of 10 MW IAEA MTR BENCHMARK [3] and a good agreement with the results available in literature is observed.

Point-Kinetics Model

Point reactor kinetics code is based on point kinetics model where a finite sized reactor is assumed to be a point one i.e. change in neutron density by virtue of reactivity insertion reflects equally at all points within a reactor. Rates of change in neutron density and precursor concentration are described by a set of coupled linear ordinary differential equations given following.

$$\frac{dn(t)}{dt}=\frac{\rho(t)-\beta}{\Lambda}n(t)+\sum_{i=1}^{g}\lambda_i C_i(t)+S(t) \qquad (1)$$

$$\frac{dC_i(t)}{dt}=\frac{\beta_i}{\Lambda}n(t)-\lambda_i C_i(t)$$

This model is connected with the thermal hydraulic model mainly through reactivity feedback resulted from the increase in fuel temperature and coolant temperature and from the formation of void in coolant. In SAC-RIT the point reactor kinetic equations are solved using fourth order Runge-Kutta method[4].

In RITAC the point reactor kinetic equations are solved using piece wise constant approximation (PCA)[5].

Reactivity Feedback Calculation: Reactivity initiated transients in nuclear reactor leads to variation of reactor power. This results in change of temperature distribution of fuel, clad and coolant system which often gives rise to reactivity feedback to the reactor core. The reactivity feedback is calculated as the summation of the feedbacks related to changes in the mean coolant density, mean fuel temperature, mean coolant temperature and the mean cladding thermal expansion and hence total reactivity inserted can be written as

$$\rho(t)=\rho_0+\rho_{ext}(t)+\rho_{clnt}\delta T_{clnt}+\rho_{fuel}\delta T_{fuel}+\rho_{clad}\delta T_{clad} \qquad (3)$$

where ρ_{fuel} ρ_{fuel}, ρ_{clad} ρ_{clad} and $\rho_{coolant}$ $\rho_{coolant}$ are temperature coefficients of reactivity of fuel, clad and coolant respectively. In case of boiling in the coolant channel, voiding coefficient of reactivity for coolant is also included in the reactivity feedback expression.

Thermal Hydraulics Model

Temperature Distribution in Fuel and Clad: The time-dependent radial temperature profile for plate type fuel-clad geometry is obtained by solving Fourier heat conduction equation as follows.

$$\rho C_p(x,t)\frac{\partial T(x,t)}{\partial t}-\frac{\partial}{\partial x}\left(k(x,t)\frac{\partial T(x,t)}{\partial x}\right)=\dot{q}'''(x,t) \qquad (4)$$

For cylindrical/ pin type fuel geometry the heat conduction equation is given by

$$\rho Cp\frac{\partial T}{\partial t}-\frac{1}{r}\frac{\partial}{\partial r}\left(\lambda r\frac{\partial T}{\partial r}\right)=\dot{q}'''(r,t) \qquad (5)$$

The first terms in equation (4) and (5) represents rate of change of heat stored in unit volume of an element, the second term represents net removal of heat from the element and the third term is rate of heat generated per unit volume of the element.

The code SAC-RIT uses explicit method based finite difference scheme to solve these equations in fuel and clad region. To solve this equation by finite difference the fuel region is divided into *N* lateral zones. Thermo dynamical properties averaged over temperature and space of each zone is taken into account for finite difference equation. Volume averaged temperatures i.e. T_1, T_2, ..., T_N and corresponding positions i.e. $\bar{x}_1$,..., $\bar{x}_i$,..., $\bar{x}_N$ are determined for each zone. For *i* th zone the average temperature position is defined as $\bar{x}_i=(x_i+x_{i+1})/2$. Similarly effective conductivity k_{ij} between *i* th and *j* th zones are estimated. Integrating (4) from $x=0$ to $x=x_1$

$$\rho C_{p1}(t)\frac{\partial T(t)}{\partial t}=\dot{q}_1'''(t)+k_1(t)\frac{\partial T(t)}{\partial x} \qquad (6)$$

. To develop finite difference equation we replace $k_1(t)\frac{\partial T(t)}{\partial x}$ by volume averaged $\bar{k}_{12}\left(\frac{T^k_1-T^k_2}{\bar{x}_2-\bar{x}_1}\right)$ in (6) where, T_1^K and T_2^k are volume averaged temperatures of zones 1 and 2 and *k* stands for *k* th time step. Similarly, $\bar{x}_1$ and $\bar{x}_2$ are average thickness of zones 1

and 2. k_{ij} is the effective thermal conductivity between *i* th and *j* th zones. For central zone of the fuel i.e. for *i=1*, the finite difference equation is given by

$$\rho_1 C_{p1}\left(\frac{T_1^{k+1}-T_1^k}{t^{k+1}-t^k}\right)=\dot{q}_1'''-\bar{k}_{12}\left(\frac{T^k{}_1-T^k{}_2}{\bar{x}_2-\bar{x}_1}\right) \tag{7}$$

For i^{th} zone (*i*=2, 3, .. , *N*-1), integrating eq.(4) from $x=x_i$ to $x=x_{i+1}$, following finite difference equation is obtained.

$$\rho_i C_{pi}\left(\frac{T_i^{k+1}-T_i^k}{t^{k+1}-t^k}\right)=\dot{q}_i'''+\bar{k}_{i-1,i}\frac{1}{(x_i-x_{i-1})}\left(\frac{T^k{}_{i-1}-T^k{}_i}{\bar{x}_i-\bar{x}_{i-1}}\right)-\bar{k}_{i,i+1}\frac{1}{(x_i-x_{i-1})}\left(\frac{T^k{}_i-T^k{}_{i+1}}{\bar{x}_{i+1}-\bar{x}_i}\right) \tag{8}$$

For outer zone of the fuel i.e. for *i*= *N*, the finite difference equation has the form

$$\rho_i C_{pi}\left(\frac{T_i^{k+1}-T_i^k}{t^{k+1}-t^k}\right)=\dot{q}_i'''+\bar{k}_{i-1,i}\frac{1}{(x_i-x_{i-1})}\left(\frac{T^k{}_{i-1}-T^k{}_i}{\bar{x}_i-\bar{x}_{i-1}}\right)-\frac{1}{(x_i-x_{i-1})}\left(\frac{T^k{}_i-T^k{}_{clad}}{R_{th,FC}}\right) \tag{9}$$

Where, $R_{th,FC}$ is the effective thermal resistance between fuel-clad interface

$$R_{th,FC}=\frac{\delta_{fuel}}{k_{fuel}}+\frac{\delta_{gap}}{k_{air}}+\frac{\delta_{gap}+\delta_{clad}/2}{k_{clad}} \tag{10}$$

For clad to coolant heat transfer, the finite difference equation has the form

$$\rho_i Cp_i\left(\frac{T_i^{k+1}-T_i^k}{t^{k+1}-t^k}\right)=\dot{q}_i'''+\frac{1}{(x_{clad}-x_{fuel})}\left(\frac{T^k{}_i-T^k{}_{clad}}{R_{th,FC}}\right)-\frac{1}{(x_{clad}-x_{fuel})}\left(\frac{T^k{}_{clad}-T^k{}_{coolant}}{R_{th,C}}\right) \tag{11}$$

where, $R_{th,C}$ is the effective thermal resistance between clad-coolant interface

$$R_{th,C}=\frac{\delta_{gap}+\delta_{clad}/2}{k_{clad}}+\frac{1}{\delta_{clad}H_{eff}} \tag{12}$$

H_{eff} is the heat transfer coefficient for clad-coolant interface.

The code RITAC uses semi-implicit method based Crank-Nicholson technique to solve these equations in fuel and clad region.

Fuel Region: As shown in Fig. 1, the entire plate is first divided into a number of vertical sections and then each such section is further divided into few lateral sections. Temperatures are calculated at the midpoints of all these lateral sections. Applying thermal energy conservation principle to this section and approximating with the help of finite difference scheme (Heath, 2002),

$$T_i(t+\Delta t)-T_i(t)=\frac{K_f\Delta t}{D_f C_f \Delta x_f{}^2}\left(T_{i+1}(t)-2T_i(t)+T_{i-1}(t)\right)+\frac{Q(t)\Delta t}{D_f C_f} \tag{13}$$

where Ti(t) is temperature at midpoint of ith section (for simplicity, further we will call the midpoint as ith node), Kf is thermal conductivity of fuel, Δt is time step for which the above approximation holds good, is fuel density, Cf is specific heat of fuel, Δxf is thickness of a section in fuel region and it is equal to (df is thickness of fuel and 2nf is the total number of sections in fuel region) and Q(t) is heat production rate per unit volume of fuel at the present elevation at time t, which is directly proportional to the reactor power n(t) coming from Eq.(1). Crank-Nicolson technique is adopted to make the above solution scheme stable (Crank and Nicolson, 1947). Hence all time dependent functions at time t on the right hand side of Eq.(13) are replaced by the average value of those functions in the time interval *(i.e. Fi(t) → {Fi(t)+ Fi(t+Δt)}/2)*. Therefore, Eq.(13) can be rewritten as

$$T_i(t+\Delta t)=F_1T_{i-1}(t+\Delta t)-2F_1T_i(t+\Delta t)+F_1T_{i+1}(t+\Delta t)+F_1T_{i-1}(t)+(1-2F_1)T_i(t)+F_1T_{i+1}(t)+\frac{Q(t)\Delta t}{2D_fC_f}+\frac{Q(t+\Delta t)\Delta t}{2D_fC_f} \tag{14}$$

where $0 < i < n_f$ and $F_1=\frac{K_f\Delta t}{2D_fC_f\Delta x_f^2}$. Setting *i=0* in Eq.(14) for the node at fuel centre-line and since T_i*-1=T-1=*T_1 for symmetric temperature distribution about *x=0*, centre-line temperature is given by

$$T_0(t+\Delta t)=-2F_1T_0(t+\Delta t)+2F_1T_1(t+\Delta t)+(1-2F_1)T_0(t)+2F_1T_1(t)+\frac{Q(t)\Delta t}{2D_fC_f}+\frac{Q(t+\Delta t)\Delta t}{2D_fC_f} \tag{15}$$

Fuel-Clad Interface: For i=n_f i.e. at the interface of fuel and clad, temperature at time t+Δt is

$$T_{n_f}(t+\Delta t)=F_{21}T_{n_f-1}(t+\Delta t)-(F_{21}+F_{22})T_{n_f}(t+\Delta t)+F_{22}T_{n_f+1}(t+\Delta t)+F_{21}T_{n_f-1}(t)-\left((F_{21}+F_{22})-1\right)T_{n_f}(t)+F_{22}T_{n_f+1}(t)+\frac{F_{21}\Delta x_f^2Q(t)}{2K_f}+\frac{F_{21}\Delta x_f^2Q(t+\Delta t)}{2K_f} \tag{16}$$

where, $F_{21}=\frac{\Delta t}{D_fC_f\Delta x_f+D_{cl}C_{cl}\Delta x_{cl}}\frac{K_f}{\Delta x_f}$,

$F_{22}=\frac{\Delta t}{D_fC_f\Delta x_f+D_{cl}C_{cl}\Delta x_{cl}}\frac{K_{cl}}{\Delta x_{cl}}$ Δx_{cl} is thickness of a section in clad region and it is equal to $\frac{d_{cl}}{n_{cl}}$ (d_{cl} is thickness of clad and n_{cl} is the total number of sections in clad

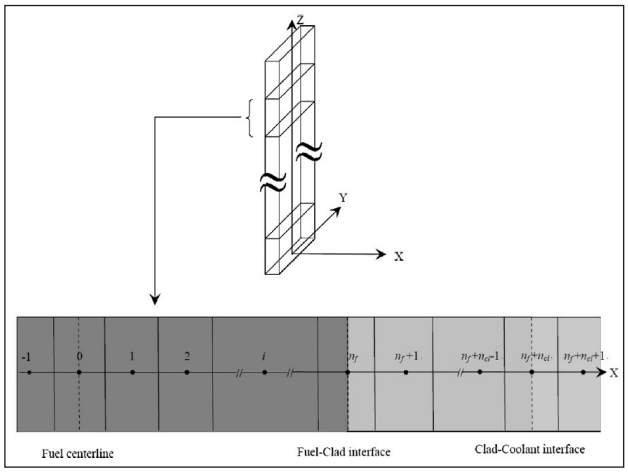

Figure 1: Fuel plate is divided into a number of vertical sections each of which is further divided into $2n_f$ number of lateral sections in fuel region and n_{cl} number of lateral sections in clad region

region), is clad density, C_{cl} and K_{cl} are specific heat and thermal conductivity of clad material respectively.

Clad Region:

Temperatures at all nodes in clad region are similar to Eq.(14) except the heat production terms.

$$T_i(t+\Delta t)=F_3T_{i-1}(t+\Delta t)-2F_3T_i(t+\Delta t)+F_3T_{i+1}(t+\Delta t)+F_3T_{i-1}(t)+(1-2F_3)T_i(t)+F_3T_{i+1}(t) \quad (17)$$

where $n_f < i < (n_f+n_{cl}-1)$ and $F_3=\dfrac{K_{cl}\Delta t}{2D_{cl}C_{cl}\Delta x_{cl}^2}$.

Clad Coolant Interface Region:

At clad coolant interface, the scenario is different from what we have considered so far for the other nodes since heat is transported from clad region to the interface by conduction process and from there onwards by convection process. So, taking into account both conduction and convection processes, temperature at clad coolant interface is

$$T_{n_f+n_{cl}}(t+\Delta t)=F_{41}T_{n_f+n_{cl}-1}(t+\Delta t)-(F_{41}+hF_{42})T_{n_f+n_{cl}}(t+\Delta t)+F_{41}T_{n_f+n_{cl}-1}(t)+(1-(F_{41}+hF_{42}))T_{n_f+n_{cl}}(t)+hF_{42}\left(T_{n_f+n_{cl}+1}(t+\Delta t)+T_{n_f+n_{cl}+1}(t)\right) \quad (18)$$

where, $F_{41}=\dfrac{K_{cl}\Delta t}{\Delta x_{cl}^2(D_{cl}C_{cl}+D_cC_c)}$, $F_{42}=\dfrac{\Delta t}{\Delta x_{cl}(D_{cl}C_{cl}+D_cC_c)}$, D_c is coolant density, C_c is specific heat of coolant and h is heat transfer coefficient of coolant.

Coolant Region:

Temperature in coolant region is based on the rate at which heat is convecting from clad to coolant and the rate at which the heat is carried away by coolant and it is given by following equation.

$$T_{n_f+n_{cl}+1}(t+\Delta t)=hF_{51}T_{n_f+n_{cl}}(t+\Delta t)-(hF_{51}+F_{52})T_{n_f+n_{cl}+1}(t+\Delta t)+hF_{51}T_{n_f+n_{cl}}(t)+(1-(hF_{51}+F_{52}))T_{n_f+n_{cl}+1}(t)+F_{52}\left(T_{in}(t+\Delta t)+T_{in}(t)\right) \quad (19)$$

where $F_{51}=\dfrac{\Delta t}{2D_cC_c\Delta x_c}$, $F_{52}=\dfrac{v\Delta t}{\Delta z}$, Δx_c is thickness of a section in coolant region and it is equal to $\frac{1}{2}(d-\Delta x_{cl})$, d is separation between two plates, v is coolant velocity, Δz is height of a vertical section, $T_{in}(t)$ is inlet temperature of the section in coolant region at an elevation z.

Final Solution:

Eq.(13)-(19) give temperatures of all lateral nodes at height z. For convenience, they are clubbed together to form a single matrix equation.

$$\vec{T}(t+\Delta t)=A\vec{T}(t+\Delta t)+B\vec{T}(t)+\vec{C}(t)+\vec{C}(t+\Delta t) \quad (20)$$

where $\vec{T}(t)$ is a *(nf+ncl+2)×1* matrix and defined as $\vec{T}(t)=\left(T_0(t)\ \ T_1(t)\ \ \ldots\ \ \ldots\ \ T_{n_f+n_{cl}+1}(t)\right)^T$. A is a $(n_f+n_{cl}+2)\times(n_f+n_{cl}+2)$ matrix.

B is also $(n_f+n_{cl}+2)\times(n_f+n_{cl}+2)$ matrix and defined as $B=I+A$, where I is an identity matrix of identical dimension. $\vec{C}(t)$ is a $(n_f+n_{cl}+2)\times1$ matrix and defined as $\vec{C}(t)=\left(\frac{Q(t)\Delta t}{2D_fC_f}\ \ \ldots\ \ \ldots\ \ \frac{Q(t)\Delta t}{2D_fC_f}\ \ \frac{F_{21}\Delta x_f^2Q(t)}{2K_f}\ \ 0\ \ \ldots\ \ 0\ \ F_{52}T_{in}(t)\right)^T$.

Therefore, temperatures at all lateral nodes inside fuel, clad and coolant at a height z at time $t+\Delta t$ is

$$\vec{T}(t+\Delta t)=(I-A)^{-1}\left(B\vec{T}(t)+\vec{C}(t)+\vec{C}(t+\Delta t)\right) \quad (21)$$

Now this equation requires $T(t=0)$ to start the transient calculation. Since reactor is at equilibrium at t=0 sec, $T(t+\Delta t) = T(t)$ and $C(t+\Delta t)=C(t)$ which modify Eq.(21) as following.

$$\vec{T}(t=0)=-A^{-1}\vec{C}(t=0) \quad (22)$$

Thermal hydraulics model for the coolant: One dimensional flow equations are applied to solve the parameter of fluid. The following assumptions are required: (1) incompressible flow, (2) in the steady state condition, inlet and outlet pressures of all channels are uniform, (3) no cross flow between two channels. The mathematical model includes general mass, momentum and energy conservation equations used in following form (Lahey and Drew, 1988).

Mass conservation equations for gas and liquid phase:

$$\frac{\partial}{\partial t}(\alpha\rho_g)+\nabla.(\alpha\rho_g v_g)=\Gamma_1+\Gamma_w \quad (23)$$

$$\frac{\partial}{\partial t}((1-\alpha)\rho_f)+\nabla.((1-\alpha)\rho_f v_f)=-\Gamma_1-\Gamma_w \quad (24)$$

Momentum conservation equations for gas and liquid phase:

$$\alpha\rho_g\frac{\partial v_g}{\partial t}+\alpha\rho_g v_g\nabla.v_g=-\alpha\nabla.P+\alpha\rho_g g-F_{wg}-F_1 \quad (25)$$

$$(1-\alpha)\rho_f\frac{\partial v_f}{\partial t}+(1-\alpha)\rho_f v_f\nabla.v_f=-(1-\alpha)\nabla.P+(1-\alpha)\rho_f g-F_{wf}-F_1 \quad (26)$$

Energy conservation equations for gas and liquid phase:

$$\frac{\partial\alpha\rho_g h_g}{\partial t}+\nabla.(\alpha\rho_g h_g v_g)=\alpha\frac{\partial P}{\partial t}+Q_{wg}+E_1+E_w \quad (27)$$

$$\frac{\partial(1-\alpha)\rho_f h_f}{\partial t}+\nabla.((1-\alpha)\rho_f h_f v_f)=(1-\alpha)\frac{\partial P}{\partial t}+Q_{wf}-E_1-E_w \quad (28)$$

Above six equations are reduced into three considering $\rho_m=\alpha\rho_g+(1-\alpha)\rho_f$. The coolant channel is divided into *N*-axial zones. An explicit difference approximation is adopted for each of these zones in the coolant channel. The coolant inlet mass flow rate should be specified as a function of time, therefore a description of the variation of the local mass velocity could be calculated. A channel averaged mass flow rate could be calculated at each time step. The coolant enthalpy at each coolant zone could be calculated by using the difference approximation.

Pressure Difference Along Vertical Fuel Channels

The hydraulic calculation of a reactor core is carried out in order to determine the pressure drop and flow distribution in coolant channels of reactor. In the calculation of total pressure drop (ΔP) coolant is considered to be a mixture of liquid and vapor flowing upward or downward. Assuming G_m and ρ_m to be mean mass flux rate and mean density of the homogenized liquid-vapor mixture, the momentum equation for a vertical constant area flow channel has the form [4]

$$\frac{\partial G_m}{\partial t}+\frac{\partial}{\partial z}\left(\frac{Gm^2}{\rho_m^+}\right)=-\frac{\partial p}{\partial z}-\frac{fG_m|G_m|}{2D_e\rho_m}-\rho_m g.\cos\theta \quad (29)$$

Where, *f is* friction factor and *g* is the acceleration due to gravity and D_e is the thermal hydraulics diameter of the flow channel.

Pressure Drop in Single Phase Flow: In single phase liquid flow the change in physical property along the heated channel can be assumed to be negligible. The total pressure drop along the channel is in the reactor core:

For constant flow area the mass flux (G_m) is constant and for $\rho_m^+=\rho_l\approx$ constant, the pressure drop due to acceleration is negligible. Therefore,

$$p_{in}-p_{out}\simeq\rho_l g(Z_{out}-Z_{in})+\frac{fG_m|G_m|}{2D_e\rho_l}(Z_{out}-Z_{in})+\Delta p_{form} \quad (30)$$

Friction factor depends upon flow velocity and channel dimension. For higher flow rate, the frictional pressure loss will be higher. Friction factor for laminar flow between rectangular cross sections is determined as: $f=(96/Re)(\mu_w/\mu_b)^{0.14}$, where *Re* is the Reynolds number and $(\mu_w/\mu_b)^{.14}$ refer to viscosity of coolant at wall and mean bulk coolant temperatures.

Pressure Drop in Two Phase Flow: Total pressure drop in two phase flow is more than that in single phase flow for the same length and mass flow rate. This is due to increased flow velocity in two phase flow. Pressure drop across a channel in which boiling takes place at $z=Z_B$ can be written as

$$p_{in}-p_{out}=\left[\left(\frac{G_m^2}{\rho_m^+}\right)_{out}-\left(\frac{G_m^2}{\rho_m^+}\right)_{in}\right]+\left[\int_{Z_{in}}^{Z_B}\rho_l g dz+\int_{Z_B}^{Z_{out}}\rho_m g dz\right]+\left[\begin{array}{l}\frac{f_{lo}G_m|G_m|}{2D_e\rho_l}(Z_B-Z_{in})\\+\frac{\overline{\phi_{lo}^2}f_{lo}G_m|G_m|}{2D_e\rho_l}(Z_{out}-Z_B)\end{array}\right]+\sum_i\left(\phi_{lo}^2K\frac{G_m|G_m|}{2\rho_l}\right)_i$$

The frictional pressure loss term Δp_{fric} is the pressure loss due to friction with channel wall surface. f_{lo} is the friction factor for liquid-only case while ϕ_{lo}^2 is the homogeneous frictional pressure drop coefficient when the effect of viscosity is neglected. The term Δp_{form} is the pressure drop because of spacers. The factor *K* depends upon the geometry or type of the spacers and it has to be determined experimentally for the channel.

Heat Transfer Coeficients

Single Phase Flow of The Coolant

Single phase flow of coolant takes place during normal full power operation in most of the research

reactors. In case of turbulent coolant flow under forced convection, the well known Dittus - Boelter correlation [5] is selected as a default model for the code. Moreover, the Gnielinski[6] and Sieder-Tate [7] correlations are also selected as alternatives to above said model. Heat transfer coefficient for single phase flow of coolant in the heated channel is expressed as

$$H_{eff} = \frac{Nu.K}{D_e} \tag{32}$$

where, *Nu* is Nusselt number, *K* is thermal conductivity and *De* is the effective hydraulic diameter of the flow channel. Nusselt number is calculated using Dittus - Boelter correlation and Sieder-Tate correlation which includes a viscosity correction to account for heated wall effects. The physical properties of coolant depend on temperature. Therefore, the coolant velocity is greatly influenced by coolant temperature. The variation of viscosity is taken care of by appropriate selection of fluid reference temperature or by introducing a multiplier $(\mu_b/\mu_w)^n$ into the correlations. When laminar flow (Re<2000) is established during normal operation of a reactor, Rohsenow and Choi's correlation [8] is used to obtain heat transfer coefficient.

Onset of Nucleate Boiling (ONB) Temperature: When the wall temperature remains below that necessary for nucleation, the mode of heat transfer is single phase convection. Onset of nucleate boiling occurs when the wall temperature exceeds the saturation temperature by the degree of superheat necessary to initiate bubble formation around the nucleation sites available on the wall surface. The temperature, where onset of nucleate boiling occurs is estimated using Bergles and Rohsenow [9] correlation over the pressure range of 1 - 136 bar given as

$$T_{ONB} = T_{sat} + 0.556\left(\frac{q''_{ONB}}{1082\,p^{1.156}}\right)^{0.463\,p^{0.0234}} \tag{33}$$

This empirical relation is widely used to predict the onset of sub-cooled nucleate boiling and is applicable for the low pressure conditions prevalent in research reactors. Onset of nucleate boiling (ONB) is not a limiting criterion in the design of a fuel element. However, it is a heat transfer regime, which should be identified for proper hydraulic and heat transfer considerations. The actual axial location at which ONB will occur depends on the axial heat flux distribution, the coolant velocity and the pressure drop along the channel.

Nucleate Boiling Region: When clad surface temperature is greater than the onset of nucleate boiling (ONB) temperature then nucleation in coolant begins. This mode of heat transfer takes place in the presence of sub-cooled liquid. Chen correlation [10] is considered to be the best correlation suitable for sub-cooled region. Initially the Chen Correlation was developed to analyze saturated boiling but it may also be used for sub-cooled nucleate boiling region with minor modifications. This correlation assumes a superposition of convection and nucleate boiling. Total heat transfer coefficient is given by

$$H_{2\phi} = h_c + h_{NB} \tag{34}$$

and the total heat flux from clad surface to the coolant is expressed as

$$q_f = h_c\left(T_w - T_b\right) + h_{NB}\left(T_w - T_{sat}\right) \tag{35}$$

The forced convective heat transfer coefficient is calculated from a modified Dittus-Boelter correlation while nucleate boiling heat transfer coefficient is obtained using Zuber-Foster [11] expression with a suppression factor.

Void Fraction Calculation : The equation used in PARET and by Munoz-Cobo et al. [12] for estimating void fraction in sub-cooled nucleate boiling region is a simplified form of Zuber's [13] equation and is given by

$$\frac{\partial \alpha}{\partial t} + SU_L\frac{\partial \alpha}{\partial z} + \lambda_s \alpha = \frac{F_s q^{''}}{h_{fg}\rho_v D} \tag{36}$$

where, λ_s is the bubble collapse frequency, F_s is the fraction of heat that produces vapor and S is the flow distribution parameter. The bubble collapse frequency (λ_s) is estimated using Jones model [14] given as $\lambda_s = c\lambda_0\phi H_I^2$ where H_1 is the degree of sub-cooling of the liquid, Φ and λ_0 are given by the following expressions:

$$\left.\begin{aligned}\phi &= \left(\frac{h_{fg}}{C_{pf}\left(T_{c0} - T_{sat}\right)}\right)^2 \\ \lambda_0 &= \frac{H_w^2}{k_f \rho_l C_{pf}}\end{aligned}\right\} \tag{37}$$

Where, T_{c0} is the clad temperature at the inception of sub-cooled boiling, H_W is the single phase heat transfer coefficient, C_{pf} is the specific heat of water at saturation temperature. The value of *c* has been taken as 0.005. In case of saturated boiling the void fraction

is estimated from steam quality x using Martinelli-Nelson correlation [15]. Void fraction (α) is calculated using Bankoff correlation [16] given as

$$\alpha = \frac{k}{1+\frac{1-x}{x}\frac{\rho_g}{\rho_l}} \quad (38)$$

where, $k = 0.71 + 0.0145\,P$.

Critical Heat Flux and Critical Heat Flux Temperature : In forced convective boiling, the boiling crisis occurs when the heat flux attains such a high value that the heated surface can no longer support continuous liquid contact. This peak heat flux is called Critical Heat Flux (CHF). The CHF is characterized by a sudden rise in surface temperature when the heated surface is covered by stable vapor blanket or alternatively, it is characterized by small surface temperature spikes when dry spots appear and disappear intermittently. A rapid increase of surface temperature of fuel elements during the boiling crisis is often sufficient to cause melting of the clad material and releasing of considerable amount of fission products into the coolant. Therefore, in nuclear reactors CHF is the most restrictive limit on the reactor power level. CHF can occur either in sub-cooled (low quality) bubbly flow regime or in saturated (high quality) annular flow regime. The former is called Departure from Nucleate Boiling (DNB) and the latter is called Dry Out. In reactor safety analysis, a minimum value of DNB ratio (DNBR), defined as the ratio of DNB heat flux and local operating heat flux, is usually accepted as the design criterion. Experiments have shown that CHF is a function of local coolant enthalpy, inlet sub-cooling, mass velocity, geometry etc.

Thermo-Physical Properties of Materials: The present computer codes, are restricted within a thermodynamic region where fuel and clad do not undergo any phase changes. Keeping this in mind, data related to thermo-physical properties of fuel and cladding materials are taken only for their solid phase. Suitable correlation for saturation properties of light and heavy water have been taken from correlations given by Crabtree and Siman-Tov, 1993[17].

Benchmarking of SAC-RIT and RITAC and Safety Analysis of Research Reactors at Trombay

Benchmark Problem: Both codes SAC-RIT and RITAC have been benchmarked against IAEA benchmark problem described in IAEA-TECDOC-643, Volume-3[3]. The problem is related to safety analysis of a 10 MWth pool type graphite reflected light water research reactor. Two types of core configuration are considered here. One is highly enriched uranium or HEU core and another is low enriched uranium or LEU core. In HEU core, fuel is UAlx–Al which comprises of 21% (% means wt.%) uranium and 79% aluminum. Results of transient cases wherein safety analysis is carried out for a fast transients of 1.5 $/0.5 s for both the cores are listed in Table-1 .The results as shown in the Table-1 shows a close agreements between the results given by SAC-RIT, RITAC and PARET/ ANL[3]. These codes were used in the analysis of PIEs related with reactivity initiated transients for Dhruva

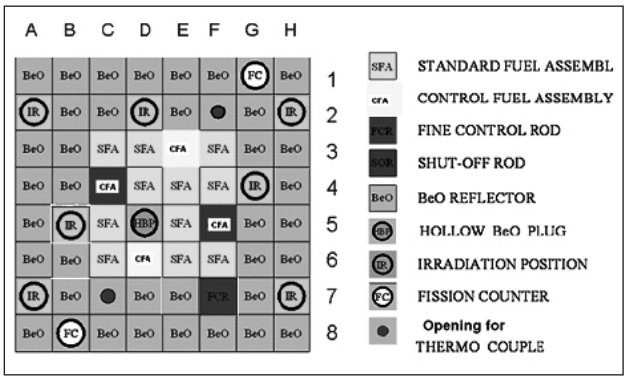

Figure 2: Core Map of 2mw Upgraded Apsara

and 2 MW Upgraded Apsara reactor. The results of the analysis using SAC-RIT and RITAC are in good agreement with other computer codes RELAP[19], COBRA[20] and SECMOD[21].

2 MW Upgraded Apsara Reactor

Upgraded Apsara Reactor is a 2 MW swimming pool type reactor. It uses Low Enriched Uranium (LEU) U_3Si_2 dispersed in Aluminum matrix (17% U^{235} enrichment) as fuel. The core is loaded with 11 Standard Fuel Assemblies (SFAs) and 4 Control Fuel Assemblies (CFAs). Out of four control fuel assemblies, two assemblies are with Control cum Shutoff Rods (CSRs) and other two assemblies are with Shut-Off Rods (SORs).

A standard fuel assembly consists of 17 fuel bearing plates and two aluminum inert plates swaged into the grooves provided in the side plates. A water gap of 2.5 mm is maintained between the fuel plates and also between fuel plate and inert aluminum plate. Each fuel plate has a meat thickness of 0.7 mm and 0.4 mm thick aluminum clad. Control fuel assembly is similar to standard fuel assembly with 12 fuel plates and water gap of 2.4 mm between the fuel plates.

Table 1: COMPARISON OF RESULTS FOR LEU CORE

Parameters	Program/Institute		
	RITAC/BARC	PARET/ANL	SAC-RIT /BARC
1. HEU CORE.			
Trip time (sec.)	0.609	0.609	0.608
Minimum period (msec.)	15	15	15
Peak power (MW)	133.36(0.655)	132.0(0.660)	131.5(0.654)
Energy at peak power(MJ)	3.24	3.26	3.090
Peak temperatures (^{0}C)			
Fuel centre	176.02(0.672)	170.9(0.670)	201.9(0.676)
Clad surface	162.51(0.674)	155.9(0.672)	196.2 (0.678)
Coolant outlet	85.76(0.770)	83.8(0.780)	81.9(0.779)
2. LEU CORE.			
Trip time (sec.)	0.572	0.573	0.572
Minimum period (msec.)	12	12	12
Peak power (MW)	137.28(0.611)	147.7(0.613)	131.43(0.611)
Energy at peak power(MJ)	2.74	2.95	2.627
Peak temperatures (^{0}C)			
Fuel centre	176.95(0.626)	183.4(0.626)	195.5(0.632)
Clad surface	157.03(0.629)	156.7(0.628)	186.6(0.634)
Coolant outlet	78.62(0.741)	82.0(0.735)	76.0(0.733)

Estimated maximum assembly powers at 2 MW are about 170 KW for SFA, 124 KW for CFA-CSR and 140 KW for CFA-SOR. Axial peaking factors for SFA, CFA-CSR and CFA-SOR are 1.36, 1.62 and 1.34, respectively; while local peaking factors are 1.45, 1.18 and 1.28, respectively. Total 4900 lpm coolant flow is provided for the core cooling.

Loss of Regulation Incident (LORI): Reactivity control and power regulation in Upgraded Apsara is achieved by controlled movement of fine control rod and control cum shut off rods in the reactor core. Fine control rod is used to adjust reactivity of smaller magnitude on auto/manual mode while the controls cum shut off

Table 2: Kinetic Parameters for 2MW Upgraded Apsara Reactor

Prompt neutron generation time	50μs
Delayed neutron fraction (β)	0.0071
Delayed neutron and prompt neutron groups	6+1
Fuel temperature coefficient of reactivity (mk/°C)	-0.014
Fuel temperature coefficient of reactivity(mk/°C)	-0.007
Void coefficient of reactivity(mk/% void)	-1.6
Shut off rod worth(mk)	69

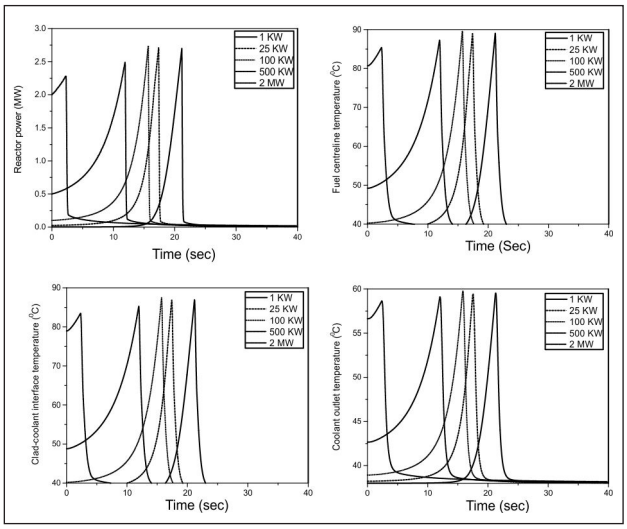

Figure 3: Transient Response of 2mw Upgraded Apsara Core

Table-3: Results of Lori for 2 Mw Upgraded Apsara Reactor at Powers 1kw and 2mw

Reactor Power	1KW	500KW	2MW
Trip point (sec)	20.74	11.58	2.37
Peak power(MW)	2.78	2.6	2.39
Total energy released (MJ)	6.35	14.2	8.61
Peak temperatures (°C)			
Fuel centerline	102.0	100.5	98.4
Clad	99.6	98.2	96.2
Coolant	62.4	62.1	61.7

rods are meant for coarse adjustment of reactivity on manual mode. A failure in control system might result in uncontrolled withdrawal of FCR resulting in insertion of positive reactivity. The analysis has been performed considering maximum drop time of SORs/CSRs as 0.5 sec for 90% drop and 2.5 sec. for the 100% drop. Results of LORI analysis are provided in Table-3 and Figure-3

Table-4: Comparison of Steady State Results Between RITAC and COBRA

Channel power (KW)	Channel flow (lpm)	Inlet plenum temperature (^{0}C)	Computer codes used	Max fuel temp (^{0}C)	Max fuel-clad interface temp (^{0}C)	Max clad-coolant interface temp (^{0}C)	Max coolant outlet temp (^{0}C)
1125	480	47	RITAC	*371.8*	*138.0*	*122.9*	*82.5*
			COBRA	377.3	138.4	127.0	80.6
1294	375	47	RITAC	*435.6*	*166.4*	*149.1*	*98.4*
			COBRA	434.7	172.6	159.5	97.4
1170	480	51	RITAC	*396.7*	*151.3*	*135.4*	*88.2*
			COBRA	-	-	135.4	87.9
1170	418	51	RITAC	*405.7*	*160.3*	*144.4*	*93.4*
			COBRA	-	-	144.8	93.2
1313	480	51	RITAC	*437.9*	*162.1*	*144.3*	*92.5*
			COBRA	-	-	144.6	92.3

Table-5: Comparison of Steady State Results Between RITAC and RELAP

Channel power (KW)	Channel flow (lpm)	Inlet plenum temperature (^{0}C)	Computer codes used	Max fuel temp (^{0}C)	Max fuel-clad interface temp (^{0}C)	Max clad-coolant interface temp (^{0}C)	Max coolant outlet temp (^{0}C)
1170	480	51	RITAC	*387.8*	*142.6*	*126.9*	*88.2*
			RELAP	389.3	-	127.3	-
1170	418	51	RITAC	*395.9*	*150.9*	*135.2*	*93.4*
			RELAP	394.5	-	134.7	-
1313	480	51	RITAC	*428.0*	*152.5*	*134.9*	*92.5*
			RELAP	422.0	-	134.1	-

Table-6: Results of LORI Initiated from 1 KW Reactor Power with Existing Assembly Power1125 KW and Coolant Channel Flow 375 lpm

Parameters (unit)	Value	
	SECMOD	RITAC
Trip actuated at (sec)	32.80	32.4
Peak Power (MW)	146	136
Maximum Reactivity Inserted (mk)	7.0	7.05
Maximum log rate (%/sec)	94	99
Maximum fuel Temperature (^{0}C)	584	614
Maximum clad Temperature (^{0}C)	223	203*/174**
Maximum coolant Temperature (^{0}C)	97	94
Total energy released in 100 sec (MJ)	461	457

** Fuel-clad interface temperature ** Clad-coolant interface temperature*

Table-7: Results of LORI Initiated from 1 KW Reactor Power with Existing Assembly Power 1170 KW and Coolant Channel Flow 418 lpm

Parameters (unit)	Value	
	SECMOD	RITAC
Trip actuated at (sec)	32.80	32.4
Peak Power (MW)	146	136
Maximum Reactivity Inserted (mk)	7.0	7.05
Maximum log rate (%/sec)	95	99
Maximum fuel Temperature (^{0}C)	595	626
Maximum clad Temperature (^{0}C)	219	201*/172**
Maximum coolant Temperature (^{0}C)	95	90
Total energy released in 100 sec (MJ)	461	457

** Fuel-clad interface temperature * Clad-coolant interface temperature*

100 MW Dhruva Reactor

Dhruva is a 100 MWth, tank type thermal research reactor at Trombay. The reactor core design is based on natural metallic uranium fuel with 7-pin cluster design. Heavy water is used as coolant, moderator and reflector. Reactor power is controlled by varying heavy water level in calandria tank while cadmium based shut off rods are used for protection/shutdown system. The calandria design provides for 146 lattice positions arranged on a regular 18 cm square lattice pitch for loading fuels, shut-off rods and isotope tray/adjuster/pneumatic carrier rods and these sites are similar in design to allow for interchangeability. Thermal hydraulics analysis using RITAC, COBRA, RELAP for steady state operation of Dhruva at thermal power of 100 MW under various condition of channel flow and inlet temperature were carried out. Results are summarized in Table-4 & 5. Results obtained using RITAC conforms well to those obtained using COBRA and RELAP.

Analysis for loss of regulation incident (LORI) in which reactivity insertion due to uncontrolled pump-up of heavy water in the calendria was considered, were carried out using RITAC and SECMOD. The analyses were carried out for the reactor power of 1 KW with channel power of 1125 KW and channel flow of 375 lpm. Results of the analysis are given in Tables-6. Similar analyses were carried out for the reactor power of 1 KW with channel power of 1170 KW and channel flow of 418 lpm. Results of the analysis are given in Tables-7.

Conclusion

SAC-RIT and RITAC are benchmarked code which can be used for safety analysis of research reactor with plate/pin type fuel design. Both computer codes can analyze events like LORI up to sub-cooled boiling regime in the fuel coolant channel satisfactorily with reasonably good accuracy. Reactivity feedback and thermal hydraulic analysis up to two phase flow for plate type geometry are incorporated into these computer codes in order to make it a complete tool for reactivity transient analysis.

References

1. Tej Singh, Jainendra Kumar, T. Mazumdar and V.K.Raina, 2013. Development of neutronics and thermal hydraulics coupled code-SAC-RIT: for plate type fuel and its application to reactivity initiated transient analysis, Annals of Nuclear Energy 62, 61-80.
2. Mazumdar, T., Singh, T., Gupta, H. P., Singh, K., 2012. RITAC: Reactivity Initiated Transient Analysis Code – An overview, Annals of Nuclear Energy 43, 192-207.
3. IAEA-TECDOC-643, 1992. Research reactor core conversion guidebook, Volume 3: Analytical verification (Appendices G and H).
4. Sanchez, J., 1989. On the numerical solution of the point reactor kinetics equations by generalized Runge–Kutta methods, Nuclear Science and Engineering 103, 94–99.
5. Todreas, N. E., Kazimi, M. S., 1993. Nuclear Systems Volume I: Thermal Hydraulic Fundamentals, second ed. Taylor and Francis, Pennsylvania.
6. Dittus, F. W., Boelter, L. M. K., 1930. Heat transfer in Automobile Radiators of the Tabular type, University of California Publications 2, 443-461.
7. Gnielinski, V., 1976. New equations for heat and mass transfer in turbulent pipe and channel flow, Int. Chem. Eng. 16, 359–367.
8. Seider, E.N., Tate, C.E., 1936. Heat Transfer and Pressure Drop of Liquids in Tubes, Ind. Eng. Chem. 28, 1429-1435.
9. Roshenow, W. M., Choi, H., 1961. Heat, Mass and Momentum Transfer, Prentice Hall, Inc., New Jursey, 141-142.
10. Bergles, A. E., Roshenow, W. M., 1963. The determination of forced convection surface boiling heat transfer, Paper 63-HT-22 presented at 6th National Heat Transfer Conference of the ASME-AlChE, Boston, 11-14th August.
11. Chen, J. C., 1963. A correlation for boiling heat transfer to saturated fluids in convective flow, ASME preprint 63-HT-34 presented at 6th National Heat Transfer Conference, Boston, 11-14th August.
12. Forster, H. K., Zuber, N., 1955. Dynamics of vapor bubbles and boiling heat transfer, AlChE Journal, I(4), 531-535.
13. Munoz-Cobo, J.L., Chiva, S., Sekhri, A., 2004. A reduced order model of BWR dynamics with sub-cooled boiling and modal kinetics: application to out of phase oscillations. Annals of Nuclear Energy 31, 1135-1162.
14. Zuber, N., Stube, F.W., Bijwaard, G., 1966. Vapor void fraction in sub-cooled boiling and in saturated boiling systems. In: From Proceedings of the Third International Heat Transfer Conference, Chicago, Illinois, August 7 to 12, 1966, vol. V. American Institute of Chemical Engineering, New York, 24–38.
15. Jones, A.B., Dight, D.G., 1963. Hydrodynamic Stability of a Boiling Channel (KAPL-2290).
16. Collier, J. G., Thome, J. R., 1996. Convective boiling and condensation, third ed. Clarendon Press, New York.
17. Bankoff, S. G., 1960. A variable density single-fluid model for two phase flow with particular reference to steam water, Trans. ASME, Ser. C, 82, 265.
18. Crabtree, A., Siman-Tov, M., 1993. Thermo physical properties of saturated light and heavy water for advanced neutron source applications, Oak Ridge National Lab., Oak Ridge, TN, ORNL/TM-12322.
19. RELAP/MOD3 Code Manual: User's guidelines. Division of Systems Research, Office of Nuclear Regulatory Research, US Nuclear Regulatory Commission, 1992.
20. Wheeler, C. L., Stewart, C. W., Cena, R. J., Rowe, D. S., & Sutey, A. M. (1976). COBRA-IV-I: An interim version of COBRA for thermal-hydraulic analysis of rod bundle nuclear fuel elements and cores (No. BNWL-1962). Battelle Pacific Northwest Labs., Richland, Wash.(USA).
21. SECMOD-A point kinetics-thermal hydraulics coupled computer code based on "Numerical integration of dynamic nuclear systems equations by optimum integrating factors," PhD thesis by Phillip Allen Seeker, Jr., The University of Arizona, (1969)

Life Cycle Reliability and Safety Engineering
Vol.4 Issue 4(2015) 54-59

A Dynamic Analysis of Circulating Fuel Reactors with Zero Dimensional Modeling

Indrajeet Singh and Anurag Gupta
Reactor Physics Design Division, Bhabha Atomic Research Centre, Trombay, Mumbai–400085, INDIA
Email: jeet@barc.gov.in

Abstract

In Circulating Fuel Reactors (CFRs), the fuel salt serves the purpose of coolant as well as fuel simultaneously resulting in strongly coupled neutronics and thermo-hydraulics system. These special features require modifications to mathematical models usually applicable to static fuel systems. In the presented work, the modified point kinetics equations have been adopted to take into account the delayed neutron precursors drift and the subsequent decay in the primary loop along with zero-dimensional thermo-hydraulic equations. To study the dynamic behavior of circulating fuel reactors, two different methods were used to solve the coupled set of differential equations. This resulting program was used to analyses the Molten Salt Reactor Experiment (MSRE) [1] for both ^{235}U based fuel mixture and the U233/U235/Pu239 based fuel mixtures.

Keywords*: Molten salt reactor, Pont Kinetics, Thorium, Delayed neutron*

1. Introduction

The Generation IV International Forum (GIF-IV) [2] has identified the Molten Salt Reactor (MSR) as one of the innovative nuclear reactor designs which promises to serve various purposes, such as breeding of nuclear fuel, actinides transmutation and high temperature operation for electricity and hydrogen production [3,4]. The MSRs are also being considered as promising candidates for the third stage of India's nuclear power program for thorium utilization. These attractive features results in a renewed interest in circulating fuel reactors especially the Molten Salt reactor. In MSRs, the fuel salt, which also serves as coolant, is in the form of molten salt of fluoride of fertile and fissile materials which circulates through reactor core and heat exchangers. The geometry of the system is designed such that only the salt within the reactor core is in critical condition. The circulation of fuel salt leads to drift of in-core born delayed neutron precursor (DNP) out of the core. Transient study of circulating fuel based system requires modifications to conventional reactor simulation tools or development of dedicated computational method to take into account drift of delayed neutron precursor (DNP) and the subsequent decay in out-of-core external primary loop [5]. It is also possible that the delayed neutron precursors re-entering the core depending upon the flow rate resulting in feedback. This poses a new challenge from the perspective of mathematical and numerical schemes for simulating the dynamic behavior of nuclear power plants [6].

The MSR technology was first studied at Oak Ridge National Laboratory (ORNL) in the middle of twentieth century and this led to Aircraft Reactor Experiment (ARE), a 2.5 MWth reactor designed for airplane propulsion and the Molten Salt Reactor Experiment (MSRE). The 8MWth MSRE went critical in 1965 and successfully operated until 1969 to demonstrate the technology for the development of power successor molten salt breeder reactor (MSBR-2250MWth) [1]. Unfortunately, MSBR project was stopped in the design stage. The theoretical and experimental data, given in Table -1, provided from the Molten Salt Reactor Experiment (MSRE) operation from Oak Ridge National Laboratory (ORNL) [7] is used as reference in the present work.

In the present work, an attempt is made to study the dynamic behavior of MSRE using modified point kinetics equations, which take into account the drift of delayed neutron precursors, with lumped thermal hydraulic model feedbacks. Two different methods, namely delay differential equation solver (dde23) and Taylor Series Expansion (TSE) method have been adopted to solve the first order coupled set of equations. The results from these two methods are compared with reference for various reactivity input transients.

The remaining paper is organized as follows. The mathematical models used to study the circulating fuel reactor are described in section 2. In section 3, the methods of solution are presented. Finally, in Section 4, the obtained results are discussed.

Nomenclature

$n(t)$: neutron density;

$C_i(t)$ i^{th} group DNP density;

λ_i : i group DNP decay constant ;

ρ_0: loss of reactivity in steady state;

ρ: reactivity;

β_i : ith group delayed neutron fraction;

β: total delayed neutron fraction;

τ_l : Loop transit time(s);

τ_c : Core transit time(s);

Λ: neutron generation time (s);

γ : fraction of power generated in the salt;

P : core power (W);

T: Temperature (K);

U: overall heat transfer coefficient between salt and graphite (WK^{-1});

M : Mass(kg);

c_p: specific heat ($Jkg^{-1}K^{-1}$);

δρ: external reactivity inserted or withdrawn;

α_s : Fuel salt temperature reactivity feedback coefficient;

α_g : graphite temperature reactivity feedback coefficient;

$T_s(0)$: initial temperature of fuel salt;

$T_g(0)$: initial temperature of graphite;

2.0 Mathematical Models

In this work, a simplified approach, based on the modified space-independent point kinetics equations is adopted, which take into account the effect of the fuel salt circulation along with zero-dimensional thermo-hydraulics equations [6]. Six group delayed neutron approximation results in seven point kinetics equations. The zero-dimensional thermal-hydraulic model consists of two equations describing the simple energy balance for the molten salt and the graphite. These two equations reduce to one if MSR core does not have any graphite moderator (For example: Molten Salt Fast Reactor).

Table-1: MSRE Parameters Used in the Study

MSRE Parameters	Fuel Type		Unit
	^{235}U	^{233}U	
β_1	22.3	23.76	pcm
β_2	145.7	85.76	pcm
β_3	130.7	71.9	pcm
β_4	262.8	82.14	pcm
β_5	76.6	15.79	pcm
β_6	28.0	10.03	pcm
λ_1	0.0124	0.0126	s^{-1}
λ_2	0.0305	0.0337	s^{-1}
λ_3	0.111	0.139	s^{-1}
λ_4	0.301	0.325	s^{-1}
λ_5	1.14	1.13	s^{-1}
λ_6	3.01	2.50	s^{-1}
l	$2.4x10^{-4}$	$4.0x10^{-4}$	s
τ_c	8.5	8.5	s
τ_l	16.5	16.5	s
α_s	-8.712	-10.443	pcm
α_g	-6.66	-5.305	pcm
M_s	1448		Kg
M_g	3687		Kg

The point-reactor model used in the present work has two additional terms

$$\frac{C_i}{\tau_c}$$

and

$$\frac{C_i(t-\tau_l)}{\tau_c} e^{(-\lambda_i \tau_l)}$$

in order to account for delayed neutron precursors (DNP) that are leaving and entering the reactor core [8]. The point-kinetics equations for circulating fuel system are as follows:

$$\frac{dn(t)}{dt} = \frac{(\rho(t)-\beta)}{\Lambda} n(t) + \sum_{i=1}^{6} \lambda_i C_i(t) \quad (1)$$

$$\frac{dC_i(t)}{dt} = \frac{\beta_i}{\Lambda} n(t) - \lambda_i C_i(t) - \frac{C_i}{\tau_c} + \frac{C_i(t-\tau_l)}{\tau_c} e^{(-\lambda_i \tau_l)} \quad (2)$$

Using equations (1-2), loss of reactivity due to drift of DNP is evaluated and given by equation (3). This loss of reactivity needs to be supplied through withdrawal of control system or fuel feed in order to maintain criticality. The loss of reactivity depends on flow rate of fuel salt which couples the thermal-hydraulic and neutronics.

$$\rho_0 = \beta - \sum_{1}^{6} \frac{\beta_i \lambda_i}{\lambda_i + \frac{1 - e^{(-\lambda_i \tau_l)}}{\tau_c}} \tag{3}$$

The zero-dimensional thermal-hydraulic model for the molten salt and the graphite is presented by equations (4) and (5).

$$\frac{dT_s(t)}{dt} = \frac{\gamma P(t)}{M_s c_{p,s}} + \frac{U}{M_s c_{p,s}}\left(T_g(t) - T_s(t)\right) + \frac{T_s^{in}(t) - T_s^{out}(t)}{\tau_c} \tag{4}$$

$$\frac{dT_g(t)}{dt} = \frac{(1-\gamma)P(t)}{M_g c_{p,g}} - \frac{U}{M_g c_{p,g}}\left(T_g(t) - T_s(t)\right) \tag{5}$$

$$T_s(t) = \frac{T_s^{in}(t) + T_s^{out}(t)}{2} \tag{6}$$

In equation (1), reactivity depends on reactivity feedback coefficients of graphite, fuel salt and external reactivity addition or withdrawal. This has been expressed in equation (7).

$$\rho(t) = \rho_0 - \alpha_s\,(T_s(t) - T_s(0) + \alpha_g(T_g(t) - T_g(0) + \delta\rho \tag{7}$$

3.0 The Solution Methods

3.1 Delay Differential Equation Solver (dde23)

The set of equations (2) are delay differential equations (DDE); a delay differential equation is a differential equation where the time derivatives at the current time depend on the solution at previous times [11]. A program has been developed to solve these first order coupled set of equations using delay differential equation solver (dde23) from pydelay [6]. The dde23 solver requires not just the value of the solution at the initial condition, but also the "history", the solutions at previous times to initial value. The initial values (at time t=0) are given by equations (3) and (4):

$$C_{i0} = \frac{n_0}{\Lambda} \frac{\beta_i \lambda_i}{\lambda_i + \frac{1 - e^{(-\lambda_i \tau_l)}}{\tau_c}} \tag{7}$$

3.2 Taylor Series Expansion Method

A program based on Taylor expansion of delay term of equation (2),

$$C_i(t - \tau_l) \approx C_i(t) - \tau_l \frac{dC_i(t)}{dt}$$

was also developed to convert set of the DDE to ordinary differential equations (ODE). With this approximation equation (2) takes ODE form as follows:

$$\frac{dC_i(t)}{dt} = \frac{\beta_i}{\Lambda}\frac{n(t)}{a_i} - \frac{b_i}{a_i} C_i(t) \tag{8}$$

where,

$$a_i = 1 + \frac{\tau_l}{\tau_c} e^{(-\lambda_i \tau_l)}$$

and

$$b_i = \lambda_i + \frac{1 - e^{(-\lambda_i \tau_l)}}{\tau_c}$$

The set of equations (8) can be easily solved by using some recently developed methods i.e. Power Series Solutions (PWS) (Aboanber, 2002, Sathiyasheela 2009), CORE (Quintero-Leyva, 2008), PCA(Kinard and Allen, 2003). The method of Taylor Series Expansion (TSE) have been used due to its simplicity in implementation and accuracy in results with small time steps (of the order of $\Lambda = 10^{-4}$). This method is based on taking a Taylor series expansion of the neutron density and delayed precursor functions at each time step [10]. The TSE method has been compared with recently developed methods by David McMahon and Adam Pierson for various generation time and reactivity inputs [10].

4. Results and Discussion

The salt flow results in loss of reactivity due to DNP decay in the circulation loop of zero importance regions. This loss has been computed using equation (3) for ^{233}U and ^{235}U based fuel salts in MSRE and compared with reference results. Subsequently, transients in MSRE are studied with methods described in section 3 for various reactivity inputs.

4.1 Loss of Reactivity with Fuel Flow Rate

The loss of reactivity at reference velocity (Vref) of ^{233}U and ^{235}U based fuel salts has been computed

using equation (3). The loss of reactivity due to fuel circulation was found to be 120pcm for ^{233}U and 250pcm for ^{235}U based fuel salt respectively. The ORNL experiment results lists the loss of reactivity in MSRE as 212 pcm for ^{235}U fuel and 100±15 pcm for the $^{233}U/^{235}U/^{239}Pu$ fuel mixture [9].

It can be seen from Table-2 that point model estimation of the relative loss of DN is 37.5 % β_{static} for the ^{235}U fuel and 41.5% β_{static} for the 233U/235U/239Pu, respectively.

Table-2: Comparison of Computed DNP Loss with Experimental Values

	^{235}U (pcm)	^{233}U (pcm)
βeff(static)	666.1	289.0
DNP Losses		
MSRE Experiment (at flow rate *Vref*)	212	100.5
DYN1D	252.6	120.4
DYN3D	269.7	129.7
PoliTO 2	278.0	134.5
Point model (Present work)	250	120

Thus, the point model result is in good agreement with DYN1D model. This is mainly due to the fact that precursor decay constants of ^{233}U are slightly greater than that of ^{233}U, as presented in Table-1 [8]. The modified point kinetics solution without feedback using dde23 solver and TSE methods at different flow rate of salt with respect to reference flow rate (Vref=0.2m/s) is shown in Fig.1.

In the steady state, the MSRE core has reactivity exactly equal to ρ_0 = 0.001117 for ^{233}U based fuel salt just to maintain the criticality condition at reference flow rate. As flow rate is changed to half of the Vref, there is gain in reactivity and neutron population increases with time as shown in Fig.1. On the other hand, relative neutron population decreases for higher fuel flow rate. It can be also seen from Fig.1 that although TSE method approximates the delay term, it results in fairly good agreement with dde23 solver.

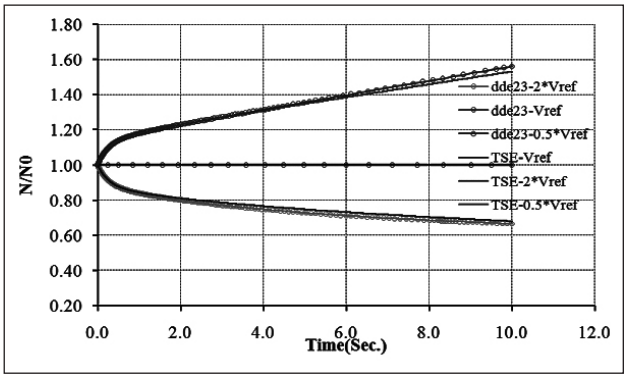

Figure 3. MSRE power for 50 pcm reactivity step at fixed inlet temperature

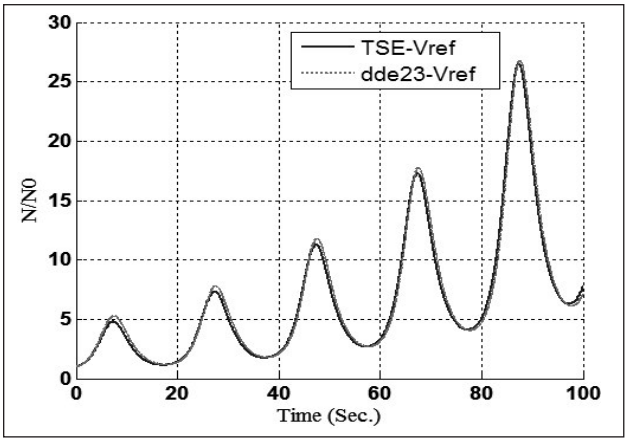

Figure 2. MSRE response for a sinusoidal reactivity

The MSRE response for a sinusoidal reactivity 0.0008*sin(3.14*t/10) was also computed by TSE and dde23 solvers with ^{233}U based fuel salt. In this study, the fuel flow rate was kept constant (equal to the reference velocity, Vref =0.2m/sec). The results of two methods for sinusoidal reactivity also were found to be in good agreement as shown in Fig.2.

4.2 Transient with Temperature Feedback

To study the dynamics of the MSRE, modified point kinetics equations were solved along with thermal hydraulic feedback equations (4-6). It is assumed that the γ = 0.93 of total thermal power is being generated in the fuel salt. In this study, reactivity initiated transients were analyses at fixed inlet salt temperature and results are compared with the reference.

4.2.1 Transient with 50 pcm Reactivity Step

Transient analyses have been carried out for 50pcm reactivity insertion at nominal power (8MW) for ^{233}U based fuel salt. At first, reactor power increases in response to reactivity insertion, subsequently negative fuel and graphite temperature feedbacks take over which results in decrease in power and stabilization at some higher power relative to initial value.

The reactor power with time for ^{233}U fuel, Fig.3, was found to be in good agreement with that of 0-0D model of used in reference study [13]. The transient for ^{235}U based fuel salt was also compared with that of ^{233}U fuel for 50pcm step reactivity and found that later fuel result in higher peak power due to large difference in the value of DNP.

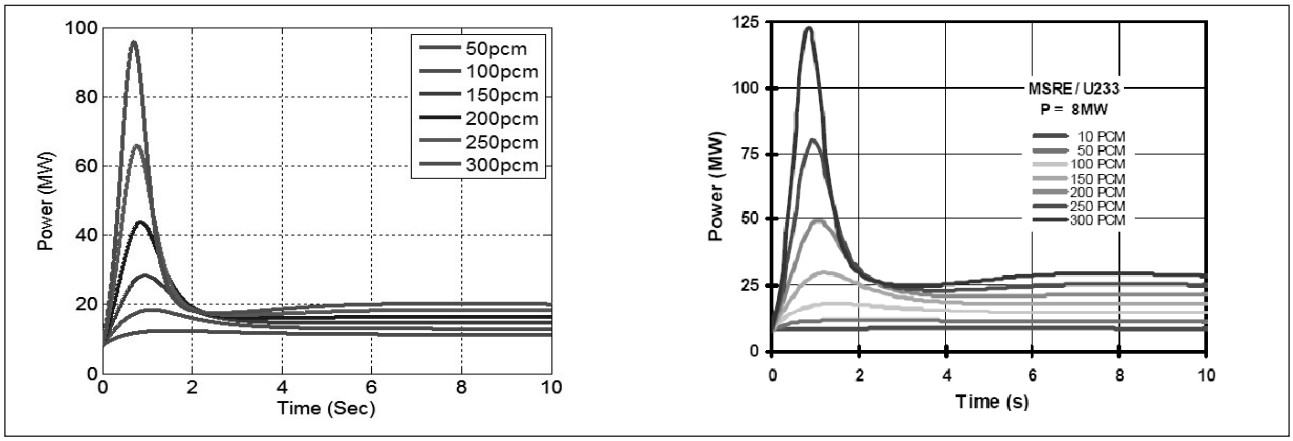

Figure 4. MSRE power for different reactivity step at fixed inlet temperature.

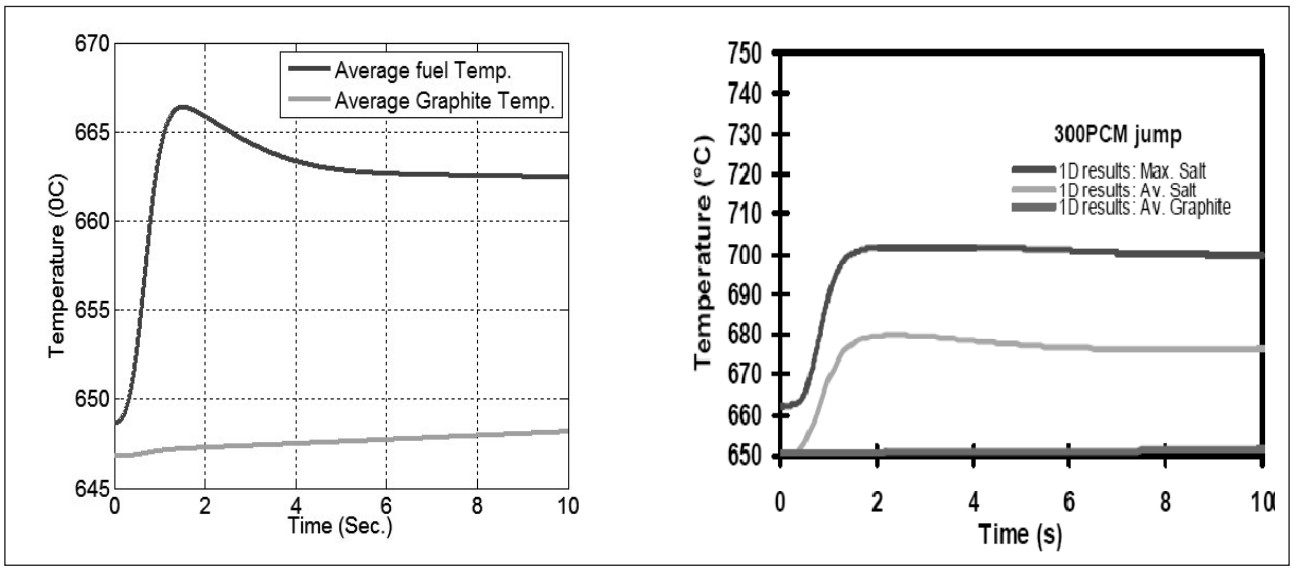

Figure 5. The average temperature of fuel salt and graphite for 300 pcm jump in the MSRE core with ^{233}U fuel.

4.2.2 Comparison of Point & 1D-Dmodels

In this study, the results of point model has been compared with that of 1D-1D model for 50, 100, 150, 200, 250 and 300pcm reactivity steps in ^{233}U loaded MSRE operating at nominal power 8MWth. Both the Point model peak power and asymptotic power was found to be about 23% lower than that of the 1D-1D model (Fig.4).

The discrepancies between these two models can be explained by observing the temperature variation of fuel salt during the transient. The initial rise in power is slowed down by temperature feedbacks caused by salt temperature increase. The loss of DNP computed by point model is 120pcm and by 1D-1D model 120.4pcm. Therefore, the reason for the difference in power variation with time is mainly due to fact that the temperature feedback is not identical in two models. The increase in average salt temperature with point model 31°C whereas it is 26.9°C with 1D-1D model as shown in Fig.4 [14].

It should be noted from various transient studies that the power transient is inherently self-limiting by virtue of the negative temperature co-efficient of reactivity of the system. This study also suggests that point model provides a good insight of transient behavior of molten salt reactor by comparing the results with higher dimensional models. At the same time, Fig.3(b) [13,14] suggests that development of Multi-physics model will be necessary for accurate safety analysis of MSR.

5. Conclusions

The loss of reactivity due to recirculation of fuel salt in steady state Molten Salt Reactor Experiment (MSRE) operation has been estimated by adopting the modified point kinetics equations. The power and

temperature transients of molten salt reactor with ^{232}Th-^{233}U & ^{235}U based fuel salts have been analyzed using a zero-dimensional model of neutronics and thermal hydraulics feedbacks. This gives a useful estimate of power and temperature peak values during transient. However, though providing a good insight of transient behavior, these models are inadequate to predict the accurate results. The results could be improved by considering the axial and radial dimensions and by taking the appropriate weighting factors for the temperature feedback and for the power distribution corresponding to the reactor regions.

References

1. Paul N. Haubenreich and J.R. Engel, "Experience with the molten-salt reactor experiment", Oak Ridge National Laboratory, oak Ridge, Tennessee TTBS7 August 1969.
2. "A Technology Roadmap for Generation IV Nuclear Energy Systems", issued by the U.S. DOE Nuclear Energy Research Advisory Committee and the Generation IV International Forum, GIF-002-00 (2002).
3. C. Forsberg et. al., "Liquid Salt Applications and Molten Salt Reactors", Proceedings of ICAPP,(2007).
4. M. Hron, J. Uhlìr, C. Renault, "Molten Salt Reactor", EUR 21231, pp. 270-286 (2006).
5. J. Krepel et. al., "DYN3D-MSR Spatial Dynamics Code for Molten Salt Reactors", ANE, 34. 2007.
6. Cammi, A., Di Marcello, V., Luzzi L., and Memoli, "A Multi-Physics Approach to the Dynamics of Molten Salt Reactors", Ann. Nucl. Energy,submitted. , V. 2010,
7. http://pydelay.sourceforge.net/
8. R. C. Stefy, Jr. P. J. Wood, "Theoretical Dynamic Analysis of The MSRE With 233U Fuel", ORNL- 'I'M- 2571.
9. Jiri Krepel, Ulrich Grundmann, Ulrich Rohde, "Development and Verification of Dynamics Code for Molten Salt Reactors" Proceedings of ICONE 12-49130: April 25-29, 2004, Arlington, Virginia, USA.
10. Mitchell, B. 1977, "Taylor series methods for the solution of the point reactor kinetic equations", Annals of Nuclear Energy 4, 169-176.
11. David McMahon and Adam Pierson, "A Taylor series solution of the reactor point kinetics equations", Department of Nuclear Safety Analysis, Sandia National Laboratories, Albuquerque, 87185-1141.
12. L.F. Shampine, S. Thompson, "Solving Delay Differential Equations with dde23", March 23, 2000.
13. Antonio Cammi, Carlo Fiorina, Claudia Guerrieri, Lelio Luzzi, "Dimensional effects in the modelling of MSR dynamics: Moving on from simplified schemes of analysis to a multi-physics modelling approach", Politecnico di Milano-Department of Energy, CeSNEF (Enrico Fermi Center for Nuclear Studies), via Ponzio 34/3-20133 Milano, Italy.
14. Jiri Krepel, "Dynamics Of Molten Salt Reactors", Department of Nuclear Reactors, Czech Technical University in Pargue, Ph.D. Thesis.

SRESA JOURNAL SUBSCRIPTION FORM

Subscriber Information (Individual)

Title	First Name	Middle Name	Last Name
_____	_____	_____	_____

Street Address Line 1	Street Address line 2
_____	_____

City	State/Province	Postal Code	Country
_____	_____	_____	_____

Work Phone	Home Phone	E-mail address
_____	_____	_____

Subscriber Information (Institution)

Name of Institution/ Library _____

Name and Designation of Authority for Correspondence _____

Address of the Institution/Library _____

Subscription Rates

	Subscription Quantity	Rate	Total
Annual Subscription (in India)	_____	Rs. 15, 000	_____
(Abroad)	_____	$ 500	_____
	_____		_____
	_____		_____

Payment mode (please mark)

Cheque ☐ Credit Card ☐ Master Card ☐ Visa ☐ Online Banking ☐ Cash ☐ De mand Draft ☐

Credit card Number _____

Credit Card Holders Name _____

Credit Card Holde _____

Guidelines for Preparing the Manuscript

A softcopy of the complete manuscript should be sent to the Chief-Editors by email at the address: editor@sresa.org.in. The manuscript should be prepared using 'Times New Roman' 12 font size in double spacing, on an A-4 size paper. The illustrations and tables should not be embedded in the text. Only the location of the illustrations and tables should be indicated in the text by giving the illustration / table number and caption.

The broad structure of the paper should be as follows: a) Title of the paper – preferably crisp and such that it can be accommodated in one or maximum two lines with font size of 14 b) Name and affiliation of the author(s), an abstract of the paper in ~ 100 words giving brief overview of the paper and d) Five key words which indicates broad subject category of the paper. The second page of the paper should start with the title followed by the Introduction

A complete postal address should be given for all the authors along with their email addresses. By default the first author will be assumed to be the corresponding author. However, if the first author is not the corresponding author it will be indicated specifically by putting a star superscript at the end of surname of the author.

The authors should note that the final manuscript will be having double column formatting, hence, the size of the illustration, mathematical equations and figures should be prepared accordingly.

All the figures and tables should be supplied in separate files along with the manuscript giving the figure / table captions. The figure and table should be legible and should have minimum formatting. The text used in the figures and tables should be such that after 30% reduction also it should be legible and should not reduced to less than font 9.

Last section of the paper should be on list of references. The reference should be quoted in the text using square bracket like '[1]' in a chronological order. The reference style should be as follow:

1. Pecht M., Das D, and Varde P.V., "Physics-of-Failure Method for Reliability Prediction of Electronic Components", Reliability Engineering and System Safety, Vol 35, No. 2, pp. 232- 234, 2011.

After submitting the manuscript, it is expected that reviews will take about three months; hence, no communication is necessary to check the status of the manuscript during this period. Once, the review work is completed, comments, will be communicated to the author.

After receipt of the revised manuscript the author will be communicated of the final decision regarding final acceptance. For the accepted manuscript the author will be required to fill the copy right form. The copy right form and other support documents can be down loaded from the SRESA website: http://www.sresa.org.in

Authors interested in submitting the manuscript for publication in the journal may send their manuscripts to the following address:

Society for Reliability and Safety
RN 68, Dhruva Complex
Bhabha Atomic Research Centre,
Mumbai – 400 085 (India)
e-mail : editor@sresa.org.in

The Journal is published on quarterly basis, i.e. Four Issues per annum. Annual Institutional Subscription Rate for SAARC countries is Indian Rupees Ten Thousand (Rs. 10,000/-) inclusive of all taxes. Price includes postage and insurance and subject to change without notice. For All other countries the annual subscription rate is US dollar 500 ($500). This includes all taxes, insurance and postage.

Subscription Request can be sent to SRESA Secretariat (please visit the SRESA website for details)

SRESA's International Journal of

Life Cycle Reliability and Safety Engineering

Contents

Vol.4 Issue No.4 Oct-Dec 2015 ISSN – 2250 0820